TECHNISCHE UNIVERSITÄT MÜNCHEN
Lehrstuhl für Entwicklungsgenetik

In vitro and *in vivo* analysis of corticotropin-releasing hormone receptor-dependent signal transduction using microarray technology

Cornelia Graf

Vollständiger Abdruck der von der Fakultät Wissenschaftszentrum Weihenstephan für Ernährung, Landnutzung und Umwelt der Technischen Universität München zur Erlangung des akademischen Grades eines

Doktors der Naturwissenschaften

genehmigten Dissertation.

Vorsitzender:	Univ.-Prof. Dr. A. Gierl
Prüfer der Dissertation:	1. Univ.-Prof. Dr. W. Wurst
	2. Univ.-Prof. Dr. D. Langosch

Die Dissertation wurde am 28.01.2009 bei der Technischen Universität München eingereicht und durch die Fakultät Wissenschaftszentrum Weihenstephan für Ernährung, Landnutzung und Umwelt am 25.06.2009 angenommen.

TRUTH IS EVER TO BE FOUND IN SIMPLICITY,

AND NOT IN THE MULTIPLICITY AND CONFUSION OF THINGS.

- Sir Isaac Newton -

Table of Contents

Abbreviations

AC	adenylyl cyclase
ACTH	adrenocorticotropin
ATP	adenosine triphosphate
aRNA	amplified ribonucleic acid
AVP	arginine vasopressin
b.w.	body weight
BLA	basolateral amygdala
bp	basepairs
BSA	bovine serum albumin
cAMP	cyclic adenosine monophosphate
cDNA	copy DNA
CeA	central amygdala
CNS	central nervous system
CORT	corticosterone
Cp	crossing point
CRH	corticotropin-releasing hormone
CRHR	CRH receptor
CRIB	Cdc42/Rac-interaction and binding
CSF	cerebrospinal fluid
Cy3 / Cy5	cyanine 3 / cyanine 5
DAG	diacylglycerol
DEPC	diethylpyrocarbonate
DG	dentate gyrus
DMEM	Dulbecco’s modified essential medium
DMSO	dimethyl sulfoxide
DNA	deoxyribonucleic acid
dNTP	desoxyribonucleotide triphosphate
DST	dexamethasone suppression test
DTT	dithiothreitol
E. coli	*Escherichia coli*
EDTA	ethylenediaminetetraacetic acid
EGF	epidermal growth factor
ErbB	avian erythroblastic leukemia viral (v-erbB) oncogene homolog
ERK	extracellular signal-regulated kinase
EtOH	ethanol
FCS	fetal calf serum
FGF	fibroblast growth factor
GDP	guanosine diphosphate
GO	gene ontology
GPCR	G protein-coupled receptor

GR	glucocorticoid receptor
GRB2	Growth factor receptor-bound protein 2
GTP	guanosine triphosphate
HPA	hypothalamic-pituitary-adrenocortical
i.p.	intraperitonally
i.v.	intravenous
IC	intracellular loop
IP3	inositol 1,4,5-trisphosphate
ISH	*in situ* hybridization
ko	knockout
LB	lysogeny broth
LDA	linear discriminant analysis
MAPK	mitogen-activated protein kinase
MeA	medial amygdale
MR	mineralocorticoid receptor
mRNA	messenger ribonucleic acid
NHS	N-hydroxysuccinimid
NMDA	*N*-methyl-d-aspartate
NOS	nitric oxide synthase
NCBI	National Center for Biotechnology Information
o.n.	over night
OD	optical density
ONPG	ortho-nitrophenyl-β-galactoside
P/S	penicillin/streptomycin
PBS	phosphate buffered saline
PCA	principal component analysis
pCPT-cAMP	8-(4-Chlorophenylthio) adenosine 3′,5′-cyclic monophosphate
PCR	polymerase chain reaction
PDGF	plateled-derived growth factor
PFA	paraformaldehyde
PI3	phosphoinositide 3
PKA	protein kinase A
PKC	protein kinase C
PLC	phospholipase C
POMC	proopiomelanocortin
PTB	phosphotyrosine-binding
PVN	hypothalamic paraventricular nucleus
qRT-PCR	quantitative real-time polymerase chain reaction
RNA	ribonucleic acid
RT	reverse transcription
RTK	receptor tyrosine kinase

SDS	sodium dodecyl sulfate
SEM	standard error of the mean
SH3	Src-homology-3
SHH	sonic hedgehog
SNP	single-nucleotide polymorphism
SOC	super optimal broth
SSC	standard saline citrate
TAE	Tris acetate EDTA
TEA	triethanolamine
Trk	tropomyosin receptor kinase
Tris	trisaminomethane
UCN	urocortin
UTP	uridine triphosphate
UV	ultra violet
wt	wildtype
X-Gal	5-bromo-4-chloro-3-indolyl-beta-D-galactopyranoside

Please note that all units are indicated as defined by the International System of units (SI) or are SI derived units with the respective prefixes and are therefore not considered in the list of abbreviations (except for the abbreviation of basepairs).

Abstract

Dysregulation of the hypothalamic-pituitary-adrenal (HPA) axis is a hallmark of complex and multifactorial psychiatric diseases such as anxiety and mood disorders. About 50-60% of patients with major depression show HPA axis dysfunction, i.e. hyperactivity and impaired negative feedback regulation. The neuropeptide corticotropin releasing hormone (CRH) is a key regulator of this neuroendocrine stress axis. The biological actions of CRH and CRH-like neuropeptides are mediated by G protein-coupled receptors, CRH receptor type 1 and 2 (CRHR1, 2). CRHR1 is widely expressed in the mammalian brain and in the pituitary gland whereas the CRHR2 is mainly found in the periphery. Mice deficient for CRHR1 display decreased anxiety-like behaviour and dysregulation of the hypothalamic-pituitary-adrenal axis. Ligand binding increases the affinity of the CRHR to G proteins. Binding of a $G_{\alpha s}$ protein will activate adenylyl cyclase and protein kinase A as well as other cAMP dependent pathways. Coupling to other G proteins to CRHR1 suggests that multiple second messengers are involved in CRHR1-signaling. As CRHR1 is a potential novel target for the therapeutic intervention in major depressive disorder, a more precise understanding of involved intracellular signaling mechanisms is an essential prerequisite towards the development of efficient and less pleiotropic CRHR1-specific antagonists.

In order to identify specific target genes of CRHR1-mediated signaling pathways, cDNA and oligonucleotide microarray technology was applied using a mouse pituitary corticotrope cell line (At-T20), a well-established *in vitro* model for CRHR1 signal transduction, and pituitary glands of stressed mice lacking CRHR1. Applying two different bioinformatical approaches - Bayesian model-based hierarchical clustering and multivariate genetic algorithms in combination with graphical models – a robust subset of known and new CRHR1-specific target genes was obtained *in vitro*. *In vivo*, simple cut off settings resulted in more than 400 genes stress- and CRHR1-dependently regulated. A subset of candidate genes was validated in independent material by quantitative real time PCR. These candidates are involved e.g. in cAMP, mitogen activated protein kinase or epidermal growth factor receptor signaling. In order to examine their functional role the effect of these genes on different known target genes downstream of CRHR1 signaling was analyzed using reporter assays in mouse corticotrope and neuronal cell lines, respectively.

1. Introduction

1.1 Stress and the hypothalamic-pituitary-adrenal axis

The ability to cope with stress is indispensable to life for every organism. The pioneer of stress research, Hans Selye, defined stress as the non-specific response of the body to any demand for change, the so called general adaptation syndrome (Selye, 1951).

Different stressors, internal or external stimuli, activate the stress system of an organism and lead to biochemical, functional and behavioral changes. The behavioral adaption includes enhanced vigilance and cognition and an increase of analgesia and body temperature whereas vegetative functions such as appetite, sex drive and sleep are suppressed. Additional physical changes like activation of the cardiovascular system, respiration and metabolism cause a shift in the energy balance in order to produce essential biomolecules (Chrousos, 1998). The response to stress and thereby the maintenance of homeostasis are the main functions of the activated stress system to ensure survival.

The major neuroendocrine stress system is the hypothalamic-pituitary-adrenal (HPA) axis mediating the stress response of an organism at multiple levels. The main component of the HPA system is the 41-amino acid neuropeptide corticotropin-releasing hormone (CRH) which was discovered in 1981 (Vale *et al.*, 1981). CRH plays a central role in the coordination of neuroendocrine, autonomic, immune and behavioral responses to stress (Vale *et al.*, 1983). In response to physical or psychological stress, increased amounts of CRH are released from the hypothalamic paraventricular nucleus (PVN) into the median eminence which subsequently reach the adenohypophysis and activate the corticotropin-releasing hormone receptor type 1 (CRHR1). The activation of CRHR1-dependent signaling cascades stimulates the synthesis of proopiomelanocortin (POMC), the precursor of the adrenocorticotropic homone (ACTH), and β-endorphine. Arginine vasopressin (AVP) has been shown to act synergistically with CRH to augment the release of ACTH, suggesting that AVP may also play a physiological role in modulating the ACTH response mediated by CRH (DeBold *et al.*, 1984).

ACTH is released into the circulation and in turn, glucocorticoids are synthesized in the adrenal cortex, mainly cortisol in humans and corticosterone in rodents, and secreted into the bloodstream. Glucocorticoids mediate a variety of physiological and metabolic reactions. They are involved in emotional and cognitive processes and modulate fear and anxiety-related behavior (DeKloet, 2004; Herman et al., 2003; Sapolsky et al., 2000; Tronche et al., 1999). Glucocorticoid levels in the blood are strictly regulated by an endocrine negative feedback mechanism acting at the pituitary and other brain regions to decrease the secretion of ACTH and CRH, respectively (Fig. 1).

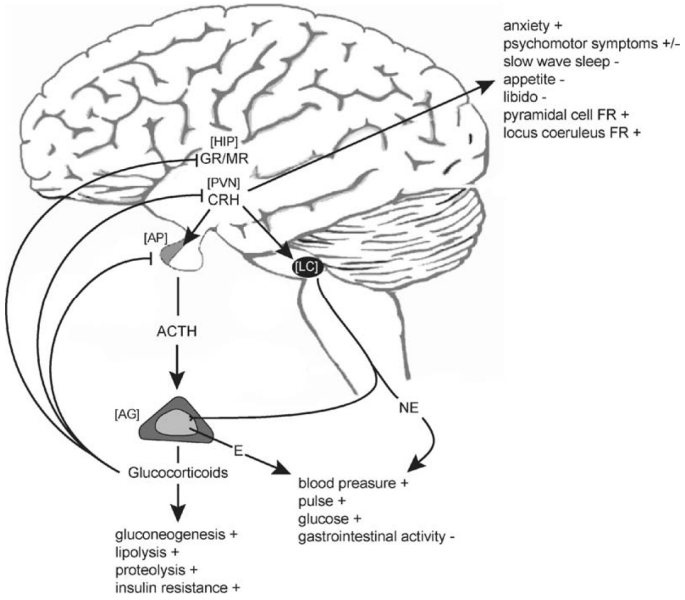

Figure 1. CRH-mediated endocrine, autonomic and behavioral responses to stress (Deussing and Wurst, 2005). AG, adrenal gland; ACTH, adrenocorticotropic hormone; AP, anterior pituitary; CRH, corticotropin-releasing hormone; E, epinephrine; FR, firing rate; GR, glucocorticoid receptor; HIP, hippocampus; LC, locus coeruleus; MR, mineralocorticoid receptor; NE, norepinephrine; PVN, hypothalamic paraventricular nucleus.

In addition, CRH acts as neuromodulator regulating neuronal activity. Whereas the hypothalamic CRH system modulates endocrine and metabolic responses to stress, extrahypothalamic regions such as the central nucleus of the amygdala, the bed nucleus of the stria terminalis, the hippocampus, the nucleus accumbens and the cerebellum mediate the behavioral adaptation to stress (DeSouza, 1985; Koob, 1999). CRH has been shown to modulate various behavioral attributes in rodents including learning and memory, food intake, anxiety, arousal, startle and fear responses, general motor activity and sexual behavior (Bale et al., 2000; Hauger et al., 2006; Radulovic et al., 1999).

1.2 Dysregulation of the HPA axis and psychiatric disorders

Persistent enhancement of stress reactivity leads to dysregulation of the HPA axis. As soon as the feedback inhibition is disrupted, hyper- or hypoactivation of the stress adaptation system resulting from increased CRH levels occur. Genetic abnormalities, exposure to stress in early life or to traumatic events can increase the individual´s sensitivity to stress (Hauger *et al.*, 2006). Chronically increased CRH concentrations lead to elevated ACTH and glucocorticoid blood levels. Moreover, the ability of circulating glucocorticoids to exert their effect on negative feedback through binding to mineralocorticoid (MR) and glucocorticid (GR) receptors is impaired and thus, causes hypercortisolemia (Gold *et al.*, 1988; Nemeroff, 1996). In contrast, hypoactivation of the stress system with chronically reduced secretion of CRH may result in pathological hypoarousal and an enhanced HPA negative feedback (Juruena *et al.*, 2004).

As the CRH-HPA system controls behavioral, neuroendocrine and autonomic adaptation to stress, disturbances of this system play an important role in the pathophysiology of

various disorders (Table 1). Increased and prolonged activation of the HPA axis is associated with e.g. melancholic depression, anorexia nervosa, obsessive-compulsive disorder, panic, anxiety and alcoholism, whereas hypoactivation of the stress system contributes to post-traumatic stress disorder, atypical or seasonal depression and the chronic fatigue syndrome (Tsigos and Chrousos, 2002).

Table 1. Disorders associated with disturbed HPA axis activity (Tsigos and Chrousos, 2002)

Increased HPA axis activity	Decreased HPA axis activity	Disrupted HPA axis activity
Severe chronic disease		
Melancholic depression	Atypical depression	Cushing syndrome
Anorexia nervosa	Seasonal depression	Glucocorticoid deficiency
Obsessive–compulsive disorder	Chronic fatigue syndrome	Glucocorticoid resistance
	Fibromyalgia	
Panic disorder	Hypothyroidism	
Chronic excessive exercise	Adrenal suppression	
Malnutrition	Post glucocorticoid therapy	
Diabetes mellitus	Post stress	
	Nicotine withdrawal	
	Postpartum	
Hyperthyroidism	Menopause	
Central obesity	Rheumatoid arthritis	
Childhood sexual abuse		
Pregnancy		

The overall lifetime-prevalence in industrialized countries for anxiety disorders is above 25% and depression and anxiety rank among the most prevalent and costly diseases. According to the estimations of the World Health Organization, depression will be the second leading cause of disability in 2020. Recent epidemiological studies indicate that severe forms of depression affect 2-5% of the population worldwide, and up to 20% are afflicted by milder forms of the disease (Kessler *et al.*, 2003). Moreover, depressive patients have a 2-4 fold increased risk of developing cardiovascular diseases and 10-15% of individuals with major depression commit suicide (Keck, 2006).

Many clinical signs and symptoms characteristic for depression and anxiety disorders as sleep disturbance, loss of libido, psychomotor and autonomic changes as well as decreased appetite are associated with unrestrained CRH secretion. Depressed patients display elevated levels of CRH in the cerebrospinal fluid (CSF) (Nemeroff *et al.*, 1984) and increased secretion of ACTH and cortisol into the blood (Holsboer, 2000). CRH expression in the hypothalamic PVN is increased (Raadsheer *et al.*, 1994) while CRH

binding to receptors in the prefrontal cortex of depressed patients who committed suicide is diminished, indicating an adaptive downregulation in response to CRH hypersecretion (Nemeroff, 1988). Additionally, in the standard dexamethasone suppression test (DST) patients with various affective disorders have elevated cortisol levels, indicating an alleviated suppressive effect of dexamethasone (Carroll, 1982) and thus, an impaired negative feedback mechanism through GR. Finally, direct application of CRH into the central nervous system (CNS) as well as overexpression of CRH in transgenic mice result in phenotypic depression-like symptoms observed similarly in patients with major depression (Deussing and Wurst, 2005; Dunn and Berridge, 1990).

1.3 CRH-like peptides and their receptors

Besides CRH as regulator of the HPA axis the mammalian CRH family comprises three distinct CRH-like peptides: urocortin (UCN), urocortin 2 (UCN2) and urocortin 3 (UCN3) (Hsu and Hsueh, 2001; Vaughan et al., 1995). Two receptors, CRHR1 and CRHR2, and the CRH-binding protein (CRH-BP) have been identified and characterized (Dautzenberg and Hauger, 2002; Hauger *et al.*, 2003). Ligands and receptors differ in their tissue distribution and pharmacology.

In the mammalian CNS, CRH-expressing neurons are widely distributed. CRH, the key stimulator of the stress response, is present in the central nervous system in the PVN, central nucleus of the amygdala and hindbrain regions as well as in the periphery in the gut, skin and adrenal gland (Bale and Vale, 2004; Swanson et al., 1983). UCN is mainly expressed in cell bodies of the Edinger Westphal nucleus in the brain. UCN2, also known as stresscopin-related peptide, is found in the hypothalamus, brainstem and spinal cord. Expression of UCN3, known as stresscopin, occurs in the hypothalamus and in the amygdala in the CNS (Fig. 2A). As CRH also UCN, UCN2, and UCN3 are present in the periphery in different tissues. Both CRH and UCN have high affinities for the CRH-binding protein (CRH-BP) whereas neither UCN2 nor UCN3 bind to this protein (Dautzenberg and Hauger, 2002).

CRHR1 is mainly expressed in the pituitary and brain regions like cerebral cortex, sensory relay nuclei and in the cerebellum, whereas CRHR2 expression is limited to some peripheral organs and to specific brain areas like the olfactory bulb, lateral septum, medial amygdala, dorsal and median raphe as well as hypothalamus (Chalmers *et al.*, 1995; Van Pett *et al.*, 2000) (Fig. 2B).

The CRH-BP, a 37 kDa N-linked glycoprotein, is expressed in the brain and the pituitary (Potter *et al.*, 1992). CRH-BP is present in the liver and in the bloodstream, where it binds CRH as dimer and probably inactivates CRH to prevent inappropriate stimulation (Lowry *et al.*, 1996).

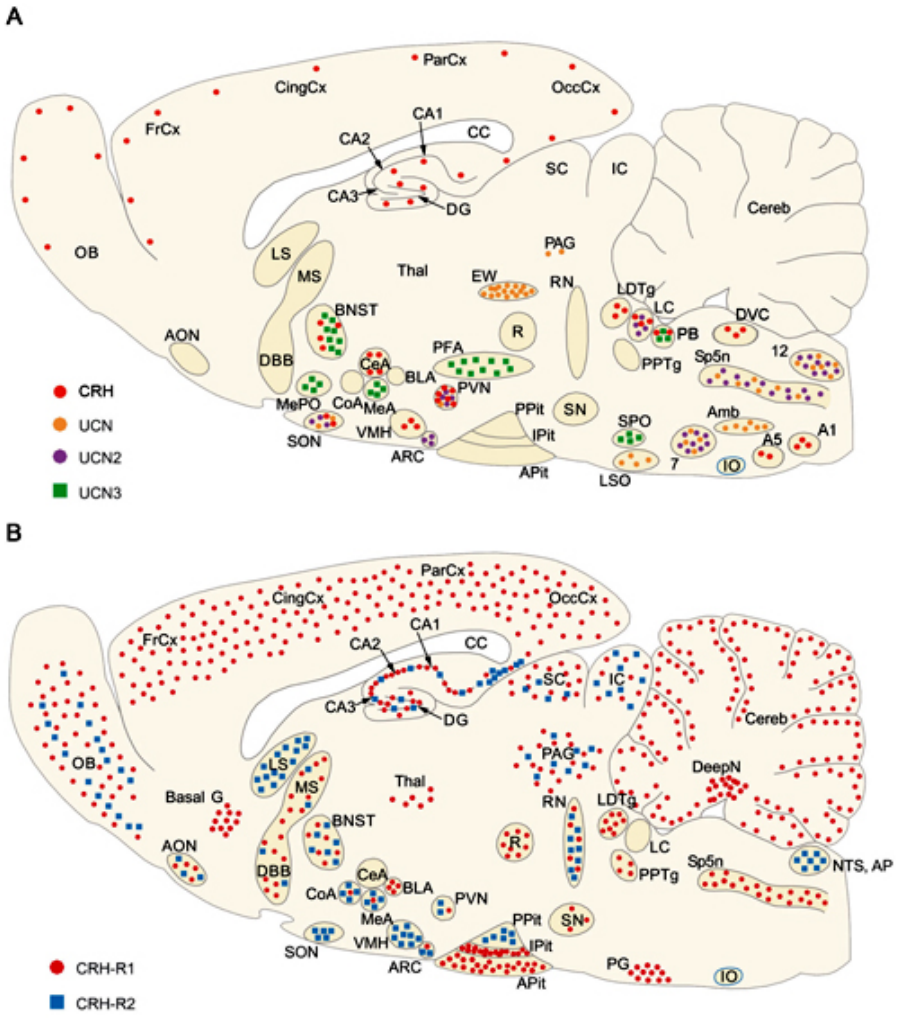

Figure 2. Expression of (A) CRH-related peptides and (B) cognate receptors CRHR1 and CRHR2 in the rodent brain (Reul and Holsboer, 2002). 7, facial nucleus; 12, hypoglossal nucleus; Amb, ambiguous nucleus; AON, anterior olfactory nucleus; AP, area postrema; Apit, anterior pituitary; ARC, arcuate nucleus; Basal G, basal ganglia; BLA, basolateral amygdala; BNST, bed nucleus of the stria terminalis; CA1-3, fields CA1-3 of Ammon's horn, CC, corpus callosum; CeA, central nucleus of the amygdala; Cereb, cerebellum; CingCx, cingulate cortex; CoA, cortical nucleus of the amygdala; DBB, diagonal band of Broca; Deep N, deep nuclei; DG, dentate gyrus; FrCx, frontal cortex; IC, inferior colliculi; IO, inferior olive; IPit, intermediate pituitary; LC, locus coeruleus; LDTg, laterodorsal tegmental nucleus; LSO, lateral superior olive; MeA, medial nucleus of the amygdala; MePO, median preoptic area; MS, medial septum; NTS, nucleus tractus solitarii; OB, olfactory bulb; OccCx, occipital cortex; PAG, periaquaductal gray; ParCx, parietal cortex; PFA, perifornical area; PG, pontine gray, PPit, posterior pituitary; PPTg, pedunculopontine tegmental nucleus; PVN, hypothalamic paraventricular nucleus; R, red nucleus; RN, raphe nuclei; SC, superior colliculi; SN, substantia nigra; SON, supraoptic nucleus; Sp5n, spinal trigeminus nucleus; SPO, superior paraolivary nucleus; Thal, thalamus

CRHRs belong to the class B1 group of G protein-coupled seven transmembrane receptors (GPCRs). CRHR1 and CRHR2 are encoded by two distinct genes, but share more than 70% homology on the amino acid level (Hauger and Dautzenberg, 1999). Importantly, the intracellular loop (IC) 3, the putative G protein-coupling site, is 100% conserved in all CRH receptors discovered to date (Dautzenberg and Hauger, 2002; Hauger *et al.*, 2003).

However, both receptors have various splice variants. Eight splice variants are known for CRHR1, isoform α, β, and c-h. Several of these isoforms have been shown to be nonfunctional (Grammatopoulos and Chrousos, 2002). CRHR2 appears in three functional isoforms, α, β, and γ, whereas the γ isoform has only been detected in humans (Dautzenberg and Hauger, 2002).

CRH has a tenfold higher affinity for CRHR1 than for CRHR2. UCN has equal affinities for both receptors (Perrin *et al.*, 1995), whereas UCN2 and UCN3 appear to be selective for CRHR2, although UCN2 may activate CRHR1 at higher concentrations (Lewis *et al.*, 2001) (Fig. 3).

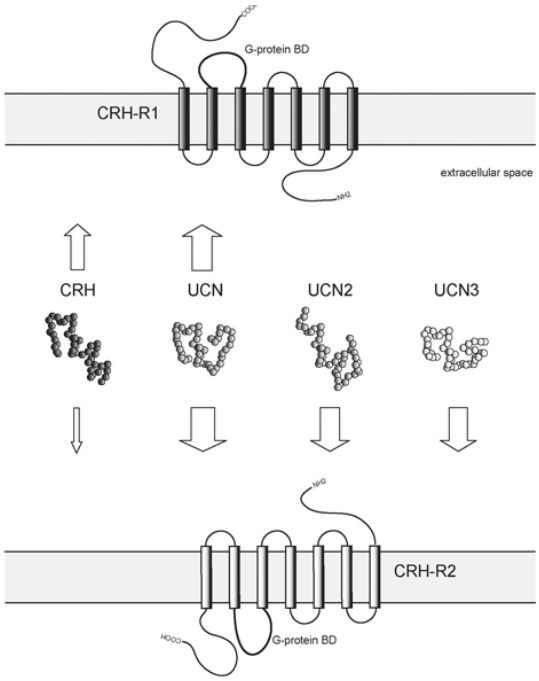

Figure 3. Mammalian family members of CRH-related neuropeptides and their receptors. Arrows represent ligand-receptor interactions. The thickness of arrows reflects relative binding affinities (Deussing and Wurst, 2005). CRH, corticotropin releasing hormone; UCN, urocortin; UCN2, urocortin 2; UCN3, urocortin 3; CRH-R1, CRH receptor 1; CRH-R2, CRH receptor 2.

1.4 G protein-coupled receptor-dependent signaling cascades

Upon activation, GPCRs interact with their cognate G proteins. G proteins are heterotrimers localized at the inner surface of the plasma membrane. The three subunits, G_α, G_β and G_γ, communicate their signals either by the G_α subunit or the $G_{\beta\gamma}$ complex. Currently, there are 20 known G_α, 6 G_β, and 11 G_γ subunits. On the basis of sequence similarity, the G_α subunits have been divided into four families: $G_{\alpha s}$, $G_{\alpha i}$, $G_{\alpha q}$ and $G_{\alpha 12/13}$.

These G_{α} subunits regulate the activity of several second messenger-generating systems. In the inactive state, G_{α} carries guanosine diphosphate (GDP) in its binding site. When a ligand binds to the associated GPCR, a conformational change occurs which triggers an allosteric change in G_{α} causing GDP to leave and be replaced by guanosine triphosphate (GTP). GTP activates G_{α} causing its dissociation from $G_{\beta\gamma}$ subunits. The dissociated G_{α} and $G_{\beta\gamma}$ subunits interact with a variety of effector molecules including adenylyl cyclase (AC), phospholipase C (PLC) isoforms and ion channels (Pierce *et al.*, 2002).

The interactions of $G_{\alpha s}$ and $G_{\alpha i}$ with AC respectively stimulate or decrease the production of cyclic adenosine monophosphate (cAMP) and thereby regulate the activation of protein kinase A (PKA). Activation of PLC by $G_{\alpha q}$ promotes the formation of inositol (1,4,5)-triphosphate (IP3) and diacylglycerol (DAG), leading to elevation of intracellular Ca^{2+} levels and activation of protein kinase C (PKC) isoforms. The $G_{\beta\gamma}$ subunit of G proteins directly couples to at least four effector molecules: PLCβ, K^{+}-channels, AC and PI3-kinase. Additionally, $G_{\alpha s}$, $G_{\alpha i}$ and $G_{\beta\gamma}$ subunits were found to be sufficient to stimulate or inhibit mitogen-activated protein kinase (MAPK) pathways including members of the kinase families such as RAP, RAF, MEK and extracellular signal-regulated kinases (ERK) (Gutkind, 1998; Lefkowitz *et al.*, 2002; Luttrell, 2002). Moreover, β-arrestins, which are known to terminate G protein activation by desensitization and internalization of phosphorylated GPCRs, have been shown to function as GPCR signal transducers by linking GPCR signaling to MAPKs cascades (Luttrell and Lefkowitz, 2002).

CRHR1 and CRHR2 are class B G protein-coupled receptors that are capable to activate different G proteins and signaling cascades upon ligand-binding. The dominant CRHR signaling pathway in endogenous and recombinant cell lines is the activation of the AC-PKA pathway via $G_{\alpha s}$ (Aguilera *et al.*, 1983; Olianas *et al.*, 1995). But in dependency of species, tissue and cell type, both receptors are known to activate $G_{\alpha q}$/ PLC-, AKT/PI3-kinase-, NOS/guanylyl cyclase-, caspase pro apoptotic- and NFκB or NURR1/NUR77 transcription factor signaling pathways (Fig. 4) (Hauger *et al.*, 2006).

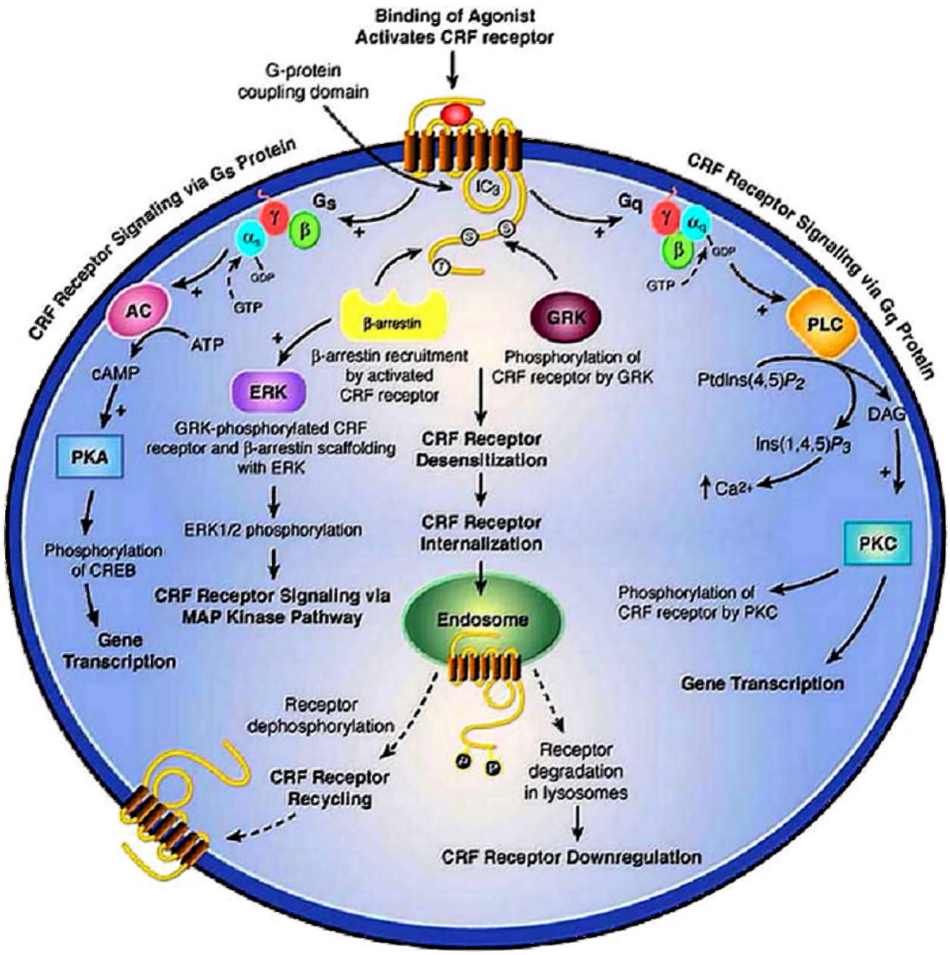

Figure 4. Major intracellular pathways for signal transduction by CRHR1 and CRHR2 (Hauger *et al.*, 2006)

To investigate the molecular mechanisms of CRH signaling, corticotrope AtT-20 cells were analyzed in culture. As *in vivo* in the pituitary gland, CRH has major effects on the AtT-20 cell line through the CRHR1 (Iredale and Duman, 1997; Rosendale et al., 1987). Kovalovsky and colleagues described proopiomelanocortin (POMC) induction by CRH in AtT-20 cells via NUR transcription factors (Fig 5.). Thereby, PKA activation triggers on the one hand a Ca^{2+}-dependent signaling pathway via CAMKII which increases Nur77 and Nurr1 transcription, on the other hand PKA activates a MAP kinase pathway including RAP1, B-RAF, MEK1 and ERK1/2 resulting in NUR77 phosphorylation/transactivation and Pomc transcription (Kovalovsky *et al.*, 2002). Recently, it was shown that sonic hedgehog (SHH), a morphogen involved in development, and components of its signal transduction pathway are expressed in AtT-20 cells. Crosstalk mechanisms between the signaling pathways of CRH and SHH play a functional role in the regulation of Pomc transcription and CRHR1 expression (Vila *et al.*, 2005).

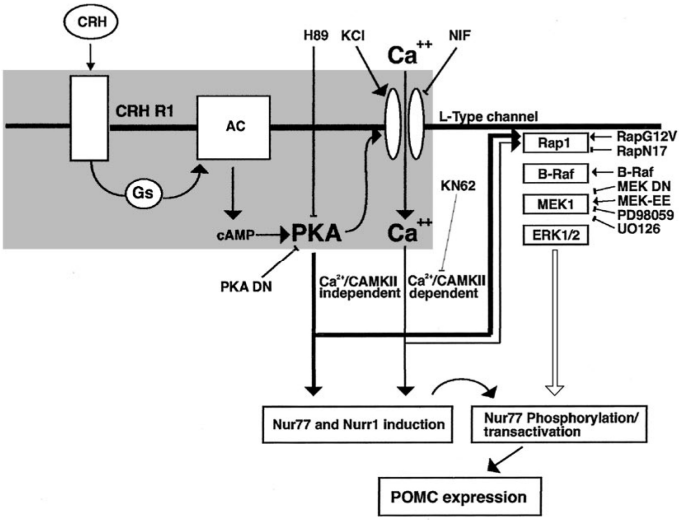

Figure 5. Pathways involved in CRH and cAMP induction and activation of NUR factors and Pomc expression in AtT-20 cells (Kovalovsky *et al.*, 2002).

1.5 Animal models of anxiety and depression based on the CRH system

To analyze effects of a gene of interest on behavior, cognition and physiology as well as therapeutic consequences of pharmacological treatments, genetically engineered mice are an important tool in psychiatric research (Bucan and Abel, 2002; Seong *et al.*, 2002). According to McKinney and Bunny, a valid animal model of depression should first be reasonably analogous to the human disorder in its symptomatology (face validity); second it should cause behavioral changes that can be monitored objectively. Moreover such an animal model should produce behavioral changes that are reversed by the same treatment modalities that are effective in humans (predictive validity) and it should be reproducible between different investigators (McKinney and Bunney, 1969). In face of the variety of different mouse models that have been established to understand the pathophysiology of psychiatric diseases, it remains difficult to mimic the complexity of such a disorder. Therefore, animal models with only certain sub-features of a disease, so called endophenotypes, are used to analyze parts of a complex disease (Hasler *et al.*, 2004).

The HPA axis and in particular the central CRH/CRH receptor system as key regulator of the manifold stress responses, probably provide the most reasonable basis for the development of genetic mouse models for depression (de Kloet et al., 2005; Deussing, 2006; Grigoriadis, 2005; Hillhouse and Grammatopoulos, 2006; Todorovic et al., 2005).

Several mouse models related to the HPA system have already been generated. Two whole animal CRHR1-knock out (ko) mouse lines, created by Smith *et al.* and Timpl *et al.*,

showed decreased anxiety-related behavior but no alterations in depression-like behavior (Smith *et al.*, 1998; Timpl *et al.*, 1998).

A conditional CRHR1-ko mouse line in which CRHR1 function is specifically inactivated in CamKIIa-expressing forebrain cells but not in the pituitary displayed reduced anxiety with normal basal HPA system activity (Muller *et al.*, 2003). Moreover, inhibition of CRHR1 expression by central administration of antisense oligonucleotides or specific antagonists exhibited anxiolytic effects (Deak et al., 1999; Liebsch et al., 1999; Lundkvist et al., 1996; Skutella et al., 1998).

Until now, three different CRHR2-ko mouse lines have been developed but contradictory and inconclusive results have been obtained (Bale *et al.*, 2000; Coste *et al.*, 2000; Kishimoto *et al.*, 2000). Whereas Bale *et al.* and Kishimoto *et al.* detected increased anxiety-like behavior revealing an anxiolytic role for CRHR2, Coste *et al.* found no differences in CRHR2-ko mice. CRHR2 deletion did not cause changes in basal ACTH and corticosterone levels but enhanced HPA activity under stressful stimuli suggesting an important role for CRHR2 in regulating HPA axis homeostasis by probably counterbalancing CRHR1-mediated effects on the endocrine stress system.

Different transgenic CRH overexpressing mouse lines displayed a Cushing´s syndrome-like phenotype including elevated ACTH and corticosterone levels, enhanced anxiety-like behavior and learning deficits (Heinrichs et al., 1996; Stenzel-Poore et al., 1994; van Gaalen et al., 2002). Spatially restricted CRH overexpression in the entire central nervous system, but not when overexpressed in specific forebrain regions, resulted in stress-induced hypersecretion of stress hormones and increased active stress-coping behavior (Lu *et al.*, 2008).

Overall, studies with transgenic and knockout mouse models including mice overexpressing CRH-BP, CRH-BP-ko mice as well as CRHR1/2 double-ko mice have confirmed the impact of the CRH/CRHR system in HPA axis stress response (Bale and Vale, 2004; Deussing and Wurst, 2005).

1.6 CRHR1 antagonists as novel class of antidepressants

For more than 30 years treatment of depressive-like disorders is based on three different groups of antidepressants. (i) Tricyclic antidepressants block non-selectively the reuptake of serotonin and/or norepinephrine from the synaptic cleft by inhibition of the corresponding transporter systems. (ii) Selective reuptake inhibitors for serotonin or noradrenaline (SSRIs or SNRIs, respectively) influence mainly one neurotransmitter system reducing side effects produced by non-selective modulation of other neurotransmitter systems as it is the case for tricyclic antidepressants. (iii) Monoamino oxidase inhibitors (MAOs) restrain the activity of the enzyme monoamino oxidase which

catalyzes the degradation of neurotransmitters. All drug classes lead to an increased neurotransmitter (serotonin, nordadrenalin and dopamine, respectively) concentration in the synaptic cleft (Nestler *et al.*, 2002). The effect on the biochemical level occurs rapidly, whereas, in a patient, the approvement of symptoms needs weeks to appear. Overall, the mechanisms how antidepressants act are not fully understood. Thus, the development of improved antidepressants based on other biochemical mechanism is in the focus of current research.

Because of the involvement of the CRH system in anxiety- and depression-like disorders, the CRHR1 is a target of recent drug research. The first tested compounds were peptidergic CRH antagonists which were all poorly selective for CRHR1 but interfered with CRH/CRHR1-dependent signaling. Several studies have shown that α-helical CRH-(9-41), D-Phe-CRH-(12-41) and astressin are able to blunt stress-induced alterations on intracellular signaling level and on behavior as well as autonomic activity in rodents (Brauns et al., 2001; Britton et al., 1986; Chen et al., 1993; Kalin et al., 1988; Korte et al., 1994; Sajdyk and Gehlert, 2000). Various non-peptidergic, more selective CRHR1 antagonists, most of them based on the structure of pyrrolopyrimidine, were synthesized in the last years. In signaling and behavioral experiments small molecules such as CP 154,526, NBI 27914 and antalarmin inhibit CRH-dependent stimulation of cAMP and ACTH release and show anxiolytic effects (Deak et al., 1999; McCarthy et al., 1999; Schulz et al., 1996). The development of a very promissing non-peptidergic CRHR1 antagonists, R121919, had to be stopped because of liver toxicity (Zobel *et al.*, 2000). Another CRHR1 antagonist, NBI-34041, displayed reduced hormonal stress response in animals and humans without ablating the ability of the organism to respond appropriately to stressors with an HPA axis response, properties of an ideal drug candidate. (Holsboer and Ising, 2008; Ising et al., 2007).

1.7 Microarray technology

1.7.1 The role of the transcriptome

Phenotypes are created by networks including transcriptional regulation, signaling pathways, protein-protein and protein-nucleic acid interactions. Trancriptional changes affect molecular actions and control the dynamics of cells such as survival, apoptosis, growth, differentiation and signal transduction. Global transcriptional response, and not single genes, is nowadays expected to constitute biological phenotypes. Although protein levels are often regulated without underlying transcript changes, transcript changes usually result in protein changes.

One method to examine transcriptional changes is the high-throughput technology of microarrays. Microarrays consist of tenthousands of nucleotide probes – either cDNA

clones or oligonucleotides – attached to a solid surface. By hybridization of the array with cDNA samples of interest, probe-target hybridization of complementary nucleotides is detected and quantified by fluorescence-based detection of fluorophore-labeled targets to determine relative abundance of nucleic acid sequences in the target. Thereby, the whole transcriptome is analyzed in a genome-wide assay. Genes which are associated with biological processes such as genotypes of transgenic mice, single-nucleotide polymorphisms (SNPs) or stimulus-dependent changes can be screened at the same time. In clinical research, expression profiling is used to discover patterns of expression that classify disease phenotypes, genetic vulnerability, drug responsiveness or molecular targets.

1.7.2 Microarray technology

The first microarray was developed in 1994 using plasmid DNA immobilized on a membrane. As target radioactive-labeled cDNA samples were hybridized to the membrane (Chalifour *et al.*, 1994). During the last decade, a variety of technologies for microarray fabrication was developed. For spotted microarrays, probes are synthesized prior to deposition on the array surface and are then spotted onto glass slides (Schena *et al.*, 1995). Probes are oligonucleotides, cDNAs or small fragments of PCR products that correspond to mRNAs. The MPIP 24 k chip, developed at the Max-Planck-Insitute of Psychiatry in Munich, Germany, e.g. consists of 24192 PCR products derived from different mouse cDNA libraries (sources: Research Genetics, RZPD Deutsches Ressourcenzentrum für Genomforschung, proprietary clones) representing 12387 different unigene clusters (unigene build #143) (Deussing *et al.*, 2007). Optimized protocols for RNA amplification, labeling, hybridization, data acquisition and statistical analysis are established and reproducible. The technology performed by Illumina couples 50-mer oligonucleotides to beads which are then etched into the surface of a slide-sized silicon substrate. Oligonucleotide arrays are produced by printing short oligonucleotide sequences designed to represent a single gene or a family of gene splice variants by synthesizing this sequence directly onto the array surface instead of depositing intact sequences (Lockhart *et al.*, 1996). This technique is e.g. used by Agilent® and Affymetrix®. The advantage of using synthesized oligonucleotides is the possibility to detect not only whole transcripts but also to differentiate between splice variants. Moreover, the synthesis of short oligonucleotides eliminates the necessity of preparing and handling clones, PCR products and cDNAs.

In addition to the different techniques of array fabrication, microarrays differ in the demanded experimental design. Aside from RNA amplification and hybridization protocols, one main difference is the color labeling of the target. In two-color experiments,

target RNA and control RNA are labeled with two different types of fluorophores (e.g. Cy3 and Cy5), mixed and hybridized on the same array. Direct comparison of target and control sample reduces variability and increases sensitivity and accuracy (Patterson *et al.*, 2006). To mitigate dye-specific biases, dye-reversed replicates are performed (dye-swap). The advantage of one-color microarrays is the simple and flexible experimental design. All samples are labeled with one fluorescent dye and are hybridized on different arrays. In the data analysis, different arrays and samples are compared. Therefore, no previous combination of RNA pairs is required. To avoid data inconsistency caused by variability in microarray fabrication and processing, sufficient biological and technical replicates have to be evaluated.

For data analysis a variety of statistical methods are available. Data analysis normally includes preprocessing (image processing, normalization), inferential statistics (fold change, shrinkage, false-disvovery rate) and classification (supervised, unsupervised) (Allison et al., 2006; Hastie et al., 2001b). Many algorithms have been developed in the last years to define e.g. co-regulated gene networks or to predict gene-gene interactions.

One limitation of the microarray technology is the difficulty to reproduce data across laboratories and platforms. For reliable data production it is very important to control all experimental conditions in the same way (Barnes *et al.*, 2005; Shi *et al.*, 2006). Another limitation of microarrays is the sensitivity. Genes with low expression levels (low-abundant genes) are hardly detected. Moreover, posttranslational modifications are not measured by these genome-wide assays (Bunney *et al.*, 2003). Another disadvantage of this technology is that many, technical and biological, replicates are required to get reliable data which amplifies the experimental costs.

Data revealed by microarray technology present a good basis for further experiments. But validation of expression profiling results is required. Independent methods such as *in situ* hybridization, Northern blot and quantitative real-time PCR (qRT-PCR) are used for confirmation of microarray results. Nevertheless, microarrays provide the unique opportunity to analyze the whole transcriptome at once and help to increase our understanding of molecular mechanisms involved in biological phenotypes.

1.7.3 Microarrays in psychiatric research

Psychiatric disorders such as anxiety and depression are multifactoral diseases not caused by a single gene abnormality but by a set of abnormal genes. Fundamental understanding of genes that increase the risk for those disorders is missing. Moreover, limited progress has been made to identify new, unique drug targets or diagnostic markers. The high-throughput analysis of the whole transcriptome using microarray

technology offers the opportunity to discover candidate genes and pathways associated with psychiatric disorders.

Comparison of the transcriptome of mouse models for anxiety and depression and antidepressant treatment, revealed new classes of genes involved in the corresponding phenotype: Using microarray and proteomic analyses, glyoxalase-I was identified as biomarker for anxiety-related behaviour (Kromer *et al.*, 2005). Comparing the brains of CRHR1-wt and -ko mice identifies the CRH-system as modulator of neurovascular gene activity (Deussing *et al.*, 2007). Genes involved in glucocorticoid signaling, myelination, cell proliferation and extracellular matrix formation were obtained by expression profiling of different brain areas of CRH-overexpressing mice which showed that lifelong exposure to excessive CRH leads to adaptive changes in the brain (Peeters *et al.*, 2004a).

Expression analysis of e.g. AtT-20 cells stimulated with leukemia inhibitor factor or CRH revealed new target genes involved in the regulation of POMC transcription (Abbud *et al.*, 2004; Peeters *et al.*, 2004b). Moreover, changes in the expression profile of hippocampi of stressed mice suggest novel stress-elicited pathways including genes involved in neuronal plasticity (Tsolakidou *et al.*, 2008).

The use of genome and transcriptome analysis in appropriate *in vitro* and *in vivo* models with microarrays will help to understand the genetic networks behind complex psychiatric disorders.

2. Objective of this study

The aim of this study was to identify new target genes regulated by CRH/CRHR-dependent signaling cascades which are potentially capaple of regulating CRH/CRHR1-mediated signaling. CRHR1 as key molecule orchestrating the neuroendocrine and behavioral responses to stress has attracted major interest as a potential novel target for the therapeutic intervention in major depressive disorder (Holsboer and Ising, 2008; Ising and Holsboer, 2006; Ising et al., 2007; Zobel et al., 2000). However, CRH/CRHR1-dependent signal transduction mechanisms are only partially understood. Therefore, a more precise understanding of involved intracellular signaling mechanisms is an essential prerequisite towards the development of efficient and less pleitropic CRHR1-specific antagonists (Arzt and Holsboer, 2006).

The aim of this work was to dissect the stress- and CRH-dependent alterations of CRHR1-mediated signal transduction pathways *in vitro* and *in vivo*. As *in vitro* model system the mouse pituitary corticotrope cell line AtT-20 was cused. *In vivo*, the stress response of conventional CRHR1-wildtype (wt) and -ko mice was activated by restraint stress. CRHR1-mediated changes on mRNA transcription were investigated *in vitro* as well as *in vivo* using the high-through put technology of microarrays.

Based on the transcriptome analyses *in vitro* and *in vivo* the following questions were investigated using different bioinformatical and biomolecular methods:

a) What classes of genes are regulated by CRH/stress via CRHR1? Are there differences of gene regulation in a time-dependent manner?

b) Are there common signal transduction mechanisms *in vitro* and *in vivo*?

c) Are the new candidate genes themselves regulating CRHR1-mediated signaling mechanisms?

d) Are there common CRHR1-dependent signaling pathways in corticotrope and neuronal cells?

e) Is there a crosstalk of CRH/CRHR1-dependent signaling and receptor tyrosine kinase-regulated signaling mechanisms (in particular ErbB receptor signaling)?

3. Material and Methods

3.1 Material

3.1.1 Buffers and solutions

3.1.1.1 Buffers for electrophoresis

1 x TRIS acetate EDTA (TAE) buffer

4.84 g	tris(hydroxylmethyl)-aminomethane (TRIS, Sigma-Aldrich, Munich, Germany)
1.142 ml	acetic acid (Karl Roth, Karlsruhe, Germany)
20 ml 0.5 M	ethylendiaminetetraacetate (EDTA, Sigma-Aldrich), pH 8.0
800 ml	H_2O_{bidest}

adjust pH to 8.3 with acetic acid

adjust volume to 1 liter with H_2O_{bidest}

6 x DNA loading buffer (orange)

1 g	orange G (Sigma-Aldrich)
10 ml	2 M TRIS/HCl, pH 7.5
150 ml	glycerol

adjust volume to 1 liter with H_2O_{bidest}

3.1.1.2 Metyrapone

for 150 mg/kg bodyweight (b.w.)

40%	propyleneglycol (Sigma-Aldrich)
60%	0.9% saline
37.5 mg/ml	metyrapone (Sigma-Aldrich)

for 100 mg/kg b.w.

40%	propyleneglycol
60%	0.9% saline
25 mg/ml	metyrapone

3.1.1.3 Microarray

20 x standard saline citrate (SSC)

3 M	NaCl (Karl Roth)
300 mM	sodium citrate (Sigma-Aldrich)

pH 7.4

ad. H_2O_{bidest}, add 1 ml diethylpyrocarbonate (DEPC)/liter

incubate over night (o.n.), 2 x autoclave

pre-hybridization buffer

50 %	formamide (Karl Roth)
5x	SSC
0.1 %	sodium dodecyl sulfate (SDS) (Sigma-Aldrich)
0.1 mg/ml	bovine serum albumin (BSA) (Sigma-Aldrich)

hybridization buffer

50 %	formamide
5x	SSC
0.1 %	SDS
0.1 mg/ml	murine Cot1-DNA (Invitrogen, Karlsruhe, Germany)

3.1.1.4 Solutions for *in situ* hybridization (ISH)

H_2O-DEPC

2 ml DEPC (Sigma-Aldrich)

ad. 2l H_2O_{bidest}

2 x autoclave

10 x phosphate buffered saline (PBS)

1.37 M	NaCl
27 mM	KCl (Karl Roth)
200 mM	Na_2HPO_4 x 12 H_2O (Merck, Darmstadt, Germany)
20 mM	KH_2PO_4 (Merck)

pH 7.4

ad. H_2O_{bidest}, add 1 ml DEPC/liter

incubate o.n., 2 x autoclave

20% paraformaldehyde (PFA)

20% w/v paraformaldehyde (Sigma-Aldrich)

in 1x PBS-DEPC

pH 7.4

10 x triethanolamine (TEA)

1 M TEA (Sigma-Aldrich)

pH 8.0

ad. H_2O_{bidest}, add 1 ml DEPC/liter

incubate o.n., 2 x autoclave

hybridization-mix (hybmix)

50 ml	formamide
1 ml	2 M TRIS/HCl, pH 8.0
1.775 g	NaCl
1 ml	0.5 M EDTA, pH 8.0
10 g	dextran sulphate (Sigma-Aldrich)
0.02 g	ficoll 400 (Sigma-Aldrich)
0.02 g	polyvinylpyrrolidone 40 (PVP40, Sigma-Aldrich)
0.02 g	BSA (Sigma-Aldrich)
5 ml	tRNA (10 mg/ml, Roche Diagnostics GmbH, Mannheim, Germany)
1 ml	carrier DNA (salmon sperm, 10 mg/ml, Sigma-Aldrich)
4 ml	5 M dithiothreitol (DTT, Roche)

store as 1 to 5 ml aliquots at - 80°C

hybridization chamber fluid

250 ml	formamide
50 ml	20 x SSC
200 ml	H_2O_{bidest}

5 M DTT/DEPC

7.715 g	DTT
4 ml	H_2O-DEPC

shake the falcon tube until the powder is nearly solved

adjust volume to 10 ml with H_2O-DEPC

5 x NTE

146.1 g	NaCl
50 ml	1 M TRIS/HCl, pH 8.0
50 ml	0.5 M EDTA, pH 8.0

adjust volume to 1 liter with H_2O_{bidest}, add 1 ml DEPC

incubate o.n., autoclave

3 M NH_4OAc

3 M	NH_4OAc (Sigma)

ad. H_2O_{bidest}

autoclave

alcohol(denat.)-solutions

Alcohol conc.	Vol. of EtOH 100% / ml	Vol. of 3M NH_4OAc / ml	Vol. of H_2O_{bidest} / ml
30% EtOH/NH_4OAc	150	50	300
50% EtOH/NH_4OAc	250	50	200
70% EtOH/NH_4OAc	350	50	100
96% EtOH	480 + 20ml aqua dest		
100% EtOH	500		

cresyl violet staining solution

2.5 g cresyl violet (Merck)

0.102 g Na-acetat (Sigma-Aldrich)

1.55 ml acetic acid

ad. 500 ml H_2O_{bidest}

pH 3.5

filtrate

3.1.2 Media for *Escherichia coli* (*E. coli*)

lysogeny broth (LB) medium

1% (w/v) bacto-tryptone (BD, Heidelberg, Germany)

0.5% (w/v) bacto-yeast-extract (BD)

1.5% (w/v) NaCl

pH 7.4 with NaOH (Karl Roth)

autoclave

LB agar plates

1% (w/v) bacto-tryptone

0.5% (w/v) bacto-yeast-extract

1.5% (w/v) NaCl

1.5% (w/v) bacto-agars (BD)

pH 7.4 with NaOH

autoclave

super optimal broth (SOC) medium

2.0% (w/v) bacto-tryptone

0.5% (w/v) bacto-yeast-extract

10 mM NaCl

2.5 mM KCl

→ pH = 7

autoclave

add

10 mM	MgSO4 (Merck)
10 mM	MgCl2 (Karl Roth)
20 mM	glucose (Sigma-Aldrich)

filter sterile

3.1.3 Media and materials for cell culture

3.1.3.1 Media

growth medium

500 ml Dulbecco's modified eagle medium (DMEM, #41965, Invitrogen)

50 ml fetal calf serum (FCS; Invitrogen)

10 ml penicillin/streptomycin (5000 U/ml, Invitrogen)

transfection and treatment medium (serum-free)

500 ml Dulbecco's modified eagle medium (DMEM, Invitrogen)

freezing medium

90 % FCS

10 % dimethylsulfoxide (DMSO, Sigma-Aldrich)

3.1.3.2 Agonist and antagonist stock solutions

CRH (H-2435, Bachem, Bubendorf, Switzerland): 200 µM in sterile 0.01 M acetic acid

pCPT-cAMP (C3912, Sigma-Aldrich): 500 µM in sterile H2Obidest

3.1.3.3 Reporter assays

2x 2-Nitrophenyl β-D-galactopyranoside (ONPG)-buffer

44ml	1 M Na_2HPO_4
16.13 ml	1 M NaH_2PO_4
270 ml	H_2O
123 mg	$MgCl_2x6H_2O$
398 mg	ONPG (N-1127, Sigma)

→ stir for 40 min

→ + 2 ml β-mercaptoethanol (14M)

3.1.3.4 Plastic material

T75-flasks with vent	TPP, Trasadingen, Switzerland
10-cm plates	Nunc
6-well plates	Nunc
12-well plates	Nunc
24-well plates	Nunc
cell scraper	TPP
serological pipettes	Sarstedt, Nürmbrecht, Germany

3.1.4 PCR Primer

3.1.4.1 RT-PCR

Table 2. RT-PCR primer sequences, amplicon size and PCR settings

name	orientation 5´ → 3´	amplicon [bp]	x [°C]	y [s]	z [min]	company
T3 pT3T7	GCTAAAATTAACCCTCACTAAAGGGAATAAGC	vector insert dependent				MWG BiotecH
T7 pT3T7	CGAATTTAATACGACTCACTATAGGGAATTTG					Sigma-Aldrich
T7	GAATTGTAATACGACTCACTATAGGGCGAATTG					
BGH_rev	TAGAAGGCACAGTCGAGG					Sigma-Aldrich
Sp6	CCAAGCTATTTAGGTGACACTATAGAATACT					Sigma-Aldrich
CRHR1 fw	GCCGCCTACAACTACTTCCA	521	59	60	5	MWG Biotech
CRHR1 rev	CAGAAAACAATAGAACACAGACAC					MWG Biotech
CRHR2 fw	GGCAAGGAAGCTGGTGATTTG	378	59	60	5	MWG Biotech
CRHR2 rev	GGCGTGGTGGTCCTGCCAGCG					MWG Biotech
EGFR1_nest_fwd	ACAAGTAACAGGCTCACCCAAC	884	56	60	3	Sigma-Aldrich
EGFR1_nest_rev	TTTTTACACTTGCGGATGCC					Sigma-Aldrich
EGFR1_fwd2	TCAACACCGTGGAGAGAATC	192	55	0	1	Sigma-Aldrich
EGFR1_rev2	AGAGGATGGGGTTGTTGC					Sigma-Aldrich
ErbB2_nest_fwd	ATCTTGAAGGGAGGAGTTTTG	830	56	60	3	Sigma-Aldrich
ErbB2_nest_rev	ACACTGAGGTCTTGGAAGC					Sigma-Aldrich
ErbB2_fwd2	TGCCTCCACTTCAATCATAG	207	55	0	1	Sigma-Aldrich
ErbB2_rev2	TGTGACCTCTTGGTTGTTC					Sigma-Aldrich
ErbB3_fwd2	ACTACAATACCAACTCCAGC	204	55	0	1	Sigma-Aldrich
ErbB3_rev2	AGACTTCGTGACAGGGTG					Sigma-Aldrich
ErbB4_nest_fwd	CTTCCCTACAGTTCCAGTCTCT	912	56	60	3	Sigma-Aldrich
ErbB4_nest_rev	GGATTTTCACTGTTTCACCTTC					Sigma-Aldrich
ErbB4_fwd2	TCCATCTGTGTTGAGTGTGAC	298	55	0	1	Sigma-Aldrich
ErbB4_rev2	TAGCGTGTTGTGGTAAAGTG					Sigma-Aldrich
HPRT fw	GTCAAGGGCATATCCAACAACAAAC	351	59	60	5	Metabion
HPRT rev	CCTGCTGGATTACATTAAAGCACTG					Metabion

3.1.4.2 qRT-PCR

Table 3. RT-PCR primer sequences, amplicon size and PCR settings

name	orientation 5´ → 3´	amplicon [bp]	x_1 [°C]	x_2 [s]	y [s]	company
9630033F20Rik_fw	ACTCCAGGCTCCGAGAAAG	129	58	5	6	MWG Biotech
9630033F20Rik_rev	GCTCAACTGTCTCTCCTCCAG					MWG Biotech
Acsl4_fwd	GGAGCCAAGCCAGAAAAC	144	60	5	11	Sigma-Aldrich
Acsl4_rev	GCCTGTCATTCCAGCAATC					Sigma-Aldrich
BC055107_fw	GACCAGAGTACAGAGAGTGGAAC	212	62	5	10	MWG Biotech
BC055107_rev	CCTCTAGCTCCTCCTCCTTC					MWG Biotech
Calm2_fw	TGACCAACTGACTGAAGAGC	202	55	4	10	MWG Biotech
Calm2_rev	TTTCTTGCCATCATTGTCAG					MWG Biotech
Cirbp_fw	CAGAGACTACTATGCCAGCC	396	56	5	16	MWG Biotech
Cirbp_rev	CCAAAACCCACACAACCC					MWG Biotech
Cldn10_fw	AGAGGACTAATGATCGCTGC	252	57	5	10	MWG Biotech
Cldn10_rev	TGGGTCCGTTGTATGTGTAG					MWG Biotech
Crem_fw	ACATGCCAACTTACCAGATCC	222	55	4	10	MWG Biotech
Crem_rev	TTTTCAAGCACAGCCACAC					MWG Biotech
Cyp20a1_R_fw	TTCAACCCCAATAAGACTTCG	125	54	6	12	MWG Biotech
Cyp20a1_R_rev	GTCACGGCATCTCCATACAG					MWG Biotech
Dusp14_fw	TCACTGTAACAAGCACCGC	125	57	4	14	MWG Biotech
Dusp14_rev	ATTGATGACGCAGGTGATG					MWG Biotech
Enc1_R_fw	AAAGAAAGCACGCATGAGC	130	55	5	14	MWG Biotech
Enc1_R_rev	GATGGTATTCGAGGAGTCTCAGTAG					MWG Biotech
Errfi1 fw	CAATCTGAACTCCCCTGCTC	170	62	7	8	MWG Biotech
Errfi1 rev	CTTGATCCTCTTCACGCTGTC					MWG Biotech
Fos_fw	TCAACGCCGACTACGAGGC	193	62	4	10	MWG Biotech
Fos_rev	GCTGGTGGAGATGGCTGTCAC					MWG Biotech
Fosl2 fw	GGTAGATATGCCTGGCTCGG	240	63	7	8	MWG Biotech
Fosl2 rev	TCATCTCTCCTTCTGCGGCC					MWG Biotech
GAPDH_fw	CCATCACCATCTTCCAGGAGCGAG	326	65	5	13	MWG Biotech
GAPDH_rev	GATGGCATGGACTGTGGTCATGAG					MWG Biotech
Hmgb1_fw	ATCCTGGCTTATCCATTGG	237	61	4	10	MWG Biotech
Hmgb1_rev	TCCTCTTCATCCTCCTCATC					MWG Biotech
H2Aa_2_fw	AGGTCAAATTCCACCCCAG	243	56	5	10	MWG Biotech
H2Aa_2_rev	AGAAGGGATGAAGGTGAGATAAG					MWG Biotech
Hbb-b1_R_fw	TGCATGTGGATCCTGAGAAC	125	59	5	10	MWG Biotech
Hbb-b1_R_rev	CACTCCAGCCACCACCTT					MWG Biotech
HPRT fw	ACCTCTCGAAGTGTTGGATACAGG	167	57	5	8	Metabion
HPRT rev	CTTGCGCTCATCTTAGGCTTTG					Metabion

name	orientation 5´ (3´	amplicon [bp]	x1 [°C]	x2 [s]	y [s]	company
Hmgcs1_fwd	AATGCCGTGAACTGGGTCG	267	60	5	11	Sigma-Aldrich
Hmgcs1_rev	TGAGGTAGCACTGTATGGAGAGC					Sigma-Aldrich
Hnrpa2b1_fw	GGAACACCACCTTAGAGATTAC	360	56	5	16	MWG Biotech
Hnrpa2b1_rev	TAGCCATCCCCAAATCCAC					MWG Biotech
Hspb1_fw	ACAGTGAAGACCAAGGAAGG	111	56	5	7	MWG Biotech
Hspb1_rev	TGGAGGGAGCGTGTATTTC					MWG Biotech
Kcnma1_fw	CTTCACAACATCTCCCCTAAC	130	57	5	7	MWG Biotech
Kcnma1_rev	CATCTGCTGACTCTATCTTGAC					MWG Biotech
Kif3a_fw	ATCAACCTTTCATTGTCTACCC	325	59	4	14	MWG Biotech
Kif3a_rev	ACACTTCTTCCCCTTCCTC					MWG Biotech
Mest_fw	TGGCTGCGTACCTGCACATC	224	61	5	10	MWG Biotech
Mest_rev	TCACTCGATGGAACCTCAGGG					MWG Biotech
Mpp7_fw	TATTGCCTCCCGTGCCTG	208	57	4	10	MWG Biotech
Mpp7_rev	GATTCCATTCACTTCCCTCAGC					MWG Biotech
Mrpl13_R_fw	CTTCCCCAGAGTGTGGACT	140	59	5	10	MWG Biotech
Mrpl13_R_rev	ACAGGGAGTTCCCATGGTTT					MWG Biotech
Mt1_fw	TAAGCGTCACCACGACTTC	269	57	5	12	MWG Biotech
Mt1_rev	TCACATCAGGCACAGCAC					MWG Biotech
Ndrg4_fw	AGGTGGGAGCGTCACAGT	269	60	7	10	MWG Biotech
Ndrg4_rev	TGTCTGGTAAAGTGCTGGTC					MWG Biotech
Nf2_fw	TTCAAGAGATCACGCAACAC	234	59	4	10	MWG Biotech
Nf2_rev	TTCTCTCCTCCCACATTTCC					MWG Biotech
Nnat_R_fw	CACCCACTTTCGGAACCAT	108	56	5	10	MWG Biotech
Nnat_R_rev	TGCAGCATTCCAGGAACA					MWG Biotech
Npn3_fw	ATCCACTCGGGCTGCATC	186	59	5	10	MWG Biotech
Npn3_rev	AATAGTAGTAGTCGCCACCCTG					MWG Biotech
Nr4a2_fw	ATCGCAGTTGCTTGACACGC	268	59	4	12	MWG Biotech
Nr4a2_rev	TAACCATCCCAACAGCTAGGCAC					MWG Biotech
Pak3_fw	GAACAGAAGAAGAACCCACAAG	180	57	4	14	MWG Biotech
Pak3_rev	TACAGGAGGAGCCAAAGGAG					MWG Biotech
Pcsk2_fw	ACGCTGATGCAAGTTATGAC	197	59	4	10	MWG Biotech
Pcsk2_rev	TGTCATAAAGGGCTGGTC					MWG Biotech
Pex13_fw	TCCTGTTCTTTGCTGTTATCC	109	56	5	6	Sigma-Aldrich
Pex13_rev	TCATCCTCACCACTTGCC					Sigma-Aldrich
Peg3_fw	CAGTGACATGAACAGTGACGACG	289	61	5	12	MWG Biotech
Peg3_rev	TGTCATCATCTCTGTCCAGTCC					MWG Biotech
Pomc_fw	ATAGATGTGTGGAGCTGGTGC	284	64	4	12	MWG Biotech
Pomc_rev	GGCTCTGGACTGCCATCTC					MWG Biotech

name	orientation 5´ → 3´	amplicon [bp]	x_1 [°C]	x_2 [s]	y [s]	company
Rbm3_fw	TTCATCACCTTCACAAACCC	196	57	5	8	MWG Biotech
Rbm3_rev	CATATCTTCCACTTCCATATCCC					MWG Biotech
Rbp4_fw	ACACTGAAGATCCTGCCAAG	151	56	5	10	MWG Biotech
Rbp4_rev	ACAGGTGCCATCCAGATTC					MWG Biotech
RGS4 fw	TGCAAGCAACAAAAGAGGTG	97	55	20	10	MWG Biotech
RGS4 rev	CTGGGCTTCATCAAAACAGG					MWG Biotech
RGS9_R_fw	TCGGTGTCTCTTGGAGGAA	107	60	7	10	MWG Biotech
RGS9_R_rev	TGGGTGTCGTCTGTTATCCA					MWG Biotech
Sfrs6_fw	AGATGCTCACAAAGAACGAAC	216	55	5	14	MWG Biotech
Sfrs6_rev	CTTCTGCGACTCCTACTCC					MWG Biotech
Slc27a2_fw	AACCATCAATCATCATCGCC	340	57	5	12	MWG Biotech
Slc27a2_rev	CTCTCTCCACACATCTCCTC					MWG Biotech
Stmn1_fw	CAGGTGAAAGAGCTGGAGAA	259	54	5	12	MWG Biotech
Stmn1_rev	AAGTTGTTGTTCTCCTCGATG					MWG Biotech
Syt4 fw	TGATGTCATTGGAGAAGTCCTG	168	58	5	8	MWG Biotech
Syt4 rev	ACCACAGTGAGCGTGTTTGT					MWG Biotech
Tcfe3_R_fw	TCCTGGAACAAGCCAAC	127	58	5	6	MWG Biotech
Tcfe3_R_rev	CAGAGACCGAACTCGTGGTT					MWG Biotech
Timm13 fw	AGGTGGAGATGATGGCTGAC	190	61	5	8	MWG Biotech
Timm13 rev	TCATCCTGCATTGACAGCTC					MWG Biotech
Ttr_fw	CCTCGCTGGACTGGTATTTG	121	60	4	10	MWG Biotech
Ttr_rev	TTACAGCCACGTCTACAGCAG					MWG Biotech

3.1.5 Plasmids

For cloning, subcloning and reporter assays the following plasmids were provided as indicated:

Table 4. Origin of used plasmids

name	origin
pCR®II-TOPO® Vector	Invitrogen
pcDNA3.1(+)	Invitrogen
Pomc-Luc	kindly provided by Günter K. Stalla
Cre-Luc	kindly provided by Dietmar Spengler
NurRE-Luc	kindly provided by Jacques Drouin
pEGFP-N1	BD Biosciences Clontech
pcDNA3.1-Hspb1	subcloning of insert of pSVKwt (kindly provided by Matthias Gaestel (Knauf *et al.*, 1994)) into pcDNA3.1 using EcoRI + XhoI
pcDNA3.1-Hspb1mut	subcloning of insert of pSVKM1M2 (kindly provided by Matthias Gaestel (Knauf *et al.*, 1994)) into pcDNA3.1 using EcoRI + XhoI
pcDNA3.1-Icer	subcloning of insert of pSG5-IcerIIγ (kindly provided by Paolo Sassone-Corsi (Liu *et al.*, 2006) into pcDNA3.1 using EcoRI + XhoI

name	origin
pcDNA3-Nf2_16	kindly provided by David H. Gutmann (Sherman *et al.*, 1997)
pcDNA3-Nf2_17	kindly provided by David H. Gutmann (Sherman *et al.*, 1997)
pcDNA3.1-HA-Pak3a	kindly provided by Jean-Vianney Barnier (Rousseau *et al.*, 2003)
pcDNA3.1-HA-Pak3b	kindly provided by Jean-Vianney Barnier (Rousseau *et al.*, 2003)
pcDNA3.1-HA-Pak3a-kd	kindly provided by Jean-Vianney Barnier (Rousseau *et al.*, 2003)
pcDNA3-Rgs4	kindly provided by Dr. Constanze Fey

3.1.6 Cell lines

AtT-20

origin cloned in October, 1966, by G. Sato; the mouse pituitary tumor was originally established in LAF1 mice by J. Furth *et al.*

cell type mouse pituitary tumor

reference Buonassisi *et al.*, 1962

obtained from Günter K. Stalla

medium DMEM, 10%FCS, 100 U/ml P/S

HN9

origin primary hippocampal cells from C57BL/g mice embryonic day 18 were immortalized via somatic cell fusion to the neuroblastoma cell line N18TG2

cell type hippocampal neurons

reference Lee *et al.*, 1990

obtained from Marcelo Paez-Pareda

medium DMEM, 10%FCS, 100 U/ml P/S

3.1.7 Animals

All animal experiments were conducted in accordance with the Guide of the Care and Use of Laboratory Animals of the Government of Bavaria, Germany.

For the *in vivo* experiments 6-12 weeks old male homozygous CRHR1-wt and -ko mice (Timpl *et al.*, 1998) were used. All animals were single-housed under standard laboratory conditions and were maintained on a 12 h light-dark cycle (lights on between 7:00 a.m. and 7:00 p.m.) with rodent laboratory chow and water *ad libitum*.

3.2 Methods

3.2.1 Microbiological methods

3.2.1.1 Culture of E.Coli

DH5α E.Coli bacteria were cultured in sterile, autoclaved lysogeny broth medium (LB medium). For liquid culture one bacteria colony was picked and inoculated in LB medium with 100 µg/ml ampicillin (Sigma-Aldrich, stock solution: 100 mg/ml in H_2O_{bidest}) over night at 37°C on a shaker (250 rpm, Swip, Edmund Bühler, Hechingen, Germany).
After transformation bacteria were plated on LB agar plates (Greiner, Frickenhausen, Germany) containing 100 µg/ml ampicillin and incubated over night at 37°C.

3.2.1.2 Preparation of electrocompetent cells

50 ml E.Coli culture was grown over night in LB medium. 1 l LB medium was inoculated on the next day with the 50 ml overnight culture and shaken at 37°C until cells have grown to an optical densitiy (OD) at 600 nm of 0.5-0.6 (DU530 photometer, Beckmann Coulter, Krefeld, Germany). Bacteria were transferred to centrifuge bottles (Beckmann Coulter) and incubated on ice for 30 min. After centrifugation at 4000xg for 15 min at 2°C (Avanti J-25 centrifuger, Beckmann Coulter) the supernatant was decanted and the bacteria pellet gently resuspended in 1 l of cold, sterile water (Ampuwa, Fresenius, Bad Homburg, Germany). Cells were centrifuged again at 4000xg for 15 min at 2°C and resuspended in 500 ml of cold, sterile water. After a further centrifugation step cells were resuspended in 40 ml of cold, sterile waster with 10% glycerol (Sigma-Aldrich). Centrifugation at 4000xg for 15 min at 2°C pelletized washed bacteria which were resuspended in 2ml of cold 10% glycerol in water by vortexing. 20 µl aliquots were frozen at -70°C.
Electrocompetence was tested by electroporating one 20 µl aliquot of electrocompetent cells with 10 pg of pUC19 vector (Invitrogen). 20, 50 and 100 µl of transformed bacteria were plated on LB agar plates with Ampicillin. After incubation over night at 37°C colonies were counted and the competence calculated with the following formula:

$$\frac{\#of\_colonies}{xng\_transformed\_DNA} \cdot \frac{10^3 ng}{\mu g} \cdot \frac{y\mu l\_total\_transformation\_volume}{X\mu l\_plated\_volume} = \frac{\#\_transformants}{\mu g\_plasmid\_DNA}$$

x = 0,01

y = 1020

X = 20, 50 or 100

3.2.1.3 Transformation

Transformation was performed by electroporation (Gene Pulser XcaII, BioRad, Munich, Germany). 1 µl of desalted plasmid was added to a 20 µl aliquot of electrocompetent cells.

After 1 min incubation on ice, bacteria were pipetted in a 1 mm electroporation cuvette (PeqLab, Erlangen, Germany) and electroporated at 1.8 kV. 500 - 1000 µl of SOC medium was added and transformed bacteria were shaken at 250 rpm for 1h at 37°C (Thermomixer, Eppendorf, Hamburg, Germany). 10-200 µl of grown bacteria were plated on LB agar plates with Ampicillin.

3.2.2 Preparation and analysis of nucleic acids

3.2.2.1 DNA plasmid preparation

Plasmid DNA was prepared using the QIAprep Spin Miniprep Kit, the QIAGEN Plasmid Midi Kit and the QIAGEN Plasmid Maxi Kit (Qiagen, Düsseldorf, Germany), respectively. The Miniprep Kit was performed for preparation of small amounts of plasmid DNA (up to 20 µg) for control digests of ligations. For isolation of higher amounts of plasmid DNA for transfections the Midi (up to 100 µg) or the Maxi (up to 500 µg) Kit were used. Single bacteria colonies were inoculated in 3 (Mini), 50 (Midi) or 200 (Maxi) ml LB medium over night. Bacteria were harvested, lysed and DNA was isolated as described in the manufacturer´s protocol. DNA was always dissolved in sterile Ampuwa water and quantified as described above.

3.2.2.2 RNA isolation with TRIzol

For RNA isolation from pituitary or neuronal cells and mouse pituitaries the TRIzol protocol (Invitrogen) was utilized. Tissue and harvested cells grown on 6-well plates or T75 flasks were homogenized in 1 ml TRIzol reagent using turrax (IKA Labortechnik, Staufen, Germany) or insulin canulas (BD). Solutions were incubated at room temperature for 5 min. After addition of 200 µl chloroform (Karl Roth) tubes were shaken by hand for 3 min at room temperature. By centrifugation for 15 min at 13000 rpm and 4°C (5403 centrifuge, Eppendorf) the phenol and water phases were separated. The aqueous upper phase containing the RNA was transferred into a fresh 1.5 ml Eppendorf tube and RNA was precipitated with 500 µl isopropanol (Karl Roth) for 1h at -20°C. Precipitated RNA was centrifuged for 10 min at 13000 rpm and 4°C. The pellet was washed with 1 ml of cold 70% ethanol (pharmacy) by centrifugation at 10000 rpm, 4°C, for 10 min. RNA pellet was dried at 37°C and dissolved in 20-50 µl H_2O_{bidest} at 65°C for 10 min.

3.2.2.3 Agarose gel electrophoresis

For DNA agarose gel electrophoresis agarose (Invitrogen) was boiled in 1x TAE buffer with agarose concentration depending on the DNA fragment size. For fragments between 100 and 1000 bp 2% agarose gels were chosen. For bigger fragments 0.8-1% agarose gels were applied. 0.1 µg/ml ethidiumbromide (Karl Roth) was added to boiled and liquid

agarose in 1x TAE which was spilt in a gel electrophoresis chamber (PeqLab). DNA or RNA samples mixed with 1/6 of 6x sample loading buffer were loaded. As size marker 1kb plus DNA ladder (Invitrogen), Smart ladder (Eurogentec, Liège, Belgium) or 50 bp DNA ladder (Fermentas, ST. Leon-Rot, Germany) were used. Electrophoresis was carried out with 80-140 V for 1-2h. The DNA fragments were detected with a UV light camera (Biometra, Göttingen, Germany).

3.2.2.4 Quantification of DNA/RNA

DNA or RNA was diluted 1/50-1/200 in water. The optical density (OD) of the nucleic acid dilution at 260 nm was measured with a spectrophotometer (DU640, Beckmann Coulter). For concentration calculation the empiric values of

1 OD_{260nm} = 50 ng DNA/µl or 40 ng RNA/µl

were taken into account.

3.2.3 Polymerase chain reaction (PCR)

3.2.3.1 Reverse transcription (RT)

Reverse transcription (RT) of RNA to cDNA was performed in a PCR machine (GeneAmp PCR System 2400, AB Applied Biosystems, Darmstadt, Germany) with the SuperScriptII Reverse Transcription Kit (Invitrogen) according to the manufacturer´s protocol. 500-1000 ng of RNA was incubated in a total volume of 11 µl with 1 µl of 0.5 µg/µl oligo(dT) primers (Invitrogen) at 70°C for 5 min and subsequently chilled on ice. Per sample,

4 µl 5x buffer
2 µl 0.1 M DTT
1 µl 10 mM dNTPs (Roche)
1 µl RNase inhibitor (Roche)
1 µl SuperScriptII

were added. After incubation at 42°C for 1 h and inactivation of the SuperScriptII at 70°C for 15 min, 1 µl of RNase H (Invitrogen) was added to digest the RNA template at 37°C for 20 min. RNase H activity was stopped at 70°C for 15 min.

To control for DNA contamination of the RNA negative controls of the RT reaction were performed using the same protocol only without SuperScriptII.

3.2.3.2 Primer design

Primers for RT-PCR and qRT-PCR were designed by hand. Primers had to have a size between 18 and 25 bp, a GC content of 40-60% and a melting temperature of 55-65°C whereby forward and reverse primer had to show less temperature difference than 5°C.

Hairpin and dimer structures were analyzed using the Vector NTI software (Invitrogen). For qRT-PCR the amplicon size had to be 100-400 bp.

3.2.3.3 PCR

To amplify specific cDNA fragments for expression analyses or expression vector clonings polymerase chain reactions were performed using the Thermoprime Plus DNA polymerase (ABgene, Hamburg, Germany) as follows:

1-2 µl cDNA
5 µl 10 x reaction buffer IV (ABgene)
3 µl 25 mM $MgCl_2$ (ABgene)
1 µl 10 mM dNTPs (Roche)
3 µl 10 µM primer fwd
3 µl 10 µM primer rev
0.5 µl Thermoprime Plus DNA polymerase (5 U/µl, ABgene)
add 50 µl H_2O_{bidest}

To assure correct transcription 1/10 of the ABgene Taq polymerase was exchanged with Phusion High Fidelity polymerase (Finnzymes, Espoo, Finland) for cloning PCRs.

PCR was carried out in a PCR machine (GeneAmp PCR System 9700, Applied Biosystems) with the following temperature settings:

program	**cycles**	**temperature**	**hold**
preincubation	1	94°C	5 min
amplification: *denaturation* *annealing* *elongation*	33	 94°C x°C 72°C	 30 sec 30 sec y sec
	1	72°C	z sec

Annealing temperature and elongation time were dependent of the melting temperature of the primers and the amplicon size (see Table 2).

3.2.3.4 Quantitative real-time PCR (qRT-PCR)

Quantitative real time PCR was performed in the Lightcycler 2.0 System (Roche) using the LightCycler® FastStart DNA MasterPLUS SYBR Green I (Roche) reagent.
Mastermix was prepared as follows (volume/sample):

2 µl 5x PCR mix (14 µl 1a plus 1 tube 1b of the Sybr Green I Kit)
0.5 µl 10 µM primer fwd
0.5 µl 10 µM primer rev
5 µl H_2O_{bidest}

8 µl mastermix were pipetted in each capillary which was fixed in the Lightcycler carousel (Roche) and closed immediately after addition of 2 µl 1/10 diluted cDNA. Dependent of primer melting temperature and amplicon size the PCR settings were chosen (see Table 3). At the end of every run a melting curve was measured to ensure the quality of the PCR product.

Programm settings:

program name	cycles	target [°C]	hold [sec]	slope [°C/s]	sec target	step size	step delay	acquisition mode
Preincubation	1	95	10 min	20	0	0	0	None
Amplification	40							
Denaturation		95	10	20	0	0	0	None
Annealing		x_1	x_2					None
Elongation		72	y	20	0	0	0	Single
Melting Curve	1	95	0	20	0	0	0	None
		50	10	20	0	0	0	None
		95	0	0,1	0	0	0	Continuous
Cooling	1	42	30	20	0	0	0	None

Crossing points (Cp) were calculated by the LightCycler®Software 4.05 (Roche Diagnostics GmbH, Mannheim, Germany) using the absolute quantification fit points´ method. Threshold and noise band were set in all compared runs on the same level. Relative gene expression was determined by the $2^{-\Delta\Delta CT}$ method (Livak and Schmittgen, 2001), using the real PCR efficiency calculated from an external standard curve, normalized to the housekeeping genes Hprt and Gapdh and related to the data of the control experiments.

3.2.4 Cloning

3.2.4.1 DNA restriction digest

Plasmid DNA was digested by restriction enzymes (Fermentas; NEB, Frankfurt/Main, Germany) to control ligated inserts (analytic restriction digest) or to isolate the targeted insert out of the vector backbone (preparative restriction digest).

For an analytic digest

2 µl plasmid DNA (Miniprep)

1 µl buffer (10x)

0.5 µl restriction enzyme (10 U/µl)

6.5 µl H_2O_{bidest}

were mixed and incubated 1h at 37°C. Fragment sizes were analyzed by agarose gel electrophoresis.

For a preparative digest

10 µg	plasmid DNA
5 µl	buffer
2.5 µl	restriction enzyme (10 U/µl)
add 50 µl	H_2O_{bidest}

were mixed and incubated over night at 37°C. Fragments were separated by agarose gel electrophoresis and the targeted insert was purified by gel extraction.

For double digests the recommendations of Fermentas were applied.

3.2.4.2 DNA gel extraction

For purification of DNA fragments out of an agarose gel the QIAquick Gel Extraction Kit (Qiagen) was used according to manufacturer´s instructions. DNA was eluted using 30 µl of H_2O_{bidest}. Extracted DNA concentration was estimated using agarose gel electrophorese and the DNA marker Smart Ladder.

3.2.4.3 TOPO TA cloning

For ligation of polymerase chain reaction (PCR) products into the expression vector pcDNA3.1 DNA was first cloned into the pCR®II-TOPO® vector using the TOPO TA cloning Dual Promoter Kit (Invitrogen).

4 µl	PCR product
1 µl	salt solution
1 µl	pCR®II-TOPO® vector

were mixed and incubated for 10 min at room temperature. The whole mixture was added to One Shot Chemically Competent Top10 *E. coli* cells (Invitrogen) and incubated on ice for 30 min. A 90 sec heat shock at 42°C was performed and after addition of 250 µl SOC medium bacteria were shaken on 37°C, 250 rpm for 1h. 50-200 µl of the bacteria suspension was plated on LB agar plates with ampicillin and 40 µl of 40 mg/ml X-Gal (Genaxxon, Biberach, Germany) in dimethylformamide (Sigma-Aldrich) (blue-white selection marker).

Minipreps of white grown colonies were inoculated and after plasmid preparation the insertion into the TOPO vector was checked by restriction digest.

In the case of correct insert insertion a preparative digest of the TOPO vector including the insert and the empty pcDNA3.1 vector was performed and the targeted insert plus the linearized pcDNA3.1 vector were extracted of an agarose gel.

3.2.4.4 Ligation

50 ng vector backbone was ligated to 3-fold molar excess of insert. The appropriate mass of insert was calculated as following:

$$m(insert) = 3 \times 50ng \times \frac{bp(insert)}{bp(backbone)} = xng$$

For ligation the Rapid DNA Ligation Kit (Fermentas) was utilized. Pipetting scheme for ligation:

50 ng	pcDNA3.1 linearized
x ng	insert gel extract
4 µl	5x Buffer
add 19 µl	H_2O_{bidest}
1 µl	T4-Ligase

After incubation of 10 min at room temperature the ligation was desalted for 30 min using mixed cellulose ester membrane discs (Millipore, Schwalbach, Germany) on 5 ml of H_2O_{bidest}. 1 µl of desalted ligation was pipetted to a 20 µl aliquot of electrocompetent bacteria and transformed by electroporation as described above.

3.2.4.5 Cloning of expression vectors

Cloning of diverse expression vectors started with RT-PCR of the desired cDNA. RT-PCR products were cloned into pCR®II-TOPO® vector and via a preparative restriction digest subcloned into the expression vector pcDNA3.1. Table 5 shows primers and restriction enzymes used for cloning.

Table 5. Cloning primer sequences, amplicon size and cloning enzymes

candidate gene	primer	cDNA size	digest TOPO → pcDNA3.1
Dusp14	fwd: 5´-CCTGATGATGATAGTGTGACC-3´ rev: 5´-AGATGCTGGTACTGCTGAG-3´	676 bp	BamHI + NotI
ErbB3	fwd: 5´-TTCACCCTCCACTGTAATC-3´ rev: 5´-TGTTCCCCAAGAGTCTCAAG-3´	4068 bp	HindIII, XbaI, PvuI pcDNA3.1: no PvuI
Errfi1	fwd: 5´-TTGAAGGCATCCCAGAGTG-3´ rev: 5´-TCATCCCATGTAACTTCTGTTG-3´	1451 bp	BamHI + NotI
Errfi1_Nterm			EcoRV digest of pcDNA3.1-Errfi1 → religation
Errfi1_oCrib	fwd: 5´-TTGAAGGCATCCCAGAGTG-3´ rev: 5´-ACTCACTGTGACTGCCCC-3´	141 bp	SpeI + XhoI pcDNA3.1: XbaI + XhoI
Errfi1_dCrib	fwd: 5´-GGGGCAGTCACAGTGAGT-3´ rev: 5´-TCATCCCATGTAACTTCTGTTG-3´	1328 bp	BamHI + XbaI
Fosl2	fwd: 5´-ACCACCCTGTTTCCTCTCC-3´ rev: 5´-AAGGGTGTGGTAATGATGG-3´	1074 bp	BamHI + NotI

candidate gene	primer	cDNA size	digest TOPO → pcDNA3.1
Mpp7	fwd: 5´-ACAGGATCGGCTTGCGAC.3´ rev: 5´-GACAATTAAGGACATTTCTCTG-3´	1740 bp	BamHI + NotI
Nf2_17trunc			EcoRV+StuI digest of pcDNA3.1-Nf2_17 → religation
Nf2_17Ntrunc	fwd: 5´-TGGAGATGTACGGTGTGAAC-3´ rev: 5´-TAGCAGGAGAAGTGGCAGG-3´	1235 bp	BamHI + XbaI

3.2.5 Cell culture

3.2.5.1 Maintaining cells

To avoid bacteria, funghi or yeast contamination every cell culture work was done under sterile conditions in a sterile hood (Heraeus Instruments, Hanau, Germany). Cells were grown at 37°C with 5% CO_2 in a sterile incubator (Heraeus). Every second day cells were split or medium was refreshed.

unfreezing of cells

A frozen vial of cells was thawed quickly at 37°C in a waterbath (GFL, Burgwedel, Germany), suspended in 10 ml of prewarmed growth medium and centrifuged at 1200 rpm for 4 min (Universal 30F centrifuge, Hettich, Tuttlingen, Germany). The cell pellet was resuspended gently in 5 ml growth medium and cells were split on a T75 flask each containing a total of 20 ml growth medium. Cells were incubated in the incubator up to a confluency of 70-90%.

splitting of cells

Medium was removed from the flasks and the cells were washed with 15-20 ml prewarmed PBS (Invitrogen). 2 ml trypsin/EDTA (Invitrogen) was added and flasks were incubated for about 5 min at 37°C until the cells were detached. To stop the reaction 8 ml growth medium was added and cell suspension was centrifuged at 1200 rpm for 4 min. The cell pellet was resuspended in 5-10 ml growth medium by pipetting up and down several times to break any cell aggregates. An appropriate amount of the cells (1/3 - 1/10) was plated immediately on new dishes containing growth medium. The flasks were swirled to ensure an equal distribution in the medium.

freezing of cells

To obtain stocks of used cell lines freshly thawed cells were passaged and amplified at least twice and then refrozen. Therefore one T75 flask with about 80% confluency was trypsinized and centrifuged. Cells were resuspended in 3 ml of freezing medium and aliquoted in 3 cryo tubes (Nalgene, Roskilde, Denmark). The tubes were cooled down

slowly over night to -70°C using an isopropanol-filled freezing container (Nalgene). Afterwards cell tubes were stored in liquid nitrogen.

counting of cells

A Neubauer chamber (Karl Roth) was used to determine the cell number. After trypsination cells were resuspended in growth medium and 10 µl of the suspension were counted. The mean value (m) of 2 counted quadrants (containing each 16 small quadrants) was used to calculate the cell number:

$$cells/ml = m \cdot 10000$$

3.2.5.2 CRH treatment

AtT-20 cells were seeded in growth medium on 10 cm plates. 24 h later when cells were 50% confluent medium was changed to serum-free medium. 18-24h afterwards, cells were treated in fresh serum-free medium with 100 nM CRH (Bachem) for 1, 3, 6, 12 and 24 h. For every time point untreated dishes were harvested as control.

3.2.5.3 ACTH radio immune assay (RIA)

The radioimmune assay of ACTH in the cell culture medium of AtT-20 cells was measured using an N-terminal-specific polyclonal rabbit antibody as primary antibody as described elsewhere (Stalla *et al.*, 1989). The ^{125}I-tracer labeling was performed according to the Chloramine-T method (Hunter and Greenwood, 1962).

3.2.5.4 Transient transfections

Transfections were performed in a 24-well format using Lipofectamine 2000 (Invitrogen). Complexes were prepared using 0.8 µg DNA with 2 µl Lipofectamine 2000 per well. Cells were transfected at a cell density of 50-70% for high efficiency, high expression levels and to minimize cytotoxicity.

In the case of AtT-20 cells, 100000 cells per 24-well were plated in 500 µl of growth medium with the usual amount of serum two days before transfection. For HN9 cells, 24-well plates were preincubated for 1h with 0.01 mg/ml poly-D-lysine (Sigma-Aldrich) at 37°C. Afterwards, plates were washed with PBS and 80000 cells per well were seeded in normal growth medium one day before transfection. Before transfection, medium was aspirated and 400 µl medium without antibiotics and serum was added to arrest the cell cycle. For each transfection sample complexes were prepared as follows: DNA (0.5 µg expression plasmid, 0.2 µg luciferase plasmid and 0.2 µg CMV-βGal plasmid) was diluted in 50 µl of Opti-MEM (Invitrogen) and mixed gently. Lipofectamine 2000 was mixed gently before use and the appropriate amount (2 µl) was diluted in 50 µl of Opti-MEM and

incubated for 10 min at RT. After the incubation, the diluted DNA was combined with diluted Lipofectamine 2000 (total volume = 100 µl), mixed gently and incubated for 20 min at RT. 100 µl of complexes was added to each well containing cells with medium and mixed gently by rocking the plate back and forth. Cells were incubated at 37°C in a 5% CO_2 incubator for 18-24 hours prior to stimulation.

To harvest cells, cells were washed with cold PBS. For RNA extraction 1 ml cold PBS was added per dish and cells were scraped off. Cell suspension was transferred to a 1.5 ml Eppendorf tube. Cells were pelletized by centrifugation at 13000 rpm, 4°C for 5 min and frozen at -70°C.

For reporter assays 100 µl 1 x passive lysis buffer (Promega, Madison, USA) per well was added to washed cells. After 15 min shaking at room temperature (Duomax 1030, Heidolph, Schwabach, Germany) cell lysates were frozen at - 70°C.

3.2.5.5 Reporter assays

The lysed cells were unfrozen, transferred to a 96-well plate and centrifuged for 10 min at 4000 rpm (Universal 30F, Hettich).

<u>firefly luciferase measurement</u>

20 µl of the supernatant were transferred to a nontransparent 96-well plate (Dynex, Berlin, Germany). In parallel, the buffer for the firefly luciferase reaction (50 µl/well; Luciferase Assay System, Promega) was prepared.

The firefly luciferase reporter is measured by adding Luciferase Assay Reagent II (LAR II) to generate a luminescent signal lasting at least one minute. Firefly luminescence was quantified in a luminometer (TriStar LB 941, Berthold Technologies), containing auto-injectors, for 10 sec.

<u>β-galactosidase (βGal) measurement</u>

As control reporter CMV-βGal was used. The β-galactosidase amount was quantified by adding 50 µl of the substrate o-nitrophenyl-b-D-galactoside (ONPG, Sigma-Aldrich) and 30 µl of H_2O_{bidest} to 20 µl of the cell lysate in a transparent 96-well plate with plane bottom (Nunc, Rochester, USA). Cleavage of ONPG by β-galactosidase leads to release of o-nitrophenol. The absorption of o-nitrophenol was monitored at 420 nm using a plate reader (Genius Pro, Tecan, Männerdorf, Switzerland).

3.2.6 *In vivo* experiment

3.2.6.1 Stress experiment

To activate CRHR1-dependent signaling in the pituitary of CRHR1-wt and -ko mice animals were stressed using 30 min restraint stress in 50 ml Falcon tubes (BD Biosciences, San Jose, USA). 12 h before stress mice were injected intraperitonally (i.p.) with 150 mg/kg b.w. metyrapone. Metyrapone is an inhibitor of the steroid β-hydroxylase, an enzyme catalyzing the biosynthesis of corticosterone. As a consequence, the negative feedback of corticosterone on the HPA axis was blocked. A second metyrapone injection (100 mg/kg b.w.) was done directly before stress. First blood samples (~ 300 µl) were collected in 1.5-ml EDTA-coated microcentrifuge tubes (KABE Labortechnik, Nürnbrecht-ElsenKarl Roth, Germany) after the second injection before stress (controls) from the retrobulbar plexus under brief isoflurane anesthesia. Second blood samples were taken after sacrification (stress values, trunk blood). Mice were slightly anaesthetized with isoflurane (Forene, Abbott, Wiesbaden, Germany) and sacrificed by decapitation 1 h and 3 h after stress begin. Brains and pituitaries were prepared and flash-frozen on dried ice/liquid nitrogen. Tissues were stored at -70°C until RNA isolation or *in situ* hybridization.

3.2.6.2 Endocrine analysis

All collected blood samples were kept on ice and later centrifuged for 20 min at 3000 rpm at 4°C. Plasma was transferred to 1.5-ml microcentrifuge tubes and stored frozen at −20°C until the determination of corticosterone and ACTH. Blood plasma corticosterone and ACTH concentrations were measured using commercially available mouse RIA kits (ICN Biomedicals, Frankfurt/Main, Germany).

3.2.7 Expression analysis using microarray technology: *in vitro*

The RNA of CRH treated cells from different time points (1, 3, 6, 12, 24 h) and their corresponding controls was isolated as described. RNA quality was verified by agarose gel electorphoresis and RNA concentration was measured at 260 nm with a spectrophotometer.

For the analysis of the differential expression pattern of untreated versus treated AtT-20 cells the MPIP 24 k chip was used containing 24192 PCR products derived from different mouse cDNA libraries (sources: Research Genetics, RZPD Deutsches Ressourcenzentrum für Genomforschung, proprietary clones) representing 12387 different unigene clusters (unigene build #143) (Deussing *et al.*, 2007).

3.2.7.1 RNA amplification

3 µg of isolated RNA were amplified using the AminoAllyl MessageAmp aRNA kit (Ambion) according to the manufacturer´s instructions. Shortly, RNA was reverse transcribed and then *in vitro* transcribed to aRNA. During *in vitro* transcription the modified nucleotide 5-(3-Aminoallyl)-UTP (Sigma) was incorporated. Per 3 technical replicates,15 µg of control and corresponding CRH-treated aRNA (5 µg/replicate), respectively, were coupled to mono-reactive Cy3 or Cy5 N-hydroxysuccinimide (NHS) esters (Amersham, Munich, Germany). A dye-swap with 3 replicates per Cy3/Cy5 combination was performed to exclude dye-biased effects.

3.2.7.2 Hybridization

Microarrays were dried for 30 min at 60°C and blocked with pre-hybridization buffer for 1 h at 42°C. Arrays were washed with water and isopropanol and dried by centrifugation (1 min, 1500 rpm, Megafuge 1.0R, Heraeus) in a 50 ml polypropylene tube.

Dye-coupled aRNA (15 µg) was combined with hybridization buffer and 20 µg poly(dA) (Amersham) and denatured (95°C, 5 minutes). Hybridizations were performed in custom-made chambers in a waterbath at 50°C overnight. The arrays were rinsed in 2xSSC/0.1%SDS at room temperature, then washed consecutively in 2xSSC/0.1%SDS at 42°C (5 minutes, shaking waterbath), 0.1xSSC/0.1%SDS at room temperature (10 minutes), four times in 0.1xSSC at room temperature (1 minute each) and in 0.01xSSC at room temperature (vigorously shaking for 10 seconds in a 50 ml polypropylene tube). Finally, the microarrays were dried by centrifugation (1 minutes, 1500 rpm) in a 50 ml polypropylene tube.

3.2.7.3 Scanning, data acquisition and normalization

Scanning was performed using a ScanArray 4000 laser scanner and ScanArray 3.1 Software (Perkin Elmer) with a fixed PMT gain of 80%, and laser power was adjusted depending on signal intensities. Quantification was performed using QuantArray software 2.1.0.0 (Perkin Elmer) and the fixed circle analysis method. Data were imported in a PSQL relational database for further analysis.

For the spot image extraction the brightness of the microarray images was globally normalized in a way that the mean spot intensity of all arrays was the same. After this, the coordinates generated during the quantification process were used to cut out the corresponding spots from each array image. These images were combined and transferred from 16 bit gray-scale to 8 bit RGB color space (Cy3 _ green channel, Cy5 _ red channel). Overlay images were created and spot acquisition areas were marked with

a blue circle. The images for Cy3, Cy5, overlay and overlay plus acquisition area were combined and stored in 8 bit Portable Network Graphics (PNG) format.
The bottom 10% of the scan intensity values were defined as background and erased. Raw data were then normalized using a nonlinear regression method according to Yang *et al.* and subjected to a t-test for significantly differential expression (Yang *et al.*, 2002). The obtained p-values were corrected for multiple testing using Benjamini-Hochberg false discovery rate (FDR) procedure (Hochberg, 1995).

3.2.7.4 Data analysis I: Bayesian model-based hierarchical clustering: Splinecluster

Cluster analysis was performed by Dr. Benno Pütz of the statistical genetics group at the MPI of Psychiatry in Munich using a Bayesian model-based software, *Spinecluster* (Heard *et al.*, 2006). This hierarchical clustering algorithm was especially developed for the analysis of time course data allowing unequally spaced time points. *Spinecluster* groups together genes that exhibit similar regulation dynamics. Thereby, groups of genes, that appear co-regulated and thus assumed to be controlled by the same biological mechanisms, were identified.
The C++ code of the cluster algorithm was applied on the whole set of normalized data filtering out genes not detected at all measured time points. All steps and settings were performed as described in Heard *et al.*.

3.2.7.5 Data analysis II: Prediction of gene-gene interactions

The data analysis to predict gene-gene interactions of the time-dependent microarray data was performed by Dr. Dietrich Trümbach of the molecular neurogenetics group at the Helmholtz Center in Munich.

<u>data preprocessing</u>

In order to reduce dye-biased effects on gene expression data a mixed linear model (two-way ANOVA) considering the factors time and dye was applied. Thus, by excluding genes showing a significant interaction between both factors ($p < 0.01$) the bias introduced by the different properties of the dyes could be removed. Only spot signals were taken into consideration which were measured at each point in time. ANOVA was performed on $\log_2$-transformed data the using statistical software R (http://www.r-project.org).

<u>supervised variable selection</u>

Univariate feature preselection was combined with a method for multivariate supervised variable selection. First, the variable selection algorithm excluded genes not differentially regulated across the time points are excluded. This reduction of the feature space can be

based on the t-statistic (Dudoit *et al.*, 2002) or on a nonparametric ranking method (Park *et al.*, 2001). With these test-statistics variables are ranked and the subsequent classifier is restricted to genes with the highest value. The number of predictor variables is a parameter which normally can be tuned via cross validation on training data. For the *in vitro* microarray data set a two way linear model was used and ranked the genes with respect to the p-value for the time-dependent effect. Due to the small sample size an optimal number of selected top ranked genes could not be determined but some trial values were used in order to get a tolerable computational burden. Therefore, no adjustment of p-values (e.g. Bonferroni correction) was performed.

To embed the genetic algorithm (GA) in the supervised variable selection procedure three parameters have to be pointed out: First, as key parameter the leave-one out cross-validation (LOOCV) procedure was chosen as measure of prediction accuracy. LOOCV has become a standard procedure to assess the performance of classification methods in microarray data analysis. The LOOCV method was applied to evaluate the fitness function that controls chromosome selection in the genetic algorithm.

Second, due to the dataset sparsity Fishers linear discriminant analysis (LDA) was utilized as classifier. LDA is a linear coordinate transformation, which maximizes between-class variance and minimizes within-class variance. The discriminant function depends on the common covariance matrix as well as on the means for every variable over all classes (time points) and can be written as

$$f_q(\vec{e}) = \vec{\mu}_q^T \Sigma^{-1} \vec{e} - \frac{1}{2} \vec{\mu}_q^T \Sigma^{-1} \vec{\mu}$$

where $\vec{\mu}_q$ is the mean vector in class q, $\vec{e}$ represents the gene expression data vector and Σ the covariance matrix. The pooled estimate of all class covariance matrices Σq is the common covariance matrix

$$\Sigma = \frac{1}{M_t - Q} \sum_{q=1}^{Q} \Sigma_q$$

with M_t acting for the number of training samples and Q for the number of classes.

Third, to identify a subset of features with good interpretability a selection procedure based on the frequency of genes covered by so called optimal chromosomes was applied. In consequence, one important parameter is the so-called chromosome size which means that the search for optimal solutions is restricted to subsets of this size. At the starting point of any GA only a small portion of the total search space is explored. Therefore, different searches are likely to provide different solutions. In order to extensively cover the space of models that can be explored it is necessary to collect a large number of variable combinations.

Finally, a gene ranking was based on the occurrence of each feature in a chromosome satisfying the goal fitness (LOOCV). With this method not only the best combination of features but also cluster of genes were identified.

For supervised multivariate variable selection *GALGO*, an R package that is based on genetic algorithm (GA) search procedure, was used (Trevino and Falciani, 2006). To avoid overfitting linear discriminant analysis was restricted to subsets of five variables (chromosome size). The search parameters in the genetic algorithm included up to 2500 iterations and an estimated classification accuracy with optimizing criteria of 100% (goal fitness). Finally, the topmost 50 genes were selected. In order to validate gene rank stability and to isolate genes occurring in several analyses the feature selection algorithm was repeated separately four times with the same input data and parameter settings.

modeling of gene interactions

To reveal groups of genes which act together, first, an unsupervised method - principal component analysis (PCA) - was used to describe the correlation structure of the selected genes. Correlations between genes determined by PCA from gene expression patterns are visualized by biplots (within the package *stats* in R). A biplot allows reduced information on both rows and columns of a data matrix to be simultaneously plotted. Complete information and further explanations of biplots can be found elsewhere (Gabriel, 1971; Gower and Hand, 1996). Additionally, a search for correlations, which cannot be explained by other variables, was performed. These partial correlations are used as a measure of conditional independence and are the basis for graphical Gaussian models (GGMs). For construction of gene association networks - GGMs that represent multivariate dependencies - the R package *GeneNet* (Schäfer *et al.*, 2006) was used. To verify the predicted network from *GeneNet* the corresponding gene-gene interactions were searched for in all PubMed abstracts with help of a text mining program (*PathwayStudio* 5.0, Ariadne Genomics, Rockville, USA) based on the Natural Language Processing (NLP) Technology.

3.2.7.6 Data analysis III: Strongest regulated genes

To identify the strongest regulated genes, simple cut off criteria with p-value < 0.05, |Z-score| $\geq$ 1.837 and |fold regulation| $\geq$ 1.3 were applied. The Z-score is an additional statistical criteria and is calculated with the $\log_2$[ratio] of the mean expression values divided by the standard deviation. With a |Z-score| $\geq$ 1.837 accept2 = true and fulfills the statistical cut off. Additionally, raw signal intensity > 950 was set as threshold ensuring the practicability of independent confirmation by qRT-PCR.

The annotation of selected and further analyzed candidate genes was verified by sequencing of the corresponding array clones (Sequiserve, Vaterstetten, Germany).

3.2.8 Expression analysis using microarray technology: *in vivo*

The RNA of pituitaries of stressed CRHR1-wt and -ko mice from different time points (1, 3 h) and their unstressed controls was isolated as described. RNA quality was verified by agarose gel electorphoresis and RNA concentration was measured at 260 nm with a spectrophotometer.

For the analysis of the differential expression pattern of unstressed and stressed CRHR1-wt versus -ko mice the Illumina Sentrix® BeadChip Array for Gene Expression Mouse-6 (Illumina, San Diego, USA) was used containing 45200 transcripts covering more than 19100 unique, curated genes in the NCBI RefSeq database (Build 36, Release 22). In average every probe is represented by 10 beads.

3.2.8.1 RNA amplification

0.5 µg of isolated RNA (pools of 2 animals per group) were amplified using the Illumina® TotalPrep RNA Amplification Kit (Ambion) according to manufacturer´s instructions. Shortly, RNA was reverse transcribed and then *in vitro* transcribed to cRNA. During the *in vitro* transcription biotin-labelled NTPs were incorporated.

3.2.8.2 Hybridization

1.5 µg cRNA per sample was hybridized to the Illumina Sentrix® BeadChip Array for Gene Expression Mouse-6 according to the manufacturer´s protocol. Hybridization was performed over night at 55°C under rotation in hybridization chambers provided by Illumina. The BeadChip was washed and blocked and bound cRNA was detected with a streptavidin-Cy3 dye (Amersham). Two technical replicates per sample were performed.

3.2.8.3 Scanning and bead level intensity extraction

Sentrix® BeadChips were scanned with the BeadStation 500G Genotyping System (Illumina) with standard settings of Illumina BeadScan software and a PMT factor of 4.5035305. The bead level intensity was extracted and the mean values of all beads per probe were calculated with activated outlier detection function.

3.2.8.4 Statistics and data analysis

Data was normalized with the BeadStudio software version 1.5.1.3 (Illumina) using the cubic spline parameter for balancing non-linear effects. For statistical analysis the Illumina custom settings were chosen which are based on a moderate t-test adjusted with

empirical factors. The diff score was used as statistical cut off criteria. The diff score is a transformation of the p-value of the statistic significance of the gene signal compared to reference. It is the $\log_{10}$ of the p-value. For selection of candidate genes the diff score had to be larger than $|13|$ (p-value < 0.05), the $|\text{differential expression}| \geq 1.5$ and the detection level > 0.99 in both compared samples.

3.2.9 *In situ* hybridization

Frozen brains were mounted on polyfreeze tissue freezing medium (Polyscience Inc., Eppelheim, Germany) and coronally cut in a cryostat (HM560, Microm, Walldorf, Germany) in 20 µm thick consecutive sections. Brain sections were mounted on super frost plus microscope slides (Menzel, Braunschweig, Germany), dried on a 37°C warming plate (ElectKarl Rothermal, Rochford, UK) and stored at - 20°C. For comparability of the results brains from basal CRHR1-wt and -ko mice or stressed CRHR1-wt and -ko mice were always cut in parallel on one slide.

3.2.9.1 Radioactive labeling of probes

The probe for Errfi1 was amplified out of the MPIP 24 k array clone 2197 inserted in the pT3/T7-Pac plasmid. The bacteria clone was inoculated in LB medium and plasmid DNA was prepared using QIAprep Spin Miniprep Kit. Using T3 and T7 primer a PCR was performed:

1 µl	plasmid DNA
5 µl	10 x reaction buffer IV (ABgene)
3 µl	25 mM $MgCl_2$ (ABgene)
1 µl	10 mM dNTPs (Roche)
3 µl	10 µM T3 pT3T7 primer
3 µl	10 µM T7 pT3T7 primer
0.5 µl	Thermoprime Plus DNA polymerase (5 U/µl, ABgene)
add 50 µl	H_2O_{bidest}

PCR was carried out in a PCR machine with the following temperature settings:

program	cycles	temperature	hold
preincubation	1	94°C	3 min
amplification: *denaturation* *annealing* *elongation*	35	 94°C 55°C 72°C	 30 sec 30 sec 90 sec
	1	72°C	5 min

The PCR fragment was extracted from an agarose gel and cloned into the pCR®II-TOPO® vector. A T7/Sp6 PCR was performed (settings like T3/T7 PCR with an annealing temperature of 67°C). This PCR product was used as Errfi1 probe for radioactive labelling.

The *in vitro* transcription was pipetted as follows (mastermix for approximately 20 slides):

2 µl	PCR product
16 µl	H_2O-DEPC
3 µl	10 x transcription buffer (Roche)
3 µl	NTP-mix (rATP/rCTP/rGTP 10 mM each; Roche)
1 µl	0.5 M DTT
1 µl	RNasin (RNAse-inhibitor; 40 U/µl; Roche)
3 µl	35S-thio-rUTP from Amersham (12,5 mCi/mM; 1250 Ci/mmol)
1 µl	T7 (antisense) or SP6 (sense) RNA polymerase (20 U/µl, Roche)

The reaction samples were mixed gently by tapping the Eppendorf tube and spinned down quickly. Then, the samples were incubated at 37°C for 3 hours in total; after 1 h another 0.5 µl of RNA polymerase was added.
To destroy the DNA template, 2 µl RNase-free DNase I (10 U/µl; Roche) were added and samples were incubated for 15 min at 37°C.

3.2.9.2 Purification of riboprobes

For purification of riboprobes the RNeasy Mini Kit (Qiagen) was used according to manufacturer´s protocol. RNA was diluted in 100 µl RNase-free water and 1 µl of the probe was measured in 2 ml scintillation fluid (Zinsser Analytic, Frankfurt, Germany) in a beta-counter (LS 6000 IC, Beckmann Coulter). For *in situ* hybridization 35000 to 70000 cmp/µl and 90 µl/slide (7 Mio/slide) were required.

3.2.9.3 Pre-treatment of cryo-slides

Slides were taken out of the - 20°C freezer and warmed up for at least 1 h at 37°C while still in the box. Then they were spread out on clean cotton tissue and dried for another 15 min. For pre-treatment the following protocol was applied:

action	duration	chemical	comments
1. fix	10 min	4 % PFA/PBS	ice-cold (4°C)
2. rinse	3 x 5 min	PBS/DEPC	
3.	10 min	0,1 M triethanolamine-HCl (pH8.0) (TEA) (200 ml)	add 600 µl acetic anhydride (Sigma-Aldrich) to rapidly rotating stirring bar of TEA
4. rinse	2 x 5 min	2xSSC/DEPC	
5. dehydrate	1 min	60 % ethanol/DEPC	
6.	1 min	75 % ethanol/DEPC	

action	duration	chemical	comments
7.	1 min	95 % ethanol/DEPC	
8.	1 min	100 % ethanol	
9.	1 min	$CHCl_3$	
10.	1 min	100 % ethanol	
11.	1 min	95 % ethanol/DEPC	
12. Air dry (dust free !)			

3.2.9.4 Hybridization

An appropriate amount of hybridization mix (hybmix) containing the riboprobe was prepared. 90 to 100 µl hybmix and 3.5 to 7 million counts per slide were required.

The hybridization mix containing the probe was heated to 90°C for 2 min, put shortly on ice, then on room temperature. The solution was pipetted onto the slides and coverslips (Marienfeld, Lauda-Königshofen, Germany) were carefully mounted, avoiding air bubbles in between. The slides were carefully placed into a hybridization chamber containing hybridization chamber fluid to prevent drying out of the hybmix and the chamber was sealed with adhesive tape. The slides were incubated in an oven (Memmert, Schwabach, Germany) at 55-68°C o. n. (up to 20 h).

3.2.9.5 Washing

After hybridization the coverslips were carefully removed and the following protocol was applied:

	duration	temperature	chemical	comments
1.	4 x 5 min	Rt	4xSSC	
2.	20 min	37 °C	NTE (20µg/ml RNaseA)	add 500 µl RNaseA(10mg/ml, Sigma-Aldrich) to 250 ml of NTE
3.	2 x 5 min	Rt	2xSSC/1 mM DTT	50 µl of 5 M DTT/250 ml
4.	10 min	Rt	1xSSC/1 mM DTT	50 µl of 5 M DTT/250 ml
5.	10 min	Rt	0,5xSSC/1mM DTT	50 µl of 5 M DTT/250 ml
6.	2 x 30 min	64 °C	0,1xSSC/1 mM DTT	50 µl of 5 M DTT/250 ml
7.	2 x 10 min	Rt	0,1xSSC	
8.	1 min	Rt	30 % Ethanol in 300 mM NH_4OAc	
9.	1 min	Rt	50 % Ethanol in 300 mM NH_4OAc	
10.	1 min	Rt	70 % Ethanol in 300 mM NH_4OAc	
11.	1 min	Rt	95 % Ethanol	
12.	2 x 1 min	Rt	100 % Ethanol	
Air dry in dust free area.				

3.2.9.6 Autoradiography

Dried *in situ* sections were exposed to a special high performance X-ray film (BioMax MR from Kodak) for 10-20 hours.

3.2.9.7 Dipping

The slides were dipped in a prewarmed photographic emulsion (KODAK NTB2 emulsion, diluted one to one with Ampuwa water, stored at 4°C) for about 4 sec and dried over night at room temperature. Then they were packed into light-tight black boxes with sufficient desiccant (silica gel capsules, Karl Roth), labelled and sealed with tape. The slides were exposed for one week at 4°C.

3.2.9.8 Development

The boxes were equilibrated to room temperature for 2 h while still sealed. The slides were developed in KODAK D 19 developer (Sigma-Aldrich, P5670) for 3 min at room temperature, rinsed 30 sec in tap water and fixed in KODAK fixer (Sigma-Aldrich, cat# 197 1720) for 5 min. Then, they were rinsed in running tap water for 30 min. Using a razor blade (NeoLab, Heidelberg, Germany) the emulsion was scratched from the back side of the slides and the slides were air dried.

3.2.9.9 Nissl staining

After development brain sections were counterstained with the synthetic dye cresyl violet. This basic aniline dye is able to stain the RNA of the rough endoplasmatic reticulum, called Nissl substance, in the cytoplasm of neurons.

	duration	**chemical**
1.	20 min	0.5% Cresyl violet acetate
2.	1 min	water
3.	2 x 1 min	70% ethanol
4.	1 min	96% ethanol + 1 ml of acetic acid
5.	2 x 1 min	96% ethanol
6.	2 x 1 min	100% ethanol
7.	2 x 5 min	xylol (Karl Roth)

3.2.9.10 Quantification of relative expression

Expression of mRNAs in different brain areas was quantified by measuring the OD on scanned ISH films using the freely available computer program *ImageJ* 1.36b (http://rsb.info.nih.gov/ij/).

3.2.9.11 Image editing

Images of the Errfi1 expression on x-ray films and of the Nissl staining on slices were taken on a binocular microscope (Leica, Wetzlar, Germany) and processed with the Adobe Photoshop CS2 software. On all pictures, background was set white and artifacts were erased.

3.2.10 Statistical analysis

Data was analyzed for two-group comparisons using unpaired Student`s t-test and the software GraphPad Prism 4. Differences were considered statistically significant when $p<0.05$. Data are presented as mean ± SEM.

4. Results

4.1 New target genes of CRHR1-dependent signaling pathways *in vitro* and *in vivo*

To identify new target genes regulated by stress and/or CRH via CRHR1-dependent mechanisms the changes in mRNA expression *in vitro* and *in vivo* caused by stimulation of CRHR1-activated signaling cascades were investigated using microarrary technology.

4.1.1 Analysis of CRH-stimulated signaling pathways in AtT-20 cells

In vitro, AtT-20 cells, a commonly used cell culture model system, were used for investigation of CRH/CRHR1-activated signaling pathways. As the CRHR2 was not found expressed in AtT-20 cells (see chapter 4.3.1), only the CRH receptor type 1 was stimulated by treatment with 100 nM CRH. To analyze time-dependent changes in mRNA expression as response to CRH, five different treatment time points (1, 3, 6, 12 and 24 h of chronic CRH stimulation) were analyzed. For every time point untreated cells were used as control.

4.1.1.1 ACTH and Pomc levels

To verify successful CRH treatment, ACTH concentrations in the cell culture medium and Pomc mRNA expression were evaluated.

ACTH protein amounts in the supernatant were measured by radioimmune assay (RIA) revealing CRH-triggered ACTH release of the corticotrope AtT-20 cells. After 1 and 3 h of chronic CRH stimulation, AtT-20 cells release approximately 2.5 and 1.5 fold, respectively, more ACTH in comparison to their untreated control cells. At 6, 12 and 24 h no increased ACTH release was detected comparing CRH-treated and control AtT-20 cells (Fig. 6)

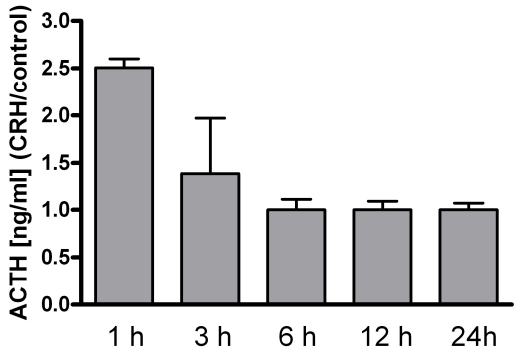

Figure 6. ACTH concentrations in cell culture medium of AtT-20 cells. Cells were treated with 100 nM CRH for indicated time periods. Values are means of biological duplicates, error bars represent SEM.

At the same time, CRH is stimulating Pomc transcription which was examined by qRT-PCR. After 3 and 6 h of stimulation, Pomc expression increased slightly but significantly.

At the 12 h time point, the activation of Pomc mRNA expression peaked out and returned to basal level after 24 h of CRH treatment (Fig. 7).

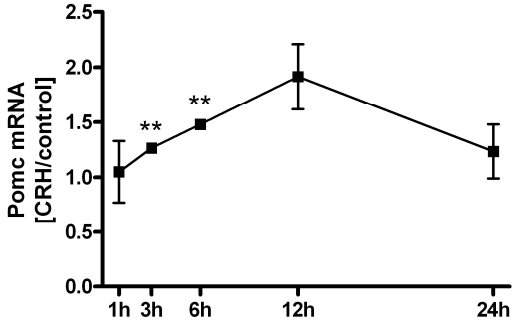

Figure 7. Pomc expression after CRH treatment of AtT-20 cells. Pomc mRNA levels of 100 nM CRH-treated AtT-20 cells were quantified by qRT-PCR and related to untreated controls at indicated time points. Pomc values were normalized to the house keeping gene Hprt and are means of biological duplicates, error bars represent SEM. $p<0.01$=** in a t-test treated vs. untreated.

4.1.1.2 Gene expression profiling using the MPIP 24 K platform

CRH stimulation of CRHR1-dependent signal transduction leads to activation or inhibition of gene expression. To detect those changes on the mRNA level, the MPIP 24 k microarray chip was used. CRH-treated and control AtT-20 cells were harvested at investigated time points (1, 3, 6, 12 and 24 h) and total RNA was isolated. RNA quality was controlled by gel electrophoresis. All RNA samples showed clear 28, 18 and 5 S ribosomal RNA bands indicating fully intact RNA without any signs of degradation (data not shown). After amplification, aRNA was again analyzed on an agarose gel which revealed similar fragment sizes of all aRNA samples mainly ranging in size from 500 to 1500 bp (data not shown). Microarray hybridization was performed in six technical replicates, three for each dye combination - meaning Cy3 control versus Cy5 treated and vice versa - in order to exclude any dye-biased effect.

After data normalization 12593 genes were found expressed at all time points whereas 15418 transcripts were detected in AtT-20 cells in at least one time point. The gene expression data have been deposited in NCBI's Gene Expression Omnibus (GEO) (Edgar *et al.*, 2002) and are accessible by the GEO Series accession numbers GSE13156 and GPL7467.

To focus on the most important genes regulated by CRH/CRHR1 three different approaches for analyzing the expression data were applied. With the Bayesian model-based hierarchical clustering genes were grouped according to their differential expression over time. Using a genetic algorithm combined with graphical Gaussian models gene-gene interactions based on the time-dependent regulation pattern were predicted. Finally, the genes showing the strongest regulation were considered for further experiments.

Bayesian model-based hierarchical clustering

The clustering methodology *Spinecluster* performs Bayesian model-based hierarchical clustering of time curve expression data. *Spinecluster* was applied on the normalized data set including the 12593 genes detected at each time point. The optimal number of clustering maximizing the log unnormalized marginal probability was 10 (Fig. 8 and 9). Clustered genes were analyzed according to Gene Ontology (GO) categories (NCBI) and grouped into the main functional classes metabolism, transport, development, signal transduction and transcription/translation. However, the majority of the clustered genes could not be classified by Gene Ontology categories. Those genes were excluded. The percentage of genes within the mentioned GO classes was calculated in relation to all genes with annotated function per cluster. Genes with diverse GO classes occur several times.

Cluster 1 contains 575 genes which showed an upregulation after 1 h of CRH stimulation and returned back to basal level after 3 h. 53% of the functionally annotated genes were assigned to the functional class of metabolism, 39% to transport, 45% to development, 28% to signal transduction and 20% to transcription/translation (Fig. 8).

In cluster 2, 179 genes were found upregulated at 1 h, downregulated at 3 h and returned to basal level after 6 h of CRH treatment. 21% of these genes are related to metabolism, 17% to transport, 29% to development, 21% to signal transduction and 17% to transcription/translation (Fig. 8).

Cluster 3 consists of 44 genes which showed a downregulation after 1 h followed by an upregulation after 3 h. At 6 and 12 h, genes were not differentially expressed comparing CRH treated and untreated cells, but after 24 h they were again slightly upregulated. Genes downregulated within the first hour of CRH stimulation are mainly transcripts involved in metabolism (69%), whereas none of them are involved in transport function. The functional classes of signal transduction (8%) and transcription/translation (31%) were respectively decreased and increased in comparison with the other clusters, but the relative number of genes involved in development (23%) was similar (Fig. 8).

The biggest cluster 4 contains the majority of the detected genes. 11378 genes did not exhibit any regulation over time according to *Spinecluster*.

59 genes were grouped in cluster 5 and were besides the 12 h time point similarly regulated over time as in cluster 3. The downregulation at 1 h and the upregulation after 3 h returned to basal level at 6 h. After 12 and 24 h these genes were again upregulated by CRH. Most of those genes were assigned to metabolism (36%), but in contrast to cluster 3, 27% of the genes were classified by transport functions. Some genes of this cluster are involved in signal transduction (9%) and transcription/translation (9%) (Fig. 8).

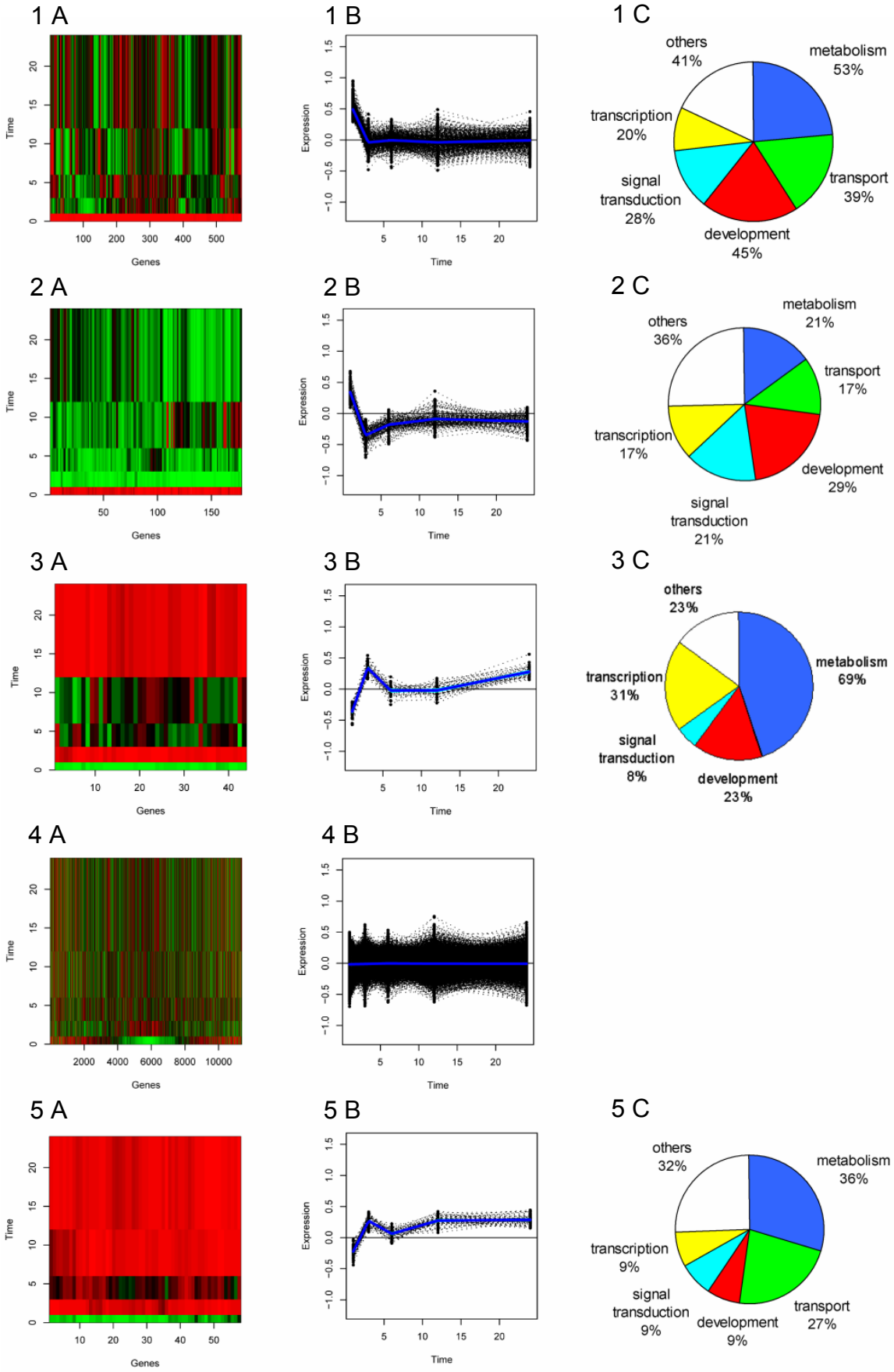

Figure 8. *Spinecluster* results for clusters 1-5. (A) Heat maps of co-regulated gene clusters, (B) corresponding scatter plots and (C) GO classification as revealed by Bayesian model-based hierarchical clustering. Blue lines show cluster mean profiles with light blue lines indicating plus or minus two posterior standard deviations of the profile from the mean.

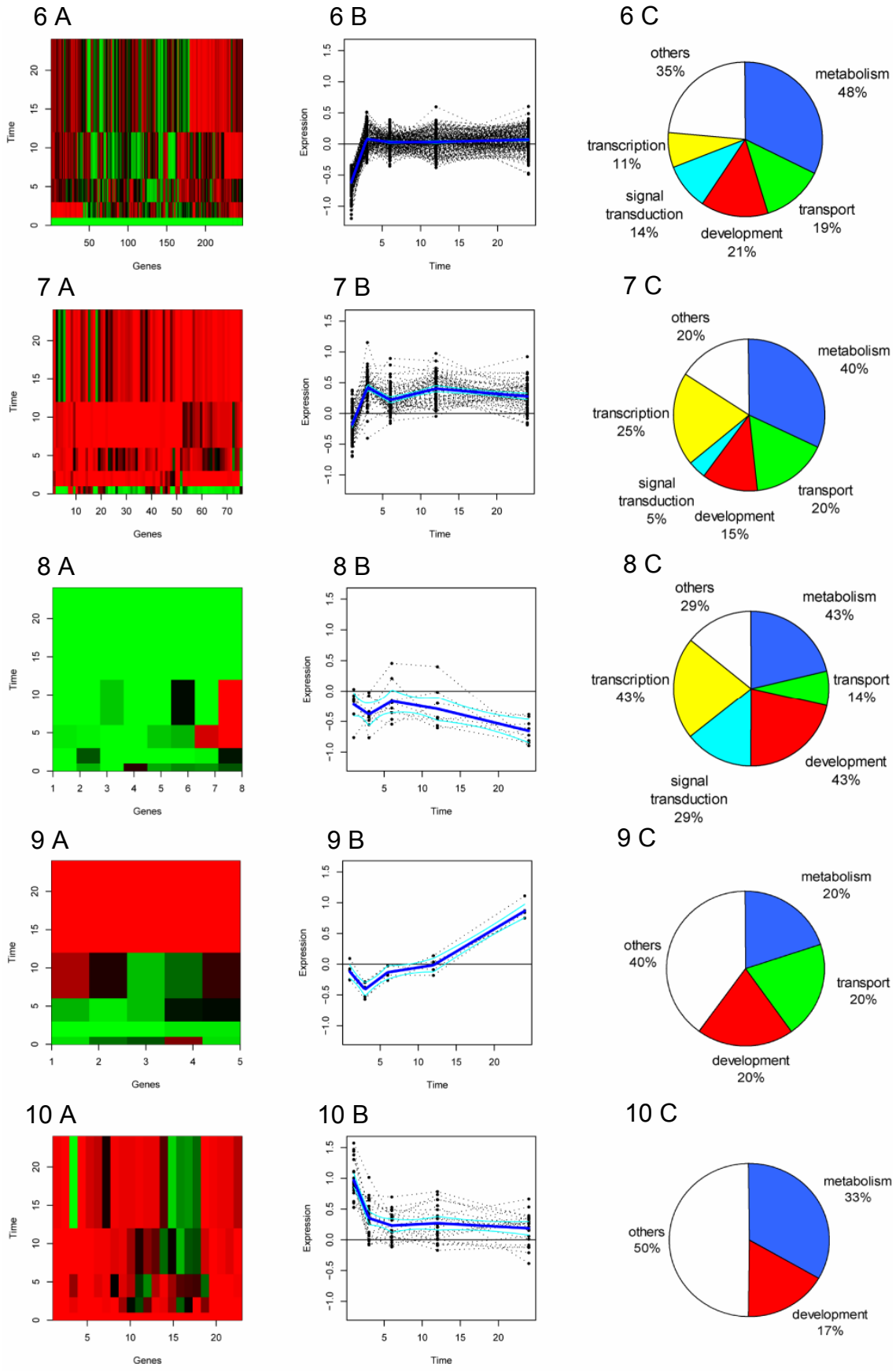

Figure 9. *Spinecluster* results for clusters 6-10. (A) Heat maps of co-regulated gene clusters 6-10, (B) corresponding scatter plots and (C) GO classification revealed by Bayesian model-based hierarchical clustering. Blue lines show cluster mean profiles with light blue lines indicating plus or minus two posterior standard deviations of the profile from the mean.

The genes of cluster 6 (248) were downregulated after 1 h, too, but after 3, 6, 12 and 24 h no differential expression was detected. The classification in GO groups is as follows: 48 % metabolism, 19% transport, 21% development, 14% signal transduction, 11% transcription/translation (Fig. 9).
In cluster 7, 76 genes were upregulated after 3, 6, 12 and 24 h. Metabolic (40%), transport (20%) and developmental (15%) functions are not over- or underrepresented in comparison to the first two clusters, but signal transducing genes (5%) are reduced while transcriptional/translational molecules (25%) are increased (Fig. 9).
In cluster 8, genes (8) downregulated at all measured time points are represented. Again, the metabolism GO group is overrepresented (43%), as it is in cluster 9 (20%) where the 5 genes were downregulated within the first 6 h, but increased after 24 h (Fig. 9).
The last cluster 10 consists of 23 genes strongly upregulated within the 1 h of CRH stimulation staying less strongly upregulated over all time points. This cluster represents genes involved in metabolism (33%) and development (17%) (Fig. 9).
The clusters 1, 2 and 10 contain all genes which were upregulated after 1h of CRH treatment. The assessed GO functions are similarly distributed in clusters 1 and 2 containing more than 20% of genes involved in signal transduction. Genes downregulated in the first hour of CRH stimulation are in the clusters 3, 5, 6, 7, 8 and 9 where genes with signal transductional function are underrepresented (< 15%). Only the functional distribution of the genes in clusters 8, 9 and 10 does not fit because of the small number of genes in those clusters.

Prediction of gene-gene interactions

To predict gene-gene interactions, an efficient variable selection strategy by consecutive application of univariate as well as multivariate methods followed by graphical models was performed. Feature preselection was used to exclude genes from the dataset not differentially regulated over time. After normalization, signals of 12593 spots measured at each time point were tested applying a mixed linear model to exclude genes showing significant dye-dependent differences in their expression profile over. Thus, differential expression values of 946 genes with a significant interaction of the factors time and dye were removed from the dataset.
It is important to further restrict microarray data before multivariate analysis since most of the genes show constant up- or down over time through CRH stimulation and thus do not contribute to the discrimination between classes. By applying a two-way linear model without interaction of the factors time and dye genes were preselected for supervised clustering with linear discriminant analysis (LDA) and variable selection using the R package *GALGO*. Within the univariate feature preselection process genes that did not

show differential regulation over time were excluded by two-way ANOVA. By this preselection process, 1175 ($p<0.05$) and 387 ($p<0.01$) genes, respectively, were identified as significantly regulated over time. To reduce the solution space and to generate more stable results the smaller set of 387 genes ($p<0.01$) was used as input for the *GALGO* program. The *GALGO* analysis was repeated separately four times and the top most 50 genes of each run were compared on the basis of their frequency ranks. The frequency rank of each gene was determined by counting the chromosomes (sets of five genes), in which the gene occurred, reaching a classification accuracy of 100% (goal fitness). Table S1 (see Supplementary Data) shows the complete list of 111 genes derived from four independent *GALGO* analyses based on the preselected genes. Genes that were not present in each of the four ranked lists were omitted. In total, 15 genes that occured in all four runs among the topmost 50 ranked genes. Excluding those genes that were not fully annotated, a total of 10 genes remained in four runs among the topmost ranked genes. Because Hmgcs1 was detected twice (Spot ID 6705 and 16977) in at least three *GALGO* analysis results this gene was also defined as possible target gene. Hence, 11 unique candidate genes were selected for further validation by qRT-PCR and modeling of gene-gene interactions via *GeneNet*.

The 11 genes identified by supervised multivariate variable selection using LDA/GA (*GALGO*) contributed strongly to the discrimination between groups (time points). Furthermore, the selected genes were expected to be highly correlated with each other in terms of gene interaction networks. In order to test whether a separation of the expression profiles of these genes into time points (after CRH treatment) can be achieved using unsupervised clustering methods a principal component analysis (PCA) was performed. The gene (column) by time point (row) matrix of expression ratios was analyzed by PCA to determine the scores for objects (time points) and the loadings for variables (gene expression patterns), respectively. Gene vectors in the biplot with similar positive values on the x-axis (PC1) and small angles between the vectors, e.g. Pex13, Cd3e and Nf2 collapsed with the 24 h data points, were well correlated with each other while Fosl2 and Crem that showed negative values on PC1 and located nearby the 1 h data points were also well correlated (Fig. 10A). If the vectors point at the same region as the data points of the objects the gene expression is increased otherwise decreased. Time points close to each other in Figure 9A had similar gene expression patterns, which is supported by the heatmap in Figure 9B showing e.g. Fosl2 and Crem (with positive values on the y-axis (PC2, Fig. 10A) upregulated after 1 h and downregulated after 24 h of CRH treatment whereas Pex13, Cd3e and Nf2 were downregulated after 1 h and upregulated after 24 h. Gene vectors appearing with an angle of approximately 90° are poorly correlated (e.g. Pex13 cf. to Fosl2) whereas angles about 180° illustrate negative correlation (e.g. Nf2 cf.

Acsl4) meaning contrary differential expression. Furthermore, Figures 10A and 10B show that the expression patterns of the 11 genes are able to clearly discriminate between the time points 1, 12, and 24 h but only partially the time points 3 and 6 h.

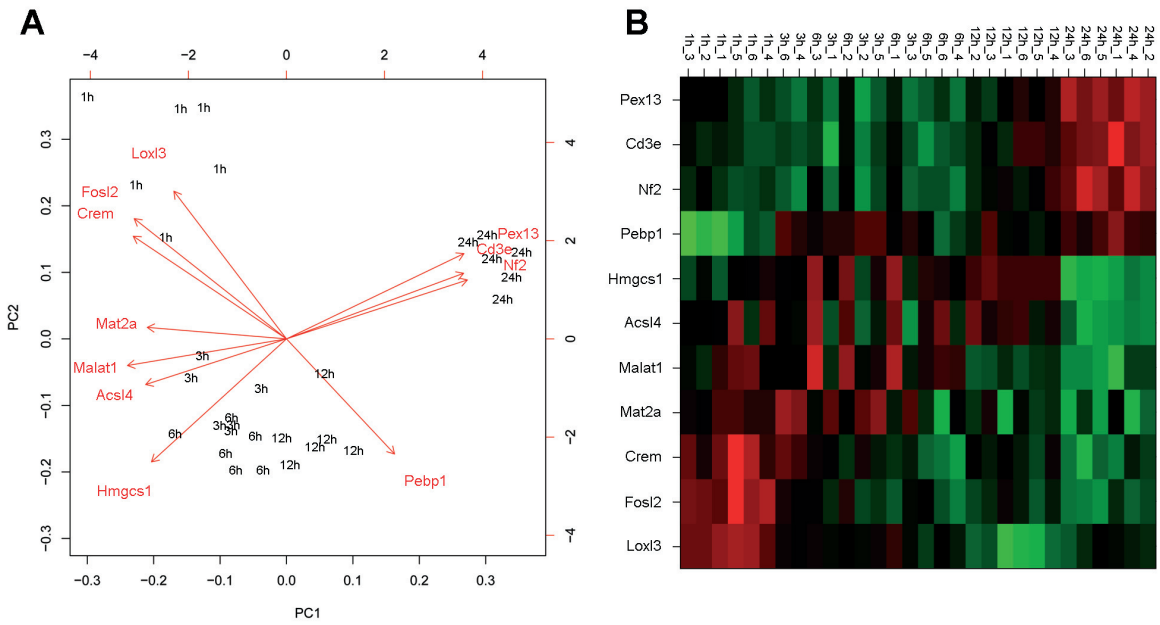

Figure 10. PCA results. (A) Biplot of 11 candidate genes (vectors) and time points after CRH treatment (scores). The first two principal components (PC1 and PC2) were used to generate the biplot. (B) The heat map represents the grouping of genes and time points by PCA. Positive and negative values of log base 2 expression ratios are colored in red and green, respectively. Black colored expression ratios illustrate no differential expression.

The same subset of 11 genes with high frequency ranks derived from the supervised variable selection procedure and investigated by PCA was further analyzed by constructing a gene association network with help of the R package *GeneNet*, another unsupervised correlation method. The resulting undirected graph from the *GeneNet* program is shown in Figure 11. Gene pairs were considered with $|pcor| \geq 0.35$ and corresponding p-values < 0.05 at their edges and additionally unconnected nodes. The association network of putatively co-regulated genes consists of four main subnetworks with the gene clusters Fosl2-Crem, Cd3e-Pex13-Nf2, Acsl4-Hmgcs1 and Loxl3-Malat1 (Fig. 11, where Hmgcs1 and Loxl3 are negatively partial correlated).

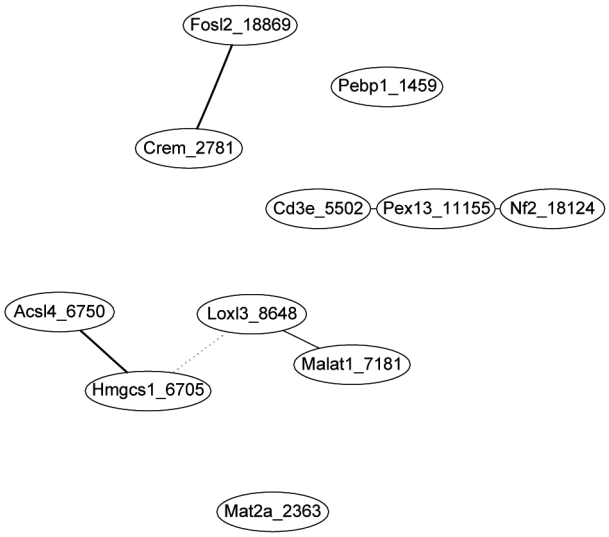

Figure 11. Undirected graph computed by *GeneNet.* Depticted are genes which occurred in four *GALGO* analyses. Additionally, Hmgcs1 was included, which occured twice in three of the *GALGO* runs among the fifty topmost ranked genes. Solid lines in black depict positive partial correlation between genes. The dotted line between Hmgcs1 and Loxl3 represents a negative partial correlation.

A complete discrimination (LOOCV=1) into time points was achieved with sets of five genes (chromosomes) in the case of Pebp1, Mat2a, Crem, Hmgcs1 and Malat1 as well as in case of Mat2a, Crem, Cd3e, Fosl2 and Malat1. The accordance of genes from these two chromosomes with genes in every subnetwork by *GeneNet* indicates that all four clusters including the two unconnected nodes (Fig. 11) play an important role for the description of the overall time response.

To validate candidate interactions revealed in PCA and *GeneNet* analyses the literature mining software *PathwayStudio* was used. As interactions direct and indirect protein-protein interactions, expression and promoter binding as well as regulation such as common regulators or targets were taken into account. Every connection found by *PathwayStudio* was confirmed manually and incorrectly associated interactions were excluded.

The link between Malat1 and Loxl3 (Fig. 11) was not verified with *PathwayStudio* software. In addition, also for the negative partial correlation between Hmgcs1 and Loxl3 no relation was found with *PathwayStudio*. Nf2, Pex13 and Cd3e clustered together in the *GeneNet* algorithm because of their regulation after 24 hours of CRH stimulation. The theoretical verification of these interactions with the *PathwayStudio* software resulted in an indirect protein-protein interaction via SH3 domains (Chadee et al., 2006; Cuevas et al., 1999; Delibrias et al., 1997; Kissil et al., 2003). According to the literature the candidate genes Hmgcs1 and Acsl4 were found indirectly connected via the peroxisomal proliferator-activated receptor α (PPARA) (Forman et al., 1997; Hertz et al., 1994; Hsu et al., 2001). Moreover, for Crem and Fosl2 literature mining revealed cAMP as the connecting molecule (Lamas and Sassone-Corsi, 1997; Schwenger et al., 2002; Spessert et al., 2000). CRH triggers the synthesis of cAMP as second messenger and Acsl4, Nf2,

Crem and Fosl2 are known to be regulated by cAMP (Alfthan et al., 2004; Cornejo Maciel et al., 2005; Lamas and Sassone-Corsi, 1997; Schwenger et al., 2002; Spessert et al., 2000) connecting those 4 candidate genes with known CRHR1 signaling cascades (Fig. 12).

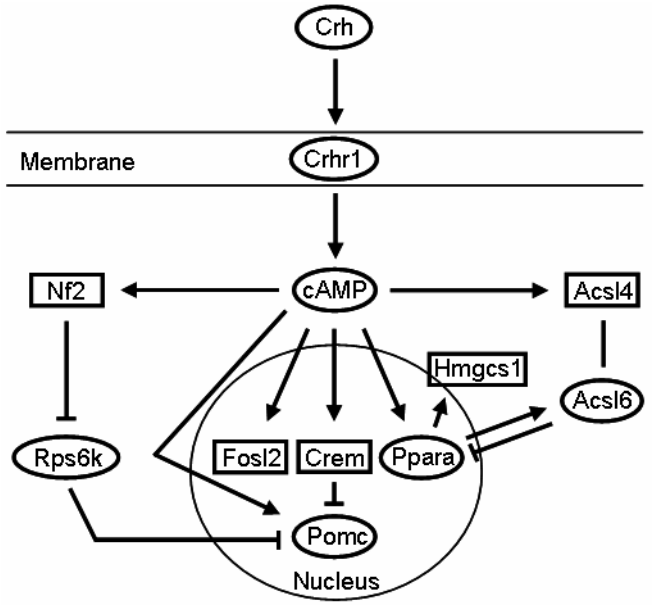

Figure 12. Potential gene interactions obtained by literature mining. Results of shortest path searches between all candidate genes investigated by *GeneNet* using the *PathwayStudio* software. After manual curation of each interaction the resulting pathways were combined in this picture. Differentially expressed in the microarray and experimentally with qRT-PCR validated genes are drawn by rectangles and intermediates are indicated by circles. Lines with an arrowhead reflect positive regulation, other lines indicate inhibition.

Strongest regulated genes

Besides the applied algorithms to cluster regulated genes time-dependently and to find gene-gene interactions based on the time curve expression data, the strongest regulated genes at each time point were examined. By setting a simple cut off of |fold regulation |≥ 1.3, accept2 = true or $p < 0.05$ and mean expression > 950, 102 transcripts were found significantly regulated in at least one time point (Table S2, Supplementary Data). These 102 candidates can be found in the clusters 1, 3, 4, 6, 7, 8, 9 and 10 of the Bayesian model-based clustering. Additionally, 8 of the candidate genes did not fit to any cluster because of missing data points. Moreover, half of the top 16 transcripts retrieved by *GALGO* analyses were significantly regulated according to chosen cut off (Table S2).

Expression differences of at least 1.5 fold are a prerequesite for reliable validation of gene regulation by independent methods such as qRT-PCR. Therefore, an additional cut off with |fold regulation| ≥ 1.7 was used to reduce the number of potential candidate genes to 20 (Table 6).

Table 6. Genes significantly regulated by CRH revealed by microarray data. Cut-off: |fold regulation| ≥ 1.7, accept2 = true or $p < 0.05$, mean expression > 950, in at least one time point; genes in boldface were chosen for qRT-PCR validation.

spot ID	accession number	gene symbol	description	fold regulation				
				1 h	3 h	6 h	12 h	24 h
7181	AI227072	2210401K01Rik[8]	Metastasis associated lung adenocarcinoma transcript 1 (non-coding RNA)	-1.11	-1.26	1.16	-1.48	-1.80
2781	AI846359	**Crem[10,G]**	cAMP responsive element modulator	3.13	2.02	1.28	1.66	1.11
9199	AI413641	D11Bwg0434e[3]	DNA segment, Chr 11, Brigham & Women's Genetics 0434 expressed	-1.74	1.29	-1.14	-1.12	1.17
5034	AI851272	**Dusp14[b]**	Dual specificity phosphatase 14	1.84	1.64	1.30		-1.19
2197	AI853531	**Errfi1[1]**	ERBB receptor feedback inhibitor 1	1.87	1.06	1.01	1.09	1.08
19524	AI851247	**Fosl2[10]**	Fos-like antigen 2	1.80	1.36	1.17	1.28	1.13
18869	AI848789	**Fosl2[10,G]**	Fos-like antigen 2	2.51	1.46	1.39	1.40	1.16
6705	AI841574	**Hmgcs1[8,G]**	3-hydroxy-3-methylglutaryl-Coenzyme A synthase 1	-1.07	-1.02	1.37	1.32	-1.76
9477	AI835922	**Kif3a[9]**	Kinesin family member 3A	-1.14	-1.30	-1.13	-1.13	1.79
12686	AI429298	**Kif3a[10]**	Kinesin family member 3A	1.80	1.26	1.25	1.27	1.01
7645	AI415104	**Mpp7[7]**	Membrane protein, palmitoylated 7 (MAGUK p55 subfamily member 7	-1.03	2.23	1.01	1.09	1.24
1333	AI842320	**Nf2[9]**	Neurofibromatosis 2	-1.15	-1.23	-1.02	-1.06	1.83
18124	AI323564	**Nf2[9,G]**	Neurofibromatosis 2	-1.14	-1.48	-1.12	1.10	2.16
12495	BE135684	Odc1[7]	ornithine decarboxylase, structural 1	1.12	1.75	1.12	1.44	1.10
8455	AI852492	**Pak3[7]**	P21 (CDKN1A)-activated kinase 3	-1.06	1.34	1.86	1.81	1.33
16914	AI847765	**Rgs4[7]**	Regulator of G protein-signaling 4	-1.84	-1.33	-1.22	-1.52	-1.45
6751	AI843967	**Syt4[10]**	Synaptotagmin IV	1.33	1.65	1.62	1.72	1.29
8023	AI323897	Tmod2[8]	Tropomodulin 2	-1.00	-1.40	-1.12	-1.01	-1.86
936	AI850053[7]		Transcribed locus	1.20	1.70	1.73	1.59	1.48
15828	W14341[7]			1.32	1.08	1.20	1.48	1.90

[1-10] Numbers of corresponding clusters revealed by Bayesian hierarchical co-clustering.
[G] Genes occurring in the top 16 candidates found by *GALGO* analysis.

For further validation and functional analyses the following genes were chosen because of strong regulation and due to interesting gene-gene interactions represented in different time-dependent clusters: Acsl4, Cd3e, Crem, Dusp14, Errfi1, Fosl2, Hmgcs1, Kif3a, Mpp7, Nf2, Pak3, Pex13, Rgs4 and Syt4.

4.1.2 Analysis of stress-stimulated CRHR1-dependent signaling pathways *in vivo*

To investigate stress-dependent activation of CRHR1-mediated signal transduction conventional CRHR1-wt and -ko mice were used. Mice were stressed for 30 min by restraint stress and subsequently stress-activated mRNA expression changes were analyzed on the Illumina Sentrix® BeadChip Mouse-6. By comparing expression differences in pituitaries of CRHR1-wt and -ko mice, genes differentially regulated by stress and via CRHR1 were identified.

4.1.2.1 ACTH and corticosterone: blood plasma concentrations

Mice were injected with metyrapone to block synthesis of corticosterone and thus glucocorticoid-mediated negative feedback on the HPA axis. The stress hormones ACTH and corticosterone were measured in blood plasma. Blood sampling was performed between the second metyrapone injection and restraint stress (basal values) and at 1 and 3 h after onset of stress, respectively (stress values).

In CRHR1-wt animals, basal ACTH blood levels increased directly after i.p. injection before restraint stress whereas in CRHR1-ko mice no ACTH increase was detected (Fig. 13A).

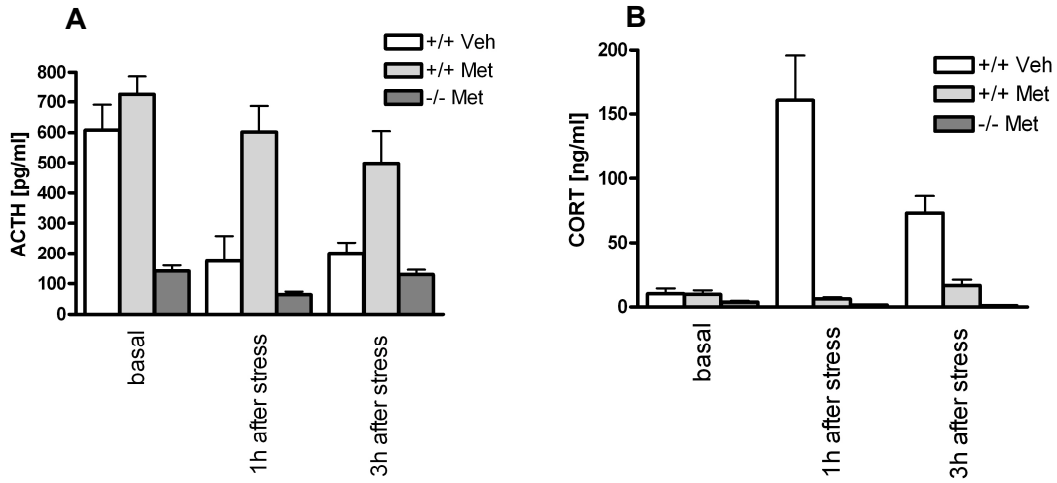

Figure 13. Basal and stress-induced hormone levels in blood plasma of CRHR1-wt and ko mice. (A) ACTH and (B) CORT levels were measured at indicated time points. +/+: CRHR1-wt mice, -/-: CRHR1-ko mice, Veh: vehicle, Met: metyrapone. Values are means of at least 2 animals per group, error bars show SEM.

1 and 3h after the start of 30 min restraint stress, ACTH concentrations of vehicle treated animals were back to basal levels. However, metyrapone injected CRHR1-wt animals showed at all time points increased ACTH blood levels indicating missing negative feedback on ACTH release by corticosterone. In CRHR1-ko mice, as expected, no changes of ACTH amount could be detected, either before or after stress.

The stress of i.p. injection did not lead to a fast increase of corticosterone in any of the animals. Metyrapone was able to block the stress-dependent increase of corticosterone in the blood plasma compared to vehicle treated animals (Fig. 13B).

4.1.2.2 Expression profiling using the Illumina Sentrix® BeadChip Mouse-6

Total RNA was isolated of pituitaries of control and stressed CRHR1-wt and -ko animals. On control agarose gels, all RNA samples showed clear 28 and 18 S ribosomal RNA bands indicating fully intact RNA with no signs of degradation (data not shown). RNA of

two animals per group was pooled and amplified. After amplification, cRNA was again analyzed on an agarose gel which revealed similar fragment sizes of all cRNA samples (data not shown). Microarray hybridization was performed in two technical replicates.
The gene expression data are accessible by the NCBI's GEO Series accession number GSE13665 (temporally reviewer link: http://www.ncbi.nlm.nih.gov/geo/query/acc.cgi?token=fjqlzekgyecycng&acc=GSE13665).
After data normalization, cut off criteria were applied as follows: First, genes had to be regulated in CRHR1-wt mice by stress in at least one time point. As regulation cut off |fold regulation| ≥ 1.5 and $p < 0.05$ were chosen. Genes were defined as detected with a detection level > 0.99. In summary, 15752 transcripts were detected in at least one of the measured time points independently of the genotype. Regarding both stress time points in CRHR1-wt mice plus the differential expression wt versus ko at basal, 1 h and 3 h time points, 9392 transcripts were expressed at all five examined time points. 991 transcripts were found regulated by stress in CRHR1-wt mice at 1 or 3 h after onset of stress (Fig. 14). 74 of these genes were regulated at both time points. Second, all genes out of the 991 candidates regulated by stress in wt mice showing a differential expression comparing wt and ko animals in at least one of the two stress time points were considered as stress- and CRHR1-dependently regulated. Thereby, 404 transcripts were found differentially expressed, among them 63 being regulated 1 and 3 h after stress comparing ko and wt (Fig. 14).

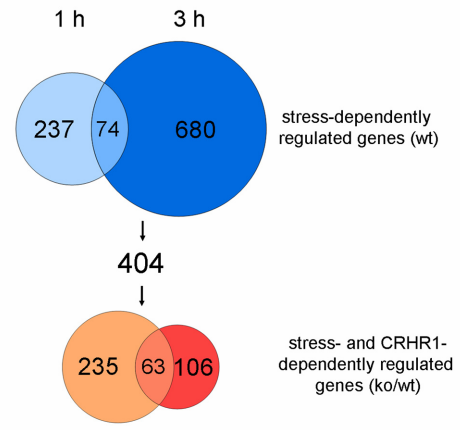

Figure 14. Overlap of stress-dependently regulated genes in CRHR1-wt and ko mice. Venn diagramm, generated by Venn Diagram Plotter software prepared by the Battelle Memorial Institute (http://omics.pnl.gov/software/VennDiagramPlotter.php). Left circles represent the 1 h, right circles the 3 h time point as indicated. Blue colored circles symbolize genes regulated in CRHR1-wt mice after stress, red colored ones those wich are additionally differentially expressed in CRHR1-ko mice after stress.

Candidates for validation were chosen applying different criteria. Genes were considered as candidates, if they fulfilled at least one of the following arguments:

a) found regulated in the *in vitro* experiment,
b) occurred several times in the list of regulated candidate genes,
c) ko versus wt expression values did not differ under basal conditions,
d) a fold regulation value ko/wt > 2,

e) differentially expressed at both stress time points comparing ko and wt,

f) regulated in other stress-/anxiety-related expression analyses (Deussing et al., 2007; Peeters et al., 2004b).

Thereby, 23 candidates were chosen and analyzed in further experiments (Table 7).

Table 7. Candidate genes in vivo.

Probe ID	accession number	gene symbol	description	fold regulation				
				wt 1h	wt 3h	ko/wt basal	ko/wt 1h	ko/wt 3h
101580739	NM_177003	9630033F20Rik	RIKEN cDNA 9630033F20 gene	0.81	0.52	1.00	1.02	1.72
6180088	NM_183187.2	BC055107		1.28	1.54	0.52	0.74	0.50
1850408	NM_007705.1	Cirbp	cold inducible RNA binding protein	0.71	2.53	1.88	3.55	0.95
6660041	NM_013498.1	Crem[a]	cAMP responsive element modulator	0.74	0.43	1.02	1.13	1.10
4810348	NM_007930.3	Enc1	ectodermal-neural cortex 1	0.87	0.30	0.89	1.14	3.21
3450273	NM_133753.1	Errfi1[a]	ERBB receptor feedback inhibitor 1	1.38	0.62	0.72	0.82	0.42
1850315	NM_010234.2	Fos	FBJ osteosarcoma oncogene	3.61	0.40	0.11	1.82	2.83
870044	NM_008037.3	Fosl2[a]	fos-like antigen 2	1.26	0.30	0.64	0.87	0.97
102030091	NM_010309	Gnas	GNAS (guanine nucleotide binding protein, alpha stimulating) complex locus	2.09	1.37	0.63	0.46	0.76
106380014	NM_010309	Gnas	GNAS (guanine nucleotide binding protein, alpha stimulating) complex locus	1.63	0.96	0.62	0.42	0.52
5290673	NM_010378.2	H2-Aa	histocompatibility 2, class II antigen A, alpha	0.80	2.94	2.56	3.92	1.38
105570373	AK003096	Hbb-b1	hemoglobin, beta adult major chain	0.67	0.97	1.61	1.59	1.14
105860114	AK010873	Hbb-b1	hemoglobin, beta adult major chain	0.65	0.95	1.85	1.68	1.22
104560707	AK011016	Hbb-b1	hemoglobin, beta adult major chain	0.51	0.66	1.66	1.46	1.40
102230086	AK011053	Hbb-b1	hemoglobin, beta adult major chain	0.20	0.23	1.41	1.82	3.42
102510156	AK011067	Hbb-b1	hemoglobin, beta adult major chain	0.37	0.52	1.45	1.61	1.62
102230020	AK011069	Hbb-b1	hemoglobin, beta adult major chain	0.55	0.92	2.03	1.70	1.13
5420300	NM_013560.1	Hspb1	heat shock protein 1	1.69	1.21	0.85	0.49	0.48
6620292	NM_008590.1	Mest	mesoderm specific transcript	1.43	0.43	0.59	0.83	1.36
102680047	XM_128966	Mpp7[a]	membrane protein, palmitoylated 7 (MAGUK p55 subfamily member 7)	1.52	1.42	1.33	0.63	0.72
4850164	NM_013602.2	Mt1	metallothionein 1	1.12	2.23	1.07	1.06	0.58
103990551	AK077465	Nnat	neuronatin	1.88	1.24	0.63	0.36	0.39
4480239	NM_029688.2	Npn3	neoplastic progression 3	1.27	1.71	0.62	0.46	0.26
3130195	NM_029688.2	Npn3	neoplastic progression 3	1.15	1.71	0.85	0.43	0.23
60273	NM_013613.1	Nr4a2	nuclear receptor subfamily 4, group A, member 2	2.14	0.20	0.92	0.55	1.53
104920411	NM_013613	Nr4a2	nuclear receptor subfamily 4, group A, member 2	2.33	0.22	1.08	0.61	0.84
430528	NM_008792.3	Pcsk2	proprotein convertase subtilisin/kexin type 2	0.96	0.60	0.99	1.03	2.63
360017	NM_008792.3	Pcsk2	proprotein convertase subtilisin/kexin type 2	0.81	0.55	0.83	1.19	2.77
5900619	NM_008792.3	Pcsk2	proprotein convertase subtilisin/kexin type 2	0.91	0.66	1.28	1.17	2.41
3710020	NM_008817.1	Peg3	paternally expressed 3	0.98	0.60	0.44	0.54	0.99
5700167	NM_016809	Rbm3	RNA binding motif protein 3	0.64	1.64	1.39	2.73	0.89
4540131	NM_011255.1	Rbp4	retinol binding protein 4, plasma	0.85	2.70	1.29	1.38	0.33
4150072	NM_013697.1	Ttr	transthyretin	1.88	0.91	0.84	0.43	0.49

[a] Genes found differentially expressed in CRH-stimulated AtT-20 cells.

4.1.3 Validation of regulation of selected candidate genes *in vitro* and *in vivo*

As described in 3.1.1, 14 candidate genes which were found differentially expressed comparing CRH-treated versus control AtT-20 cells were chosen for validation. Total RNA isolated from two independent biological replicates at different time points was reverse transcribed and cDNA was analyzed in technical duplicates by qRT-PCR. As internal standard the house keeping genes Hprt and Gapdh were used. Both genes were not differentially regulated in AtT-20 cells following CRH stimulation. A gene was defined as validated as soon as the direction of regulation of at least one time point was concordant comparing microarray and qRT-PCR results. The regulation of the following genes was investigated in independent material using qRT-PCR: Acsl4, Cd3e, Crem, Dusp14, Errfi1, Fosl2, Hmgcs1, Kif3a, Mpp7, Nf2, Pak3, Pex13, Rgs4 and Syt4 (Fig. 15).

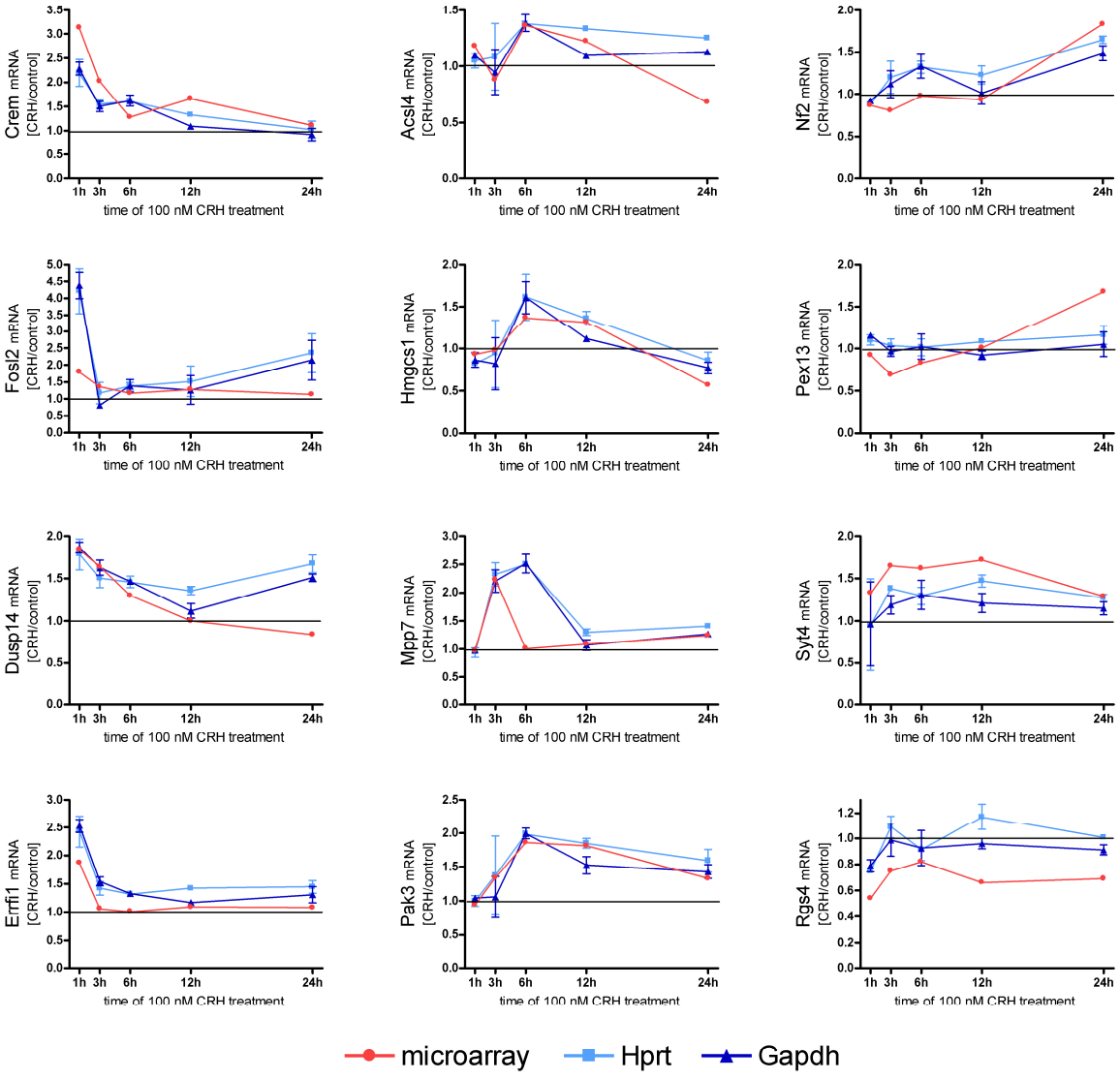

Figure 15. qRT-PCR results *in vitro*. Validation of the differential expression of a subset of candidate genes in independently treated AtT-20 cells. Values are means of biological duplicates. CRH-induced expression data was normalized to Hprt and Gapdh, respectively, and related to untreated controls. Black lines indicate the differential expression value = 1.

For Crem, Fosl2 and Dusp14 it was confirmed that after CRH stimulation the transcription was increased in the first 6 hours. Errfi1 was upregulated after 1 h of CRH treatment on the microarray which was measured by qRT-PCR in independent samples, too. Acsl4 and Hmgcs1 showed increased mRNA levels in the microarray experiment as well as in the qRT-PCR validation at 6 and 12 h. The upregulation of Mpp7 at 3 h was verified as well as the upregulation of Pak3 at 6, 12 and 24 h. Moreover, Nf2 and Pex13 were upregulated by CRH after 12 and 24 h corroborated by the qRT-PCR results. The time-dependent regulation of Syt4 was confirmed at 3, 6, 12 and 24 h. The differential expression of the candidate gene Rgs4, downregulated in the microarray experiment, was validated at the 1 h time point. With both internal references, Hprt and Gapdh, similar results were obtained (Fig. 15).
The expression of Cd3e was below the detection sensitivity of the Lightcycler instrument and thus not validated. In the case of Kif3a, none of the contradictory microarray results for both detected cDNA clones could be validated in original material. Therefore, Kif3a was not further analyzed in independent cDNA samples.
In conclusion, out of 14 selected candidates, the regulation of 12 genes was validated in independently treated AtT-20 cells. For all validated candidate genes the time-specific expression pattern caused by CRH stimulation was confirmed.

23 candidate genes which were found differentially expressed comparing control versus stressed CRHR1-wt and -ko mice were chosen for validation (Table 7). As *in vitro*, total RNA isolated from two independent biological replicates at different time points was reverse transcribed and cDNA was analyzed in technical duplicates by qRT-PCR. As internal standard the house keeping genes Hprt and Gapdh were used. A gene was defined as validated as soon as the direction of regulation of at least one time point after stress (1 or 3 h) was concordant comparing microarray and qRT-PCR results. The regulation of the following genes was investigated in independent material using qRT-PCR: 9630033F20Rik, BC055107, Cirbp, Crem, Enc1, Errfi1, Fos, Fosl2, Gnas, H2-Aa, Hbb-b1, Hspb1, Mest, Mpp7, Mt1, Nnat, Npn3, Nr4a2, Pcsk2, Peg3, Rbm3, Rbp4, Ttr.
For Cirbp, the higher mRNA expression detected by microarray analysis in ko compared to wt animals was verified by qRT-PCR on basal level and 1h after stress. The transcription factor Nr4a2 was downregulated 1 h after stress in CRHR1-ko mice in the microarray as well as in the qRT-PCR. An upregulation 3 h after stress was detected and validated in ko animals for 9630033F20Rik. The lower mRNA transcript levels of Npn3 detected by microarray in ko mice were confirmed in independent material 1 and 3 h after stress. For Rbm3, the upregulation at the 1 h time point was validated whereas Errfi1 was found downregulated 3 h after stress which was confirmed by qRT-PCR. The differential

expression of Hspb1 at all three time points, basal, 1 and 3h, was verified in independent material (Fig. 16).

For Crem, the activation by stress was validated in the original material used for microarray hybridization. However, no differential expression between ko and wt was observed, therefore this candidate was not followed up in validation experiments *in vivo*. For the other 16 genes the regulation was not validated at any time point in independent material. In summary, for 7 candidate genes out of 23 the differential expression in CRHR1-ko compared to -wt mice was confirmed.

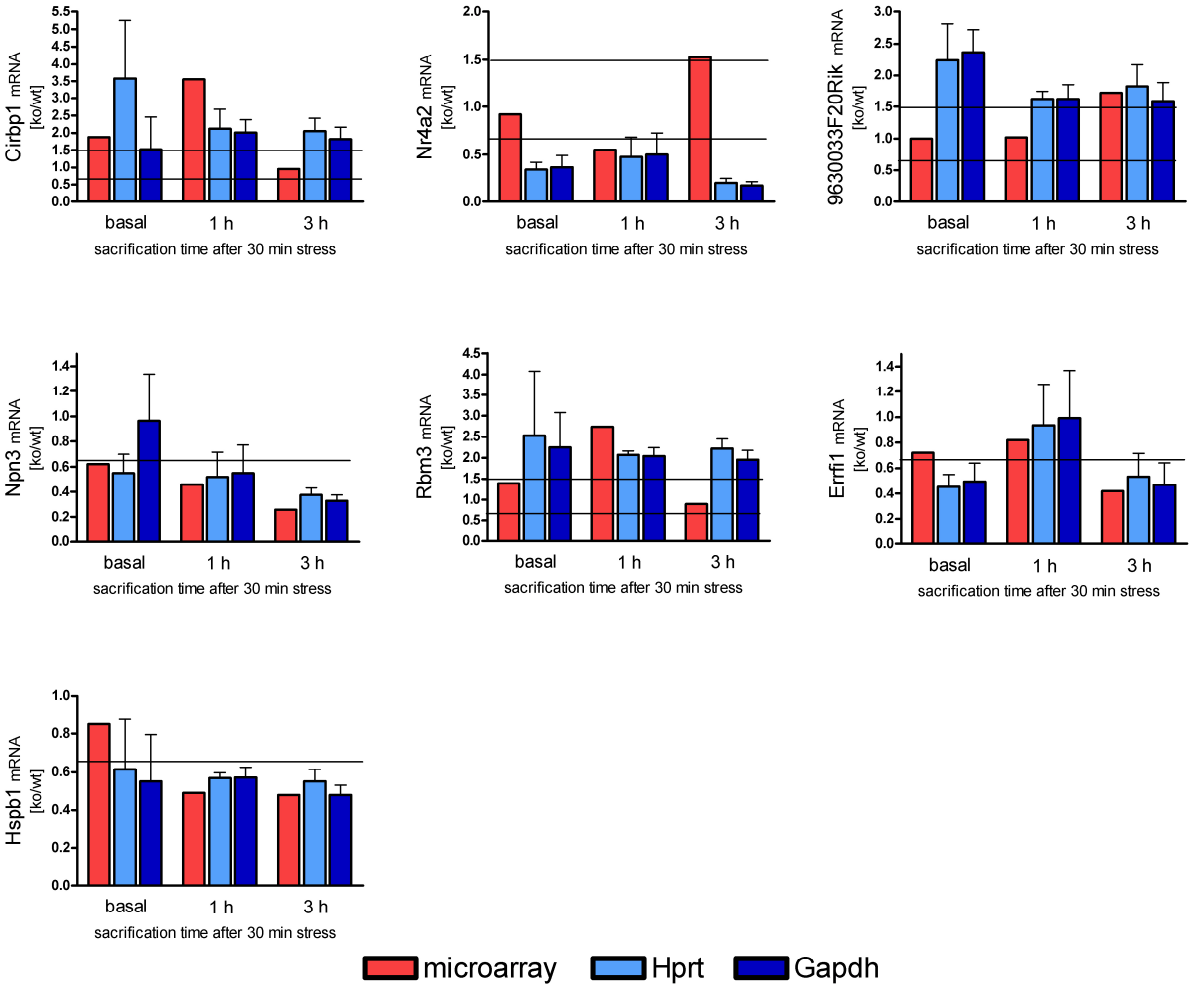

Figure 16. qRT-PCR results *in vivo*. Validation of the differential expression of a subset of candidate genes in pituitaries of independently treated basal and stressed CRHR1-wt and -ko mice. Values are means of biological duplicates. Expression data of CRHR1-ko mice was normalized to Hprt and Gapdh, respectively, and related to the corresponding CRHR1-wt mice values. Black lines indicate cut off limits |fold regulation| ≥ 1.5.

For functional validation, Errfi1 was selected because of its additional regulation in the *in vitro* experiment. Furthermore, Hspb1 was chosen for further investigation because its differential expression at all three measured time points was validated.

4.2 Common regulated genes *in vitro* and *in vivo*

Utilizing both microarray experiments stress/CRHR1-dependently regulated genes *in vitro* and *in vivo* were compared. Using this approach, commonly activated pathways in CRHR1-mediated signaling should be uncovered. Comparing the 102 genes found significantly regulated by CRH in at least one time point *in vitro* with the 991 transcripts regulated by stress *in vivo*, a small subset of genes was found differentially expressed in both experiments (Table 8).

Table 8. Candidate genes with CRH/stress-mediated differentially expression in vitro and in vivo[a]

accession number	gene symbol	description
transcription		
NM_013498.1	Crem	cAMP responsive element modulator (Crem), mRNA.
NM_008037.3	Fosl2	fos-like antigen 2 (Fosl2), mRNA.
signal transduction		
NM_133753.1	Errfi1[b]	ERBB receptor feedback inhibitor 1
protein binding		
XM_128966	Mpp7[b]	Membrane protein, palmitoylated 7 (MAGUK p55 subfamily member 7
chaperone activity		
NM_010480	Hspca	heat shock protein 1, alpha (Hspca), mRNA.
lipid metabolism		
NM_207625.1	Acsl4	acyl-CoA synthetase long-chain family member 4 (Acsl4), transcript variant 2, mRNA.

[a] Functional classification was based on Gene Ontology categories according to NCBI.
[b] Genes regulated by stress and CRHR1 *in vivo*.

Whereas Crem, Fosl2, Hspca and Acsl4 were only stress- but not CRHR1-dependently regulated *in vivo*, Errfi1 and Mpp7 show additionally a differential expression in stressed CRHR1-ko mice indicating stress- and CRHR1-mediated changes in gene expression.
While the differential expression of Crem, Fosl2, Errfi1, Mpp7 and Acsl4 was validated *in vitro*, the regulation of Fosl2 and Mpp7 *in vivo* could not be verified. Moreover, the alterations in expression of Crem and Errfi1 were confirmed *in vivo* but Acsl4 and Hspca were not investigated with qRT-PCR.
Altogether, two candidates, Crem and Errfi1, were found regulated in both analyzed models - AtT-20 cells and stressed CRHR1-wt and -ko mice. However, only Errfi1 was regulated by stress and CRHR1 *in vivo*.

4.3 Functional analysis of candidate genes

4.3.1 Expression of CRH receptors

Before the functional analysis of selected candidate genes using reporter assays, the expression of both CRH receptors was assessed in the investigated cell lines, AtT-20 and HN9, by RT-PCR. TBV2 cells were used as negative control whereas cDNA of total brain tissue served as positive control. Reverse transcription controls were performed to exclude DNA contamination. The CRHR1 is expressed in AtT-20 and HN9 cells but not in TBV2 cells (Fig. 17).

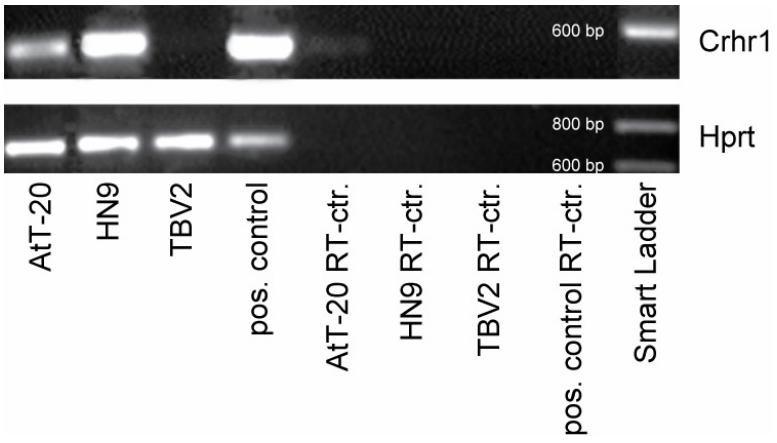

Figure 17. Expression of CRHR1. CRHR1 mRNA was analyzed in different cell lines by RT-PCR. No DNA contamination was detected in the reverse transcription controls.

For the CRHR2 no product was observed in the agarose gel after RT-PCR implying no expression of the CRH receptor 2 in AtT-20 and HN9 cells (data not shown). Therefore, the activation of the CRH receptor-mediated signaling pathways by CRH treatment in further cell culture experiments will only result from CRHR1.

4.3.2 Reporter assays: AtT-20 cells

A subset of validated candidate genes was chosen for further functional experiments. As these candidates are regulated by CRH/CRHR1-dependent signaling the question arose if those genes are themselves involved in the regulation of CRHR1-mediated signal mechanisms. Thus, reporter assays were performed. The effects of overexpression of certain genes on CRH-activated reporters including (i) CRE (cAMP responsive element), (ii) NurRE (Nur responsive element) and (iii) Pomc promoters coupled to luciferase were analyzed. Activation of the transcription factor CREB leads to initiation of CRE transcription. Nur responsive elements are activated by binding of homodimeric NUR77/NUR77 or heterodimeric NUR77/NURR1proteins. The Pomc promoter contains binding sites for CREB, NUR transcription factors and AP1 family transcription factors such as cFOS or JUNB. AtT-20 cells were transfected on the day before treatment with

reporter plasmid and expression vector for overexpression of the gene of interest. On the next day, CRHR1 signaling was stimulated with a 6-h CRH treatment.

Thereby, the overexpression of Icer, the inducible form of Crem, led to a block of CRH-stimulated Cre- and NurRE-mediated transcription (Fig. 18A and B). Increased intracellular Fosl2 levels slightly decreased CRH-induced Cre- and NurRE-dependent transcription whereas Dusp14 had an additional stimulating effect on the NurRE reporter (Fig. 18B). Neither Fosl2 nor Dusp14 showed an effect on CRH-activated Cre-mediated transcription (Fig. 18A). The full-length Errfi1 inhibited CRH-activated Cre-dependent transcription. Mutant forms of Errfi1, including a C-terminal truncated variant (Errfi-NT) with amino acids 1-263, a CRIB domain missing cDNA (Errfi-dCrib) and only the CRIB domain (Errfi1-oCrib), did not have any influence on CRHR1-dependent CRE transcription (Fig. 18A). Only on CRH-stimulated NurRE-controlled transcription, Errfi-oCrib and Errfi-dCrib had an inhibitory effect, whereas full-length Errfi1 and its N-terminus did not change NurRE-mediated transcription (Fig. 18B). Other genes augmenting CRH-increased Cre- and NurRE transcription were Mpp7 and Pak3a, a splice variant of Pak3. Pak3b, another Pak3 splice variant, did not modify CRE transcription but diminished NurRE transcription (Fig. 18A and B).

In the case of the splice variants of Nf2, Nf2_16 and Nf2_17, the CRH stimulation of CRE and NurRE was further increased by Nf2_17 whereas Nf2_16 only affected NurRE. Two truncated forms of Nf2_17, one missing the aminoacids 1-215 of the N-terminus (Nf2_17Ntrunc), the other missing the amino acids 548-596 of the C-terminus (Nf2_17trunc), enhanced the CRH-mediated CRE and NurRE transcription as Nf2_17 even though not significantly in the case of Nf_17trunc and NurRE (Fig. 18A and B). Rgs4 only reveals an inhibiting effect on CRH-initiated CRE transcription (Fig. 18A). The overexpression of the *in vivo* candidate gene Hspb1 in AtT-20 cells resulted in a weakly increasing effect on CRH-stimulated NurRE-transcription but the corresponding mutant form, S15,86A, had the same effect (Fig. 18B).

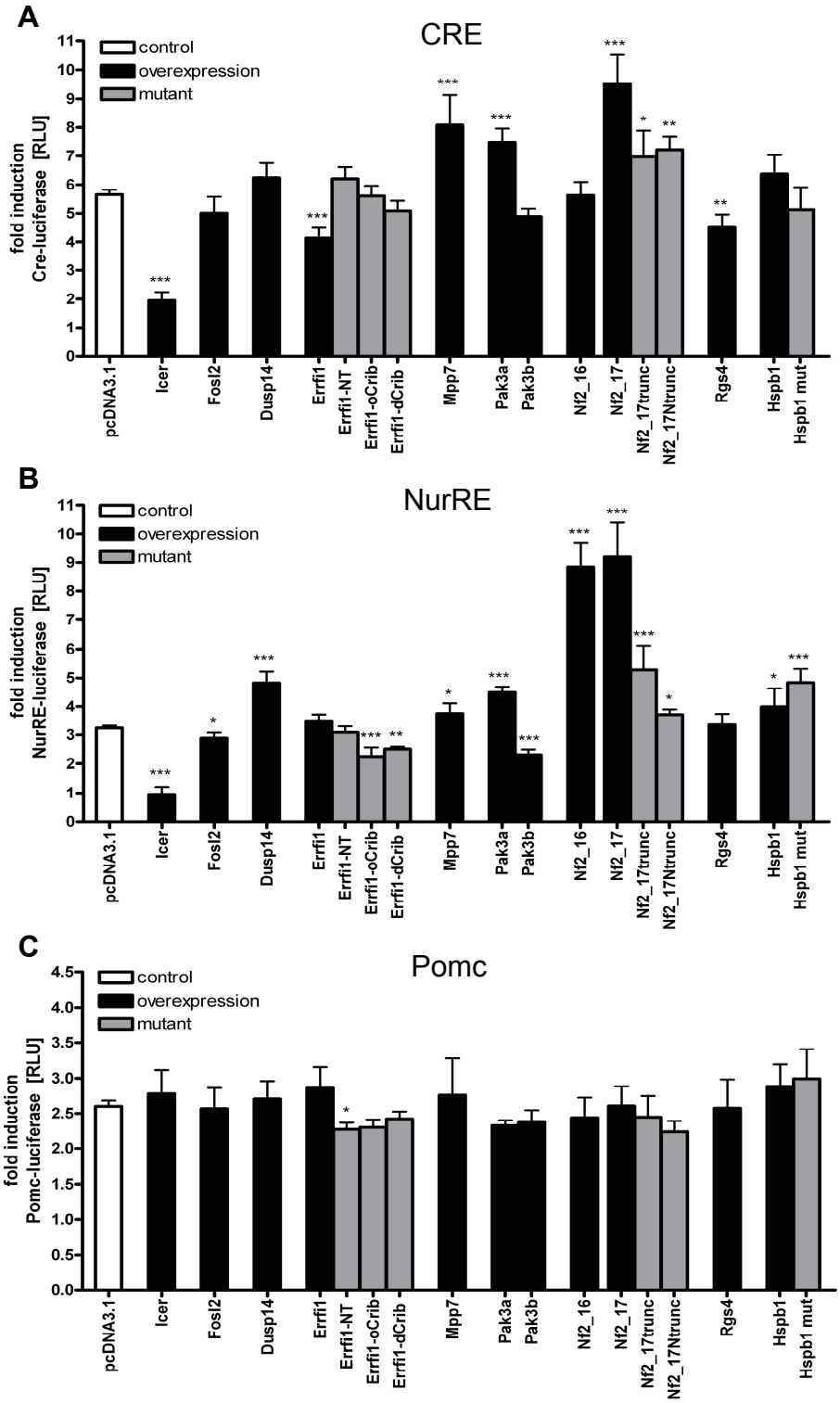

Figure 18. Reporter assay results of CRH-treated AtT-20 cells. Cells were transiently transfected with reporter vectors CRE-Luc (A), NurRE-Luc (B) and Pomc-Luc (C), respectively, plus CMV-βGal and with the indicated expression vectors 20 hours prior to 6 hours of 100 nM CRH treatment. Luciferase luminescence values were normalized to CMV-βGal values and related to the corresponding untreated controls. Values displayed are means of 3 experiments in average performed at least in duplicates. Error bars show SEM, significance values in relation to pcDNA3.1 were calculated using a t-test. $p<0.05$ = *, $p<0.01$ = **, $p<0.001$ = ***

None of the overexpressed candidate changed CRH-induced Pomc transcription itself. Only the deleted form of Errfi1, Errfi1-NT, decreased slightly the Pomc transcription.

As the activation of CRHR1 by CRH includes the formation of the second messenger cAMP, the measured effects of the candidates on the CRH-induced CRE and NurRE transcription were further investigated to assess if those results are mediated via cAMP or occur upstream and/or independent of cAMP formation (Fig. 19).

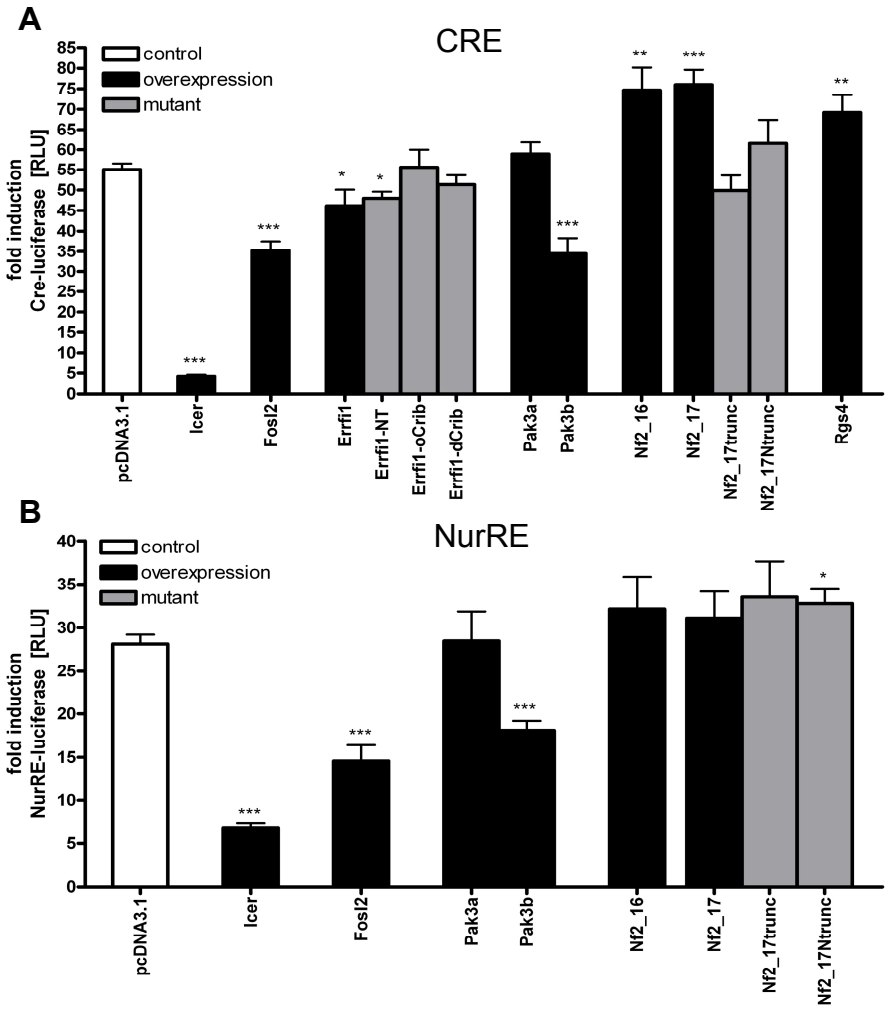

Figure 19. Reporter assay results of cAMP-treated AtT-20 cells. Cells were transiently transfected with reporter vectors CRE-Luc (A) and NurRE-Luc (B), respectively, plus CMV-βGal and with the indicated expression vectors 20 hours prior to 6 hours of 500 µM cAMP treatment. Luciferase luminescence values were normalized to CMV-βGal values and related to the corresponding untreated controls. Values displayed are means of in average 3 experiments performed at least in duplicates. Error bars show SEM, significance values in relation to pcDNA3.1 were calculated using a t-test. $p<0.05$ = *, $p<0.01$ = **, $p<0.001$ = ***

Icer and Fosl2 both inhibited cAMP-mediated CRE and NurRE transcription similar to the results with CRH (Fig. 19A and B). As full-length Errfi1 only affected CRH-activated CRE

transcription, its influence on cAMP-induced signaling was only analyzed on Cre-dependent transcriptional activation which was inhibited by Errfi1 and Errfi1-NT (Fig. 19A). In the case of Pak3, the enhancing effect of Pak3a on CRH-stimulated CRE and NurRE transcription was not mediated by cAMP. The reduction of NurRE transcription by Pak3b after CRH treatment occurred also after cAMP but in addition, Pak3b decreased cAMP-triggered CRE transcription. Both splice variants of Nf2 potentiated the cAMP-activated CRE transcription but did not influence NurRE transcription. Of the truncated mutants of Nf_17, only Nf_17Ntrunc showed a slight increase of cAMP/NurRE-mediated transcriptional activity. The inhibition of CRH-dependent CRE activation by Rgs4 was reversed after treatment with cAMP (Fig. 19).

4.3.3 Reporter assays: HN9 cells

Seven candidate genes which were not only regulated by CRH/CRHR1-dependent signaling pathways but additionally affected CRH-activated signaling according to the results in 4.3.2 were selected to assess their involvement in CRHR1 signaling in neuronal cells. Therefore, reporter assays in HN9 cells were performed using Cre-Luc as reporter and the expression vectors for Icer, Fosl2, Dusp14, Errfi1 including the mutant forms, Pak3a and b, all four variants of Nf2 and Rgs4. As Pomc is endogenously not transcribed in neuronal cells and NurRE-dependent transcription was only weakly induced by CRH, both reporters were excluded.

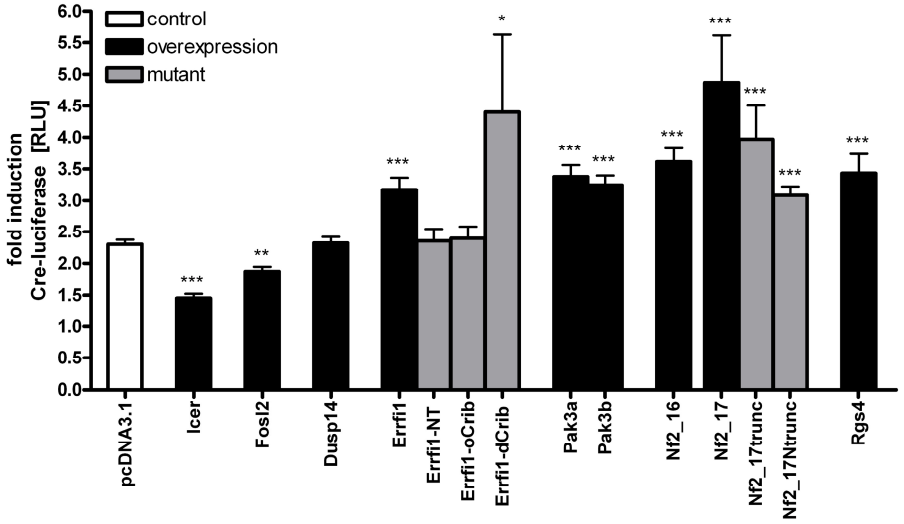

Figure 20. Reporter assay results of CRH-treated HN9 cells. Cells were transiently transfected with reporter vectors Cre-Luc and CMV-βGal and with the indicated expression vectors 20 hours prior to 6 hours of 100 nM CRH treatment. Luciferase luminescence values were normalized to CMV-βGal values and related to the corresponding untreated controls. Values displayed are means of 3 experiments in average performed at least in duplicates. Error bars show SEM, significance values in relation to pcDNA3.1 were calculated using a t-test. $p<0.05$ = *, $p<0.01$ = **, $p<0.001$ = ***

Like in the corticotrope AtT-20 cells, Icer and Fosl2 reduced CRH-stimulated CRE transcription in HN9 cells (Fig. 20). In concordance with the AtT-20 results, Dusp14 did not change CRE expression whereas in contrast to its effect in AtT-20 cells, Errfi1 enhanced CRH-dependent Cre-mediated transcription. This increase seemed to be independent of the CRIB domain because Errfi1-dCrib had the same effect as full-length Errfi1. Pak3a and b both increased CRE transcription after CRH treatment such as all four variants of Nf2. Also Rgs4 further increased CRH-activated CRE transcription (Fig. 20).
Except for Dusp14 the effect of the candidates on cAMP-triggered Cre-mediated transcription was investigated. For Icer, Fosl2, all Errfi1 forms, Pak3a, all four Nf2 variants and Rgs4, similar changes were obtained on cAMP-mediated CRE transcription as with CRH. Just the enhancing effect of Pak3b after CRH treatment did not appear after cAMP stimulation (Fig. 21).

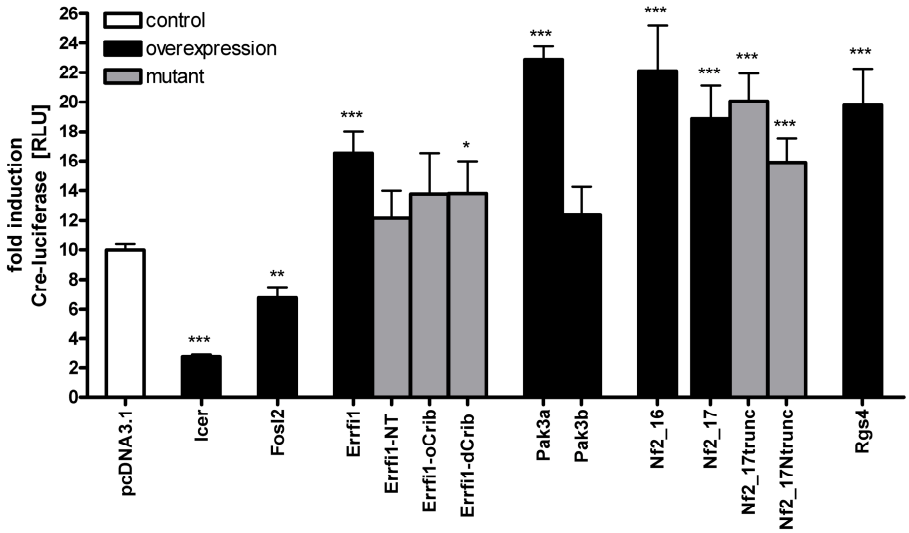

Figure 21. Reporter assay results of cAMP-treated HN9 cells. Cells were transiently transfected with reporter vectors Cre-Luc and CMV-βGal and with the indicated expression vectors 20 hours prior to 6 hours of 500 µM cAMP treatment. Luciferase luminescence values were normalized to CMV-βGal values and related to the corresponding untreated controls. Values displayed are means of 3 experiments in average performed at least in duplicates. Error bars show SEM, significance values in relation to pcDNA3.1 were calculated using a t-test. $p<0.05$ = *, $p<0.01$ = **, $p<0.001$ = ***

4.4 Interaction of CRHR1- and ErbB-activated signaling mechanisms

4.4.1 Expression of ErbB receptors

The expression of the four ErbB receptors was assessed in the investigated cell lines, AtT-20 and HN9, by nested RT-PCR performing first a PCR with the according primers (name_nest) followed by a PCR with second nested primer pairs using 1 µl of a 1/10 dilution of the first PCR product. cDNA of mouse lung tissue was used as positive, murine blood cDNA as negative control.

According to Figure 22, the Egf receptor, also called ErbB1, is expressed in neuronal HN9 cells and in pituitary tissue. ErbB2 and ErbB3 were detected in AtT-20 and HN9 cells as well as in the pituitary. ErbB4 mRNA was not found in any of the cell lines but in the pituitary.

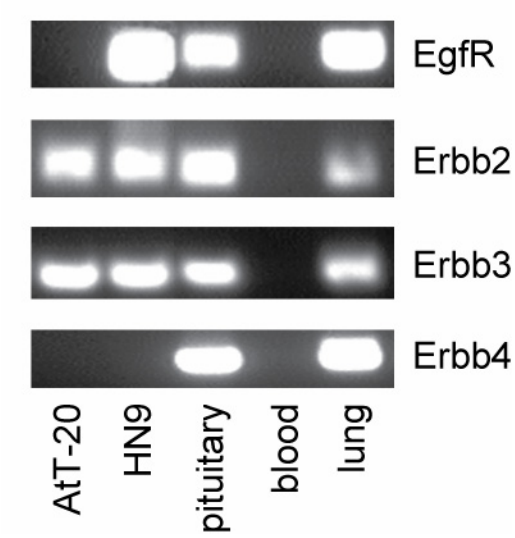

Figure 22. Expression of different Egf receptor family members. Indicated different cell lines were analyzed by RT-PCR. The cDNA content of the analyzed samples was controlled by an Hprt PCR (data not shown).

4.4.2 Effects of ErbB3 overexpression on CRHR1-dependent signaling

Some of the validated candidate genes such as Errfi1 or Nf2 are known to be involved in ErbB receptor-dependent signaling cascades. Therefore, the influence of one of the ErbB receptors, ErbB3, on CRH- and cAMP-mediated Cre, NurRE and Pomc transcription was analyzed by reporter assays.

Overexpression of ErbB3 in AtT-20 cells led to an enhanced CRH-dependent induction of CRE- and NurRE-mediated transcription whereas it did not affect Pomc expression (Fig. 23A-C). Regarding cAMP-activated signaling, ErbB3 again further increased CRE transcription whereas the effect on NurRE is independent of cAMP (Fig. 23E and F). In HN9 cells, higher intracellular ErbB3 levels augmented CRH- as well as cAMP induced CRE transcription (Fig. 23D and G).

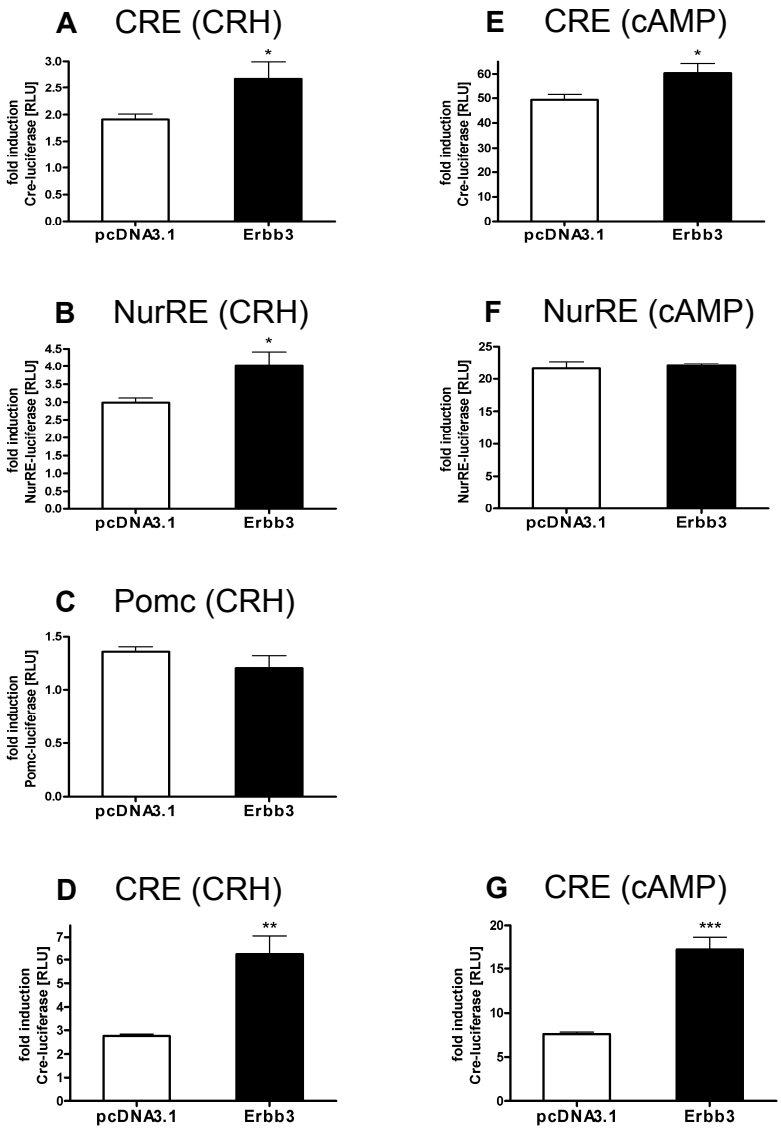

Figure 23. Reporter assay results for overexpression of Erbb3. Cells were transiently transfected with reporter vectors CRE-Luc (A, D, E), NurRE-Luc (B, F) and Pomc-Luc (C), respectively, plus CMV-βGal and expression vectors as indicated 20 hours prior to treatment with 100 nM CRH (A-D) and 500 µM cAMP (E-G). Luciferase luminescence values were normalized to CMV-βGal values and related to the corresponding untreated controls. Values displayed are means of 2 experiments performed at least in duplicates. Error bars show SEM, significance values in relation to pcDNA3.1 were calculated using a t-test. $p<0.05$ = *, $p<0.01$ = **, $p<0.001$ = ***

4.5 Errfi1 expression *in vivo*: *in situ* hybridization

The candidate gene Errfi1 was differentially expressed *in vitro* and *in vivo* after activating the CRHR1 signaling cascades. As the CRHR1 is not only expressed in pituitary but in

different brain regions and Errfi1 overexpression affected CRHR1-dependent signal transduction not only in AtT-20 but also in neuronal HN9 cells, Errfi1 expression itself and differential expression comparing CRHR1-wt and -ko mice on basal level and 3 h after stress were examined. Therefore, coronal cryostat sections of frozen brains of the animals used for the microarray experiment were hybridized with Errfi1 sense and antisense probes. With the sense probe, no signal was obtained (data not shown) whereas the antisense probe revealed a wide spread expression of Errfi1 in the murine brain. In detail, Errfi1 was detected in brain regions expressing CRHR1 including the olfactory bulb (data not shown), cortical layers, CA1 and CA3 regions of the hippocampus as well as the dentate gyrus, basolateral (BLA) and medial amygdala (MeA), substantia nigra and thalamic nuclei (Fig. 24).

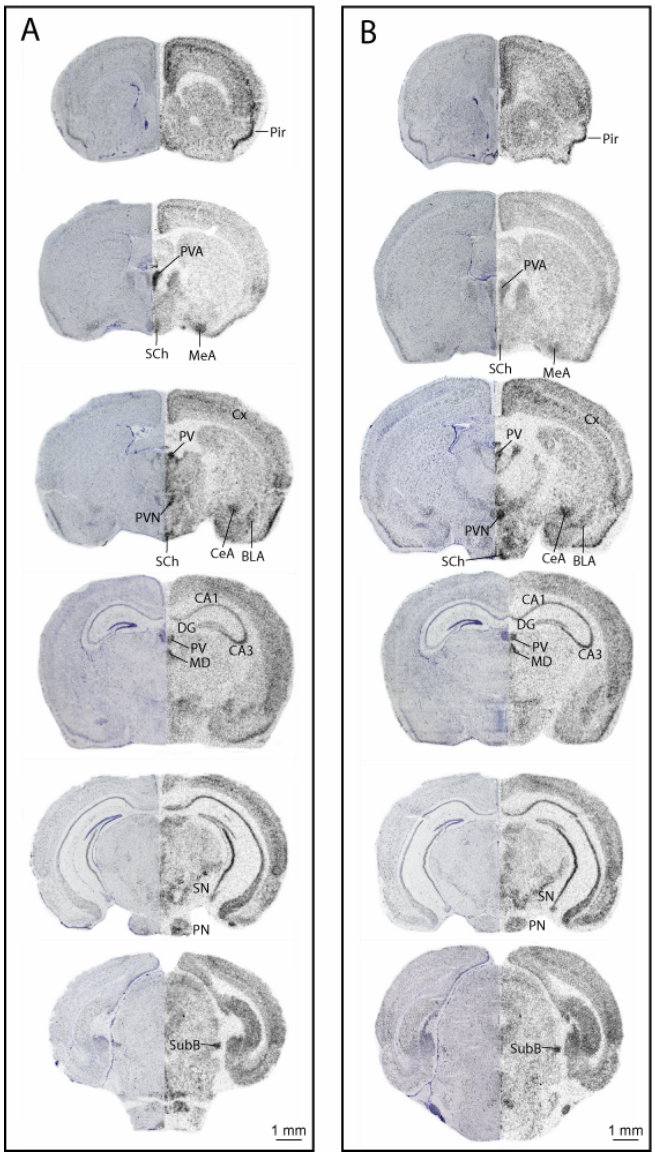

Figure 24. Basal Errfi1 expression in murine brain. A riboprobe against Errfi1 was hybridized on coronal 20 µm cryosections of basal (A) CRHR1-wt and (B) -ko mice. Left side: Nissl staining; right side: x-ray film. BLA, basolateral amygdala; CeA, central nucleus of the amygdala; CA1 and CA3, fields CA1and 3 of the hippocampus; Cx, cortex; DG, dentate gyrus; MD, mediodorsal thalamic nucleus; MeA, medial nucleus of amygdala; Pir, piriform cortex; PN, pontine nucleus; PV, paraventricular thalamic nucleus; PVA, paraventricular thalamic nucleus, anterior part; PVN, hypothalamic paratventricular nucleus; SCh, suprachiasmatic nucleus; SN, substantia nigra; SubB, subbrachial nucleus

In addition, Errfi1 was expressed e.g. in the piriform cortex, the central amygdala (CeA), the hypothalamic paraventricular nucleus (PVN), the suprachiasmatic nucleus, the pontine nucleus and the subbrachial nucleus (Fig. 24). Quantification of Errfi1 expression in the PVN, MeA, CeA and the CA1 and CA3 regions of hippocampus did not reveal any difference between basal CRHR1-wt and -ko mice.

30 min restraint stress did not change the expression pattern of Errfi1, neither in CRHR1-wt mice nor in CRHR1-ko mice (Fig. 25). Moreover, no differential expression of Errfi1 in PVN, MeA, CeA, CA1 and CA3 regions of hippocampus was measured comparing stressed wt and ko mice.

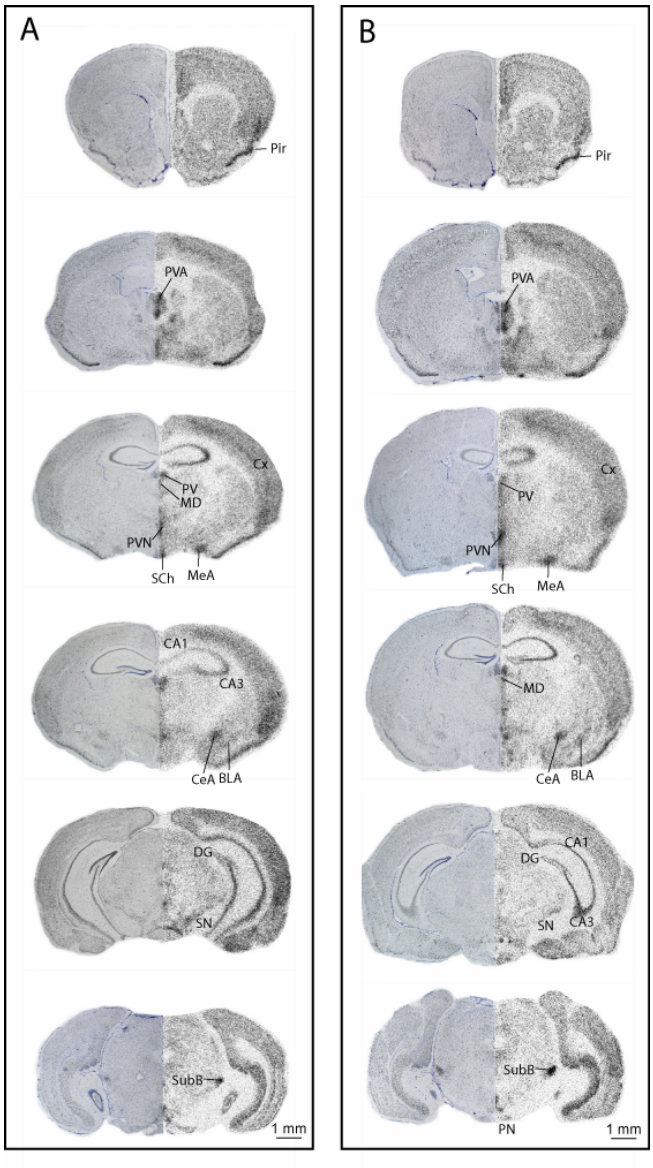

Figure 25. Errfi1 expression after stress in murine brain. A riboprobe against Errfi1 was hybridized on coronal 20 µm cryosections of stressed (A) CRHR1-wt and (B) -ko mice.Left side: Nissl staining; right side: x-ray film. BLA, basolateral amygdala; CeA, central nucleus of the amygdala; CA1 and CA3, fields CA1and 3 of the hippocampus; Cx, cortex; DG, dentate gyrus; MD, mediodorsal thalamic nucleus; MeA, medial nucleus of amygdala; Pir, piriform cortex; PN, pontine nucleus; PV, paraventricular thalamic nucleus; PVA, paraventricular thalamic nucleus, anterior part; PVN, hypothalamic paratventricular nucleus; SCh, suprachiasmatic nucleus; SN, substantia nigra; SubB, subbrachial nucleus

5. Discussion

The aim of this study was to identify new candidate genes regulated by CRHR1-dependent signaling pathways. The activation of specific signaling pathways will cause alterations in gene expression signatures. Changes on the transcriptional level usually precede changes on the protein level and provide an entry point to understand the underlying regulatory networks. In order to dissect signaling mechanisms of the CRHR1 in depth, an *in vitro* and an *in vivo* approach were conducted. The signal transduction was induced by CRH stimulation *in vitro* whereas *in vivo* conventional CRHR1-wt and -ko mice were utilized. There, the CRHR1 was activated by restraint stress. In both experiments, CRHR1-dependently regulated genes were identified by expression profiling applying high-throughput microarray technology, which allows to monitor thousands of genes simultaneously and to characterize changes in gene expression patterns induced by a defined stimulus on a genome-wide scale.

To gain insight into the dynamics of CRHR1-dependent signaling networks we investigated the alterations in expression patterns at five different time points between 1 and 24 h on the 24 k Max Planck Institute of Psychiatry (MPIP) cDNA microarray platform (Deussing *et al.*, 2007) *in vitro* whereas *in vivo* two time points (1 and 3 h) were analyzed on the Illumina Sentrix® BeadChip Array.

5.1 Reliability of new candidate genes

5.1.1 CRHR1 stimulation

To control for successful stimulation of CRHR1 signal transduction *in vitro*, secreted ACTH amounts and changes in Pomc mRNA levels were assessed. The pituitary corticotrope cell line AtT-20 is a commonly used model system for research on CRHR1 signaling, which has been demonstrated to respond with ACTH release as well as with increased Pomc transcription upon CRH stimulation (Aoki et al., 1997; Fickel et al., 1994; Kageyama et al., 2007; Peeters et al., 2004b). 100 nM CRH treatment for 1 and 3 h increased ACTH concentrations in the culture medium as expected. The dose of 100 nM CRH was chosen as 100 nM CRH evokes a response in AtT-20 cells but is still below the concentration of maximal stimulation shown in transactivation assays (Peeters *et al.*, 2004b). After 6 h and more of chronic CRH stimulation, no enhanced ACTH release was observed compared to untreated controls. As the secreted ACTH levels of untreated AtT-20 rose in a similar manner, the difference to CRH-stimulated cells disappeared. Pomc levels were augmented between 3 and 12 h as expected (Aoki *et al.*, 1997) indicating a successful stimulation of the CRH receptor type 1.

In vivo, ACTH and corticosterone blood levels were measured to control for the effectiveness of the stress procedure. On the one hand, a control, vehicle treated group

was analyzed to assess the stress effectiveness, on the other hand, the blood of metyrapone-treated CRHR1-wt and -ko mice was investigated to evaluate the influence of metyrapone on basal and stress-induced ACTH and CORT concentrations. Already the i.p. injection led to an increase in ACTH plasma levels in wt animals. 1 and 3 h after stress, ACTH levels were decreased in vehicle-treated mice caused by the negative feedback through corticosterone whereas the amount of ACTH remained increased in metyrapone-treated CRHR1-wt animals. As expected, the ACTH levels of CRHR1-ko mice did not rise above basal levels because of an impaired HPA axis due to disrupted CRHR1. CORT levels were not changed immediately after injection stress but were found increased 1 and 3 h after stress in vehicle-treated animals confirming an effective restraint stress procedure. As metyrapone is an inhibitor of the steroid 11β-hydroxylase and thereby blocks glucocorticoid synthesis (Dal-Zotto et al., 2003; Tarcic et al., 1998), stressed and metyrapone-treated CRHR1-wt animals as well as CRHR1-ko mice did not show any stress-dependent increase of corticosterone.

According to the ACTH and CORT levels, the i.p. injection itself stressed the animals already slightly. The restraint stress successfully enhanced corticosterone levels, while metyrapone blocked the stress-induced corticosterone increase and thereby the negative feedback on ACTH secretion. In CRHR1-ko mice no HPA axis activation occurred.

5.1.2 Microarray analyses

In this project, the microarray technology was chosen to identify and select new candidate genes regulated by CRH/CRHR1-dependent signaling mechanisms *in vitro* and stress-/CRHR1-regulated signaling pathways *in vivo*. *In vitro*, the MPIP 24 k cDNA array was used including more than 24000 transcripts representing 12387 genes. Six technical replicates were performed per time point to strengthen statistical power but nevertheless, a t-test failed to calculate robust p-values. Therefore, the z-score was used as statistical criterion to define statistical significance. Experimental quality was controlled by analyzing the scan images and scatter plots for conspicuous alterations. In AtT-20 cells, 15418 transcripts were detected among them 102 transcripts (0.7%; 96 genes) significantly regulated in at least one time point (fold regulation ≥ |1.3|) comparing CRH-treated versus control cells after 1, 3, 6, 12 and 24 h of chronic stimulation. 17 of these genes (18%) showed an expression difference of at least 1.7 fold. The expression analysis of Peeters *et al.* comparing different time points of CRH-stimulated AtT-20 cells to corresponding controls resulted in 88 significantly regulated genes, a similar amount as it was obtained in our experiment (Peeters *et al.*, 2004b). But only two genes, Crem and Errfi1, were regulated in both experiments. This little overlap can be explained by the different stimulation protocols (1 µM vs. 100 nM CRH, different time points) and the application of

different microarrays (oligonucleotide array of Affymetrix vs. custom cDNA microarray). Moreover, the comparison of CRH-stimulated target genes with changes on protein level revealed one candidate, Hmgcs1, upregulated in both experiments (Kronsbein *et al.*, 2008).

For the *in vivo* experiment the commercially available Illumina Sentrix® BeadChip Array for Gene Expression Mouse-6 was utilized to detect stress- and CRHR1-dependent gene expression differences. Containing 45200 transcripts covering more than 19100 unique genes, this array platform not only permits the detection of the vast majority of all murine genes but includes in average 10 probes per transcript meaning technical replicates within one microarray hybridization enforcing the statistical analyses. To reduce variability analyzed pituitaries were pooled per group (wt basal, wt 1 h, wt 3 h, ko basal, ko 1 h, ko 3 h). Using two animals per group two technical replicates were performed. Experimental quality was examined by internal controls and confirmed reliable microarray results. 9392 transcripts were detected in all five investigated comparisons (wt stress/wt basal 1 h, wt stress/wt basal 3 h, ko/wt basal, ko/wt stress 1h, ko/wt stress 3 h). Among them, 11 % were found stress- and 4 % stress- and CRHR1-dependently regulated (fold regulation ≥ |1.5|). Although *in vivo* approximately the same number of transcripts was detected in comparison to the *in vitro* experiment, a higher percentage of transcripts was differentially expressed caused by the activation of CRHR1. One explanation for this observation is presumably the unequal statistical power of the two microrarray platforms used. Though *in vitro* six technical replicates were assayed, the Illumina platform contains in average 10 replicates per transcript per array. Adding the two technical replicates, the statistical calculation seems to yield more significantly regulated genes *in vivo*. In addition, the applied version of Illumina software for data analysis did not include false discovery rate (FDR) correction. Thereby, the high number of regulated transcripts *in vivo* includes a considerable number of false positive genes. Last but not least, it was described for one-color and two-color microarray platforms that both experimental setups do not vary in sensitivity but that one-color data exhibits larger fold changes leading to more differentially expressed genes (Patterson *et al.*, 2006).

5.1.3 Selection of candidate genes *in vitro*

To elucidate molecular mechanisms and targets regulated by CRH/CRHR1-dependent signaling different bioinformatical approaches were applied. The correct identification and assembly of gene clusters that show synchronous response to CRHR1 activation is a first step to deduce CRHR1-dependently regulated signaling mechanisms. *Spinecluster* uses an unsupervised clustering approach which takes into account the temporal relationship among samples. Based on Bayesian-model hierarchical clustering this algorithm can be

applied on the whole as well as on a relevant subset of the expression profile data set. To solve the dimensionality problem (huge number of variables (genes) compared to the sample size (replicates)), it is recommended to perform the cluster analysis with the subset of CRH-responsive genes although it was originally developed for a complete expression data set (Heard *et al.*, 2006; Mutarelli *et al.*, 2008). *Spinecluster* was used for the complete *in vitro* data including all transcripts detected at all time points. The 10 different clusters revealed by *Spinecluster* represent groups of genes with similar dynamics. As the whole detected data set was used for the analyses, one big cluster was found containing 90% of the transcripts not significantly regulated over time. The remaining 9 clusters represent the candidates which are time- and CRH-dependently regulated. Candidates of each of these clusters are expected to be controlled by similar molecular mechanisms. Indeed, genes similarly regulated over time exhibit similar functions according to the GO nomenclature. All 9 clusters can be grouped into two main clusters based on the regulation within the first hour. In this way, the clusters 1, 2 and 10 contain all genes which are upregulated after 1h of CRH treatment whereas the other clusters represent genes downregulated in the first hour of CRH stimulation. Interestingly, in the first group genes with signal transduction function are overrepresented indicating that CRH induces intracellular signaling activity within the first hour after receptor activation. In addition to the assessed general GO functions, more specific functional groups occurred in dependency of the according cluster. Focusing on the strongest regulated genes obtained by simple cut-off settings (fold regulation ≥ |1.3|) those with signal transducing function were predominantly found in cluster 1 whereas in cluster 7 almost all listed GO functions (Table S2, supplementary) such as transcription, nucleic acid binding, calcium-ion transport, kinases, apoptosis and proteolysis were present. In cluster 6 three of the four strongest regulated genes related to ubiquitin-dependent catabolic processes were clustered. Altogether, *Spinecluster* successfully clustered co-regulated genes time-dependently. Moreover, in different clusters certain molecular functions were clearly found overrepresented linking CRH- and time-dependent regulation to biological function. 34% of the strongest regulated genes belonged to the unregulated cluster 4. On one hand this supports the time-dependent analysis of the microarray data. A gene significantly regulated at one time point does not have to contribute to relevant dynamic regulation which was analyzed with *Spinecluster*. On the other hand, the clusters 2 and 5 did not contain any gene defined as significantly regulated by chosen cut-off criteria. Genes of these clusters are significantly but weakly regulated over time and therefore difficult to validate with independent methods.

The second bioinformatical approach included univariate as well as multivariate methods followed by graphical models and aimed to unravel gene-gene interactions. Variable

selection is an important aspect of microarray data analysis. If it is possible to interpret a small subset of genes as biologically relevant, it may provide some insight into understanding the underlying mechanism. Variable selection methods should be oriented towards the aim to reveal combinations of genes whose expression patterns are strongly associated with time-dependent changes. Therefore, supervised methods have to be used to predict the value of an outcome measure (time point) based on expression values of genes (input measures). There is a great reservoir of multivariate statistical methods in supervised learning e.g. methods of classification, Boosting Trees (BT) and Support Vector Machines (SVM) (Hastie *et al.*, 2001a). BT and SVM are theoretically not affected by the so-called dimensionality problem. Typically, in microarray studies the number of variables (genes) is huge compared to the sample size (replicates). With this dimensionality problem - also encountered in the field of chemometrics - it is difficult to apply LDA due to the singularity of the within-class scatter matrix. The crucial point in LDA with many - normally highly correlated variables - is the stable estimation of the within-class covariance matrix. Two main strategies are known to overcome the problem: (i) truncation or dimension reduction of data or covariance matrix (Modified canonical analysis (Krzanowski *et al.*, 1995) or stabilized LDA (Läuter *et al.*, 1998)): (ii) penalizing or shrinking the covariance matrix (optimal shrinkage parameter (Ledoit and Wolf, 2003), generalized ridge discrimination (Krzanowski *et al.*, 1995)). Despite the capability of coping with high-dimensional data an intuitive approach consists of first selecting a subset of variables and then applying a supervised method. It has been demonstrated that the performance of boosting for classification of gene expression data can often be drastically improved by performing feature preselection (Dettling and Buhlmann, 2003). Multivariate approaches take into consideration that many variables (genes) may be highly correlated in terms of interaction networks. Therefore, it is risky to restrict variable selection to univariate methods, which ignore correlations or interactions among genes, which may be essential for discrimination. Here, the solution of an optimization problem with a large search space is searched for and specific methods like stochastic search strategies have to be used. Stochastic search strategies in combination with supervised classification methods have been developed and successfully applied on microarray datasets over the past years in order to address the problem of feature extraction (Deutsch, 2003; Jirapech-Umpai and Aitken, 2005; Ooi and Tan, 2003). As a robust stochastic search procedure the genetic algorithm has become popular in recent years. GA uses a randomized approach based on the process of mutation and crossover. However, these methods are able to detect only a small part of the total solution space. The origin of every GA is always a random population and different searches may deliver various solutions. Therefore, the *GALGO* analysis was repeated separately four times. The final 11 candidates revealed by

this procedure are expected to be highly correlated with each other in terms of gene interaction networks. In the principal component analysis the pronounced differential expression values observed at 1, 12 and 24 h probably reflect a dominant impact of CRH/CRHR1-dependent signaling events on processes related to an immediate response to stimulation as well as on processes related to chronic stimulation. The similar regulation at 3 and 6 h suggests the regulation of common cellular mechanisms at these time points. The graphical Gaussian model *GeneNet*, another unsupervised correlation method, was used to build up a gene association network. Primarily developed for analyzing gene expression (time series) data with focus on the interference of gene networks (Schäfer and Strimmer, 2005a; Schäfer and Strimmer, 2005b) *GeneNet* groups together genes based on their coregulation over time and its results are in agreement with the foregoing results of the PCA - an independent unsupervised clustering method - where most of the gene clusters were found to be correlated, in particular Fosl2-Crem, Pex13-Cd3e-Nf2 and Acsl4-Hmgcs1. As for all three mentioned gene-gene interaction clusters connections were confirmed by literature search using *PathwayStudio*, the combination of supervised and unsupervised algorithms led to the extraction of a small subset of significantly time- and CRH-dependently regulated genes out of a genome-wide data set. Moreover, the seven genes were linked to known CRHR1-dependent signaling pathways according to their functions and inter-gene connections (see chapter 5.3). Crem and Fosl2 (cluster 10) as well as Nf2 and Pex13 (cluster 9) clustered together in the *Spinecluster* analysis, too, proposing common regulatory and functional mechanisms for these candidates and supporting the results of the *GeneNet* analysis. Cd3e and Acsl4 were not found differentially regulated in the *Spinecluster* algorithm (cluster 4) whereas the predicted interaction partner of Acsl4, Hmgcs1, was grouped into cluster 8. The differential expression of Cd3e was not validated because of too low expression. Therefore, a potential role of this candidate in CRHR1-mediated effects is impossible to analyze. Also the maximal differential expression of Acsl4 was less than 1.5 fold in only two time points explaining the assignment to cluster 4. Comparison of the top 11 candidates from the *GALGO* analysis with the 102 strongest regulated genes according to simple cut-off criteria revealed six of them which displayed a significant differential expression in at least one time point. The missing five candidates exhibited a significant dynamic regulation but with expression differences less than 1.3 fold. Again, these genes are significantly but weakly regulated over time and therefore difficult to validate with independent methods but contribute to temporal CRHR1-dependent signaling mechanisms.

In summary, Bayesian-model based hierarchical clustering revealed CRH- and time-dependent expression changes representing co-regulated genes with different GO functions. Moreover, the combination of algorithms utilized for the prediction of gene-gene

interactions reduced the entire expression profiling data set to seven candidate genes representing important targets of CRHR1 signal transduction. Combining the results of both applied bioinformatical analyses with a fold regulation cut-off, a robust set of differentially expressed candidate genes was obtained reflecting CRHR1-dependent signal transduction *in vitro*. These results strengthen the role of CRH as a dynamic modulator of a variety of signal transduction mechanisms and cellular processes. Time-dependent changes in gene transcription as depicted in Figure 26 support in case of the early regulated genes Crem, Fosl2 and Rgs4 on one hand the regulation of established CRHR1 signaling cascades like $G_{\alpha S}$-dependent signaling via cAMP, PKA, MAPK, CREB and NUR transcription factors. On the other hand, the differential expression of Errfi1 and Dusp14 suggests previously unkown crosstalks with other signaling mechanisms such as receptor tyrosine kinase-dependent signal transduction.

After 3 h of CRH stimulation, genes involved in other cellular mechanisms such as transport appear but still signaling molecules with kinase or protein binding functions affecting signal transduction are regulated. Chronic CRH treatment for 6 h and longer stimulates in addition metabolic and proliferative molecules strengthening the involvement of CRH and CRHR1 signaling in those cellular processes (Fig. 26).

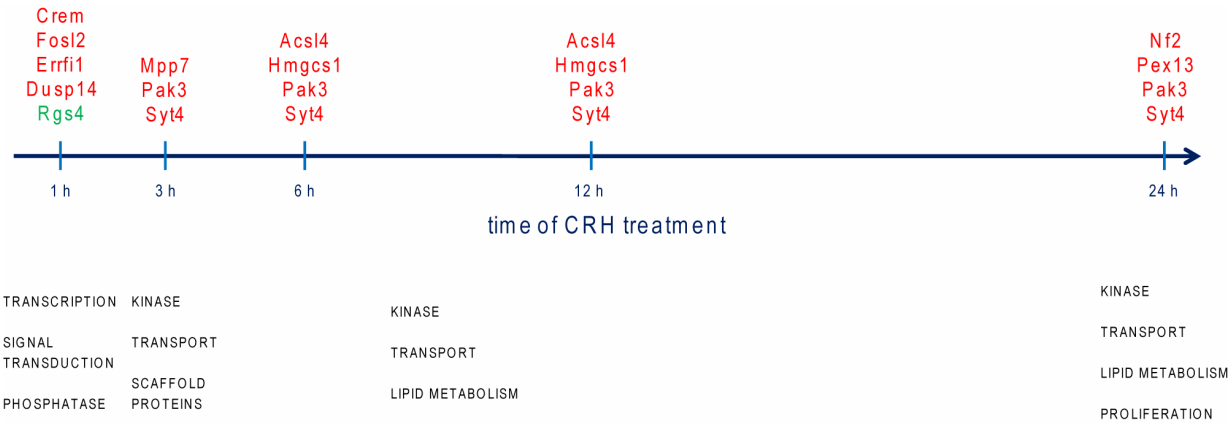

Figure 26. Time- and CRHR1- dependent functional changes of gene expression in AtT-20 cells. Upregulated genes are marked in red, downregulated genes in green. In black, corresponding functional classes according to the NCBI gene ontology nomenclature are depicted.

5.1.4 Validation of differential gene expression

Subsets of *in vitro* as well as *in vivo* candidate genes were selected for validation of differential expression in independent material. In AtT-20 cells, 12 (86%) of the 14 analyzed genes were validated by qRT-PCR. As the corticotrope cell line represents a rather uniform and stable cell population, changes of gene expression patterns due to CRH stimulation are highly reproducible among different experiments. Therefore, the *in vitro* approach resulted in expression changes that were readily validated in independent

material. In contrast, the *in vivo* experiment was confronted with two levels of complexity. First, the entire complex organ of pituitary was used consisting of different cell types. Second, stress induces complex changes modulated by the whole organism. Therefore it does not astonish that among hundreds of genes only a small subset was validated in independent material. Furthermore, individual variability of analyzed animals complicates the reproducibility of measured expression differences. In addition, the group size of examined samples was rather small impeding the validation in independent material. Nevertheless, the regulation of 30% of the chosen candidates was verified in independent material in at least one time point *in vivo*. Besides the mentioned biological variations, also differences in the compared methodologies impede the validation of differential expression. The microarray technology bases upon hybridization technology whereas quantitative real-time PCR is a PCR method. Furthermore, Canales *et al.* showed that the position of the microarray probe and of the amplicon produced by qRT-PCR within the analyzed gene could influence the comparability of the results obtained from both methods (Canales *et al.*, 2006).

5.2 Comparison of CRHR1-dependently regulated genes *in vitro* and *in vivo*

In cell culture intracellular physiological processes taking place in the entire organism are maintained but the complex *in vivo* situation is reduced to a simple and easy accessible model. Therefore, cell lines are good *in vitro* systems for basic research. AtT-20 cells are intermediate pituitary corticotrope cells and solely express the CRHR1 and not CRHR2. Thus, they are an ideal cellular system to study molecular CRHR1-dependent signal transduction (Abbud *et al.*, 2004; Peeters *et al.*, 2004b). But as cell culture conditions may differ from physiological states, *in vitro* findings should not be regarded isolated. Therefore, we additionally examined stress- and CRHR1-dependent changes of gene expression in murine pituitaries and compared the *in vitro* and *in vivo* expression profiles. Comparing gene expression profiles *in vitro* with *in vivo* data resulted in model-specific responses but included also a small subset of commonly regulated genes (Dere *et al.*, 2006; Liu *et al.*, 2007). 18865 transcripts (78% of total transcripts of the MPI 24 k chip and 42% of Illumina Sentrix® BeadChip, respectively) are presented on both applied microrrays according to their gene annotation. Therefore, the majority of transcripts analyzed by the MPIP 24 k platform is also expressed on the Illumina Sentrix® BeadChip making both experiments comparable. More than 15000 transcripts were found expressed *in vitro* and *in vivo* in at least one time point. Regarding the overlap of annotated genes of both experiments, 12119 (79% of detected transcripts *in vitro*) of these transcripts were detected *in vitro* and *in vivo* reflecting the overall overlap between the platforms.

Nevertheless, in this study, the 102 CRH/CRHR1-regulated transcripts *in vitro* were compared with the 991 stress-regulated transcripts *in vivo* what resulted in a very small overlap of six genes. Only two of these six genes were additionally CRHR1-dependently regulated (Errfi1, Mpp7). Moreover, the differential expression ko/wt was validated only for Crem and Errfi1 *in vivo*. All together, only one gene, Errfi1, was verified to be stress/CRH- and CRHR1-dependently regulated *in vitro* and *in vivo*. There are several reasons explaining the little overlap between the experiments. First, *in vivo*, candidate genes were selected including two factors, stress and genotype. This increased the data complexity and revealed more differentially expressed genes. Furthermore, genetic manipulation evokes compensatory mechanisms influencing a plethora of processes including signal transduction pathways. Conventional deletion of CRHR1 changes the expression of various genes already under basal conditions (Deussing *et al.*, 2007) which may affect CRHR1-dependent signaling molecules. Additionally, stress regulated different genes in pituitary tissue than CRH treatment in pituitary corticotrope cells in culture because the cellular composition of the anterior pituitary is more complex than AtT-20 cells. AtT-20 cells are corticotrope cells expressing the CRHR1 whereas the pituitary consists of the anterior (corticotrope, melanotrope, somatotrope, lactotrope and gonadotrope cells), intermediate and posterior lobe expressing also the CRHR2 (Van Pett *et al.*, 2000). Furthermore, AtT-20 cells are all in the same stage of proliferation and differentiation as the FCS deprivation leads to cell cycle arrest. Moreover, the direct activation of CRHR1 by CRH *in vitro* was related to the indirect activation by stress *in vivo*. Restraint stress in mice leads to various reactions of the organism including the activation of the HPA axis starting with the release of CRH and AVP. Both hormones trigger the activation of pituitary corticotropes influencing CRHR1-induced signaling cascades (DeBold *et al.*, 1984). The complexity of stress-related molecular changes *in vivo* is difficult to compare with the simple CRH-dependent activation within the *in vitro* situation. Although *in vitro* and *in vivo* the first measured time points were the same, the time delay *in vivo* until activation of the CRHR1 in the pituitary occurs has to be considered, too. Therefore, earlier time points *in vitro* are expected to be comparable with later time points *in vivo*. Indeed, three of the six overlapping candidates are regulated *in vitro* after 1h of CRH stimulation but *in vivo* after 3 h of stress. Last but not least, one important reason for the model differences is the application of two different microarray platforms. Both platforms differ in number and sequences of probes, mRNA preparation, dye-labeling and hybridization, scanning and normalization procedures. Several studies analyzed the comparability of different microarray platforms and observed a considerable discordance regarding the differentially expressed genes (Kothapalli *et al.*, 2002; Kuo *et al.*, 2002; Tan *et al.*, 2003).

In this study, the selected experimental setups are difficult to compare. Different CRHR1 activation strategies, distinct cell types and two microarray platforms complicate the dissection of common CRHR1-dependent signaling mechanisms *in vitro* and *in vivo*. In general, results obtained using *in vitro* systems are to a certain extend transferable to the corresponding *in vivo* models. CRH stimulation of *ex vivo* or primary cell cultures of pituitaries, direct activation of CRHR1 by i.p. or intravenous (i.v.) CRH injection *in vivo* and the use of a single array platform are possibilities to increase the comparability of CRHR1 signal transduction in AtT-20 cells and murine pituitaries. Nevertheless, new findings acquired in cell culture are the basis for further in depth research in *in vivo* models. Therefore, we focused especially on Errfi1 to elucidate its role in CRHR1 signaling *in vitro* and *in vivo*.

5.3 Potential role of new candidates in CRH/CRHR1-regulated signal transduction in corticotrope and neuronal cells

In vitro the differential expression of 12 candidate genes was confirmed at several time points. We focused on the role of Crem, Fosl2, Dusp14, Errfi1, Mpp7, Pak3, Nf2 and Rgs4 in CRHR1-dependent signal transduction, which was further analyzed using reporter assays. According to the reporter assay results, those candidate genes seem to be not only regulated by CRH but in turn directly influence CRH/CRHR1-mediated signaling.

Crem and Fosl2, both transcription factors, are upregulated in the first hours of CRH stimulation and appear in a common cluster as calculated by *Spinecluster* and *GeneNet* algorithms indicating similar regulatory mechanisms. **Crem** is a modulator of cAMP responsive element (CRE) -dependent transcription. The constitutively expressed variant Crem induces CRE-dependent transcription whereas the inducible variant Icer, an alternatively spliced variant, is known to inhibit CRE-dependent gene expression (Lamas and Sassone-Corsi, 1997). The expression of numerous genes such as CRH or tyrosine hydroxylase involved in psychiatric and neurodegenerative disorders, respectively, is regulated by Crem/Icer (Liu *et al.*, 2006). Moreover, Crem is known to be activated by CRH in AtT-20 cells and seems to contribute to an intracellular negative feedback on CRHR1-depedent signaling cascades (Peeters *et al.*, 2004b). This assumption was confirmed with the reporter assay results. Icer not only inhibited cAMP-controlled signaling in AtT-20 cells but affected Nur-induced transcription in AtT-20 cells probably via secondary effects demonstrating its negative regulatory role in CRHR1-dependent signal transduction. Moreover, in a microarray experiment comparing 300 nM CRH-treated primary hippocampal mouse cells at 6 and 12 h (unpublished data) Crem was upregulated after 6 h. In HN9 cells Crem also blocked CRH- and cAMP-induced CRE transcription

supporting its possible role in mediating CRHR1-dependent autoinhibitory effects on transcriptional level.

Fosl2 is a transcription factor of the Fos family. Its most prominent member is the immediate-early gene c-Fos. Heterodimerization with members of the Jun family of transcription factors leads to transcriptional regulation of genes containing an AP1-binding site in their promoter. Upon CRH stimulation of AtT-20 cells AP1 binding to the Pomc promoter is increased. Furthermore, CRH changes the protein composition of the bound AP1 complexes in a time-dependent manner. Fosl2 dimerizes with Jun-D 4 h after CRH stimulation and suppresses further Pomc transcription by controlling c-Fos/Jun-B expression (Becquet *et al.*, 2001). This autoregulatory negative feedback on Pomc transcription is likely to be mediated by CRE- and NurRE-dependent transcription in AtT-20 cells and CRE-transcription in HN9 cells downstream of cAMP.

As early regulated transcription factors Crem and Fosl2 may play an important role in an autoregulatory loop of CRHR1-dependent signal transduction, probably by suppressing the transcription of secondary involved genes.

Another validated *in vitro* candidate is synaptotagmin 4 (**Syt4**), which was also found upregulated at 6 and 12 h of CRH treatment of primary hippocampal cells (unpublished data). Syt4 is a Ca^{2+}-binding, membrane protein present in secretory vesicles and is broadly expressed in the brain. Syt4 triggers Ca^{2+}-dependent exocytosis e.g. in astrocytes (Zhang *et al.*, 2004) and is involved in mood-related behavior as Syt4-ko mice display reduced anxiety- and depression-like behavior (Ferguson *et al.*, 2004). Because of its upregulation by CRH in AtT-20 cells Syt4 may play a role in CRH-induced Ca^{2+}-dependent ACTH release whereas in hippocampal cells it may assist the release of neurotransmitters.

Mpp7, a nearly uncharacterized member of the p55 Stardust family of membrane-associated guanylate kinase (MAGUK) proteins, contains SH3 and PDZ domains and is upregulated by CRH at 3 h. MAGUK family proteins are critical adapter proteins for the assembly of multiprotein complexes and regulate the activity of interacting membrane proteins by modulating their surface delivery, endocytosis and subcellular localization. They are found at synapses, adherens junctions and tight junctions where they organize signaling complexes (Bohl et al., 2007; Kim and Sheng, 2004). It is not clear if CRH receptors exert their effects via scaffold proteins but specific interactions between CRHRs and other receptor systems through protein-protein interactions may influence downstream signaling components of CRH and other partner receptors. Indeed, overexpression of Mpp7 slightly enhanced CRH-induced CRE and NurRE transcription proposing a positive regulatory role of this scaffold protein in corticotrope CRHR1 signaling.

Together with Mpp7, the p21-activated kinase 3 (**Pak3**) was found in the same cluster based on Bayesian-model based hierarchical clustering and showed an upregulation at all time points starting from 3 h after CRH stimulation. Furthermore, Pak3 was found upregulated 6 h after CRH stimulation of primary hippocampal cells (unpublished data) supporting a general role in CRHR1-activated signaling cascades. Paks are serine-threonine kinases implicated in a number of different intracellular processes including cytoskeletal regulation, synaptic plasticity and the activation of MAP kinases (Boda et al., 2004; Manser et al., 1997; Zhang et al., 1995). Pak3 is known to inhibit neuronal apoptosis and DNA synthesis and can be activated by the small GTP-binding proteins Rac and Cdc42 and a variety of external stimuli that act through e.g. GPCRs (Knaus *et al.*, 1995; McPhie *et al.*, 2003). Pak3 contains different functional protein domains such as a CRIB domain inside the GTPase-/p21-binding domain (PBD) and an autoinhibitory domain (AID) (Jaffer and Chernoff, 2002). Binding of the GTP-bound GTPases to the CRIB domain of Pak3 leads to a blockade of the AID allowing kinase activation (Buchwald *et al.*, 2001). Membrane recruitment of Pak3 is required for its activation mediated e.g. by Nck adapter linking Pak to tyrosine kinase receptors (Li *et al.*, 2001). The expression of Pak3 was detected in the nervous system and mutations of the Pak3 gene lead to nonsyndromic mental retardation (Knaus and Bokoch, 1998; Meng *et al.*, 2005). Some years ago, a new splice variant of Pak3, Pak3b, was discovered and is characterized by an additional 45 bp exon inside the AID leading to a constitutive active kinase independent of Rac and Cdc42 binding (Rousseau *et al.*, 2003). Like Pak3a, the originally found Pak3, Pak3b expression in mice is predominantly found in the brain. The overexpression of both splice variants in AtT-20 and HN9 cells led to splice variant- and cell type-dependent differences in the effects on CRHR1-activated signal transduction. The inducible Pak3a indeed enhanced CRH-activated CRE and NurRE transcription independently of cAMP in corticotrope AtT20 cells whereas the CRE transcription in neuronal HN9 cells was enhanced downstream of cAMP. In contrast, the constitutively active form Pak3b only inhibited cAMP-induced CRE transcription independently of CRHR1 but CRH- and cAMP-dependent NurRE transcription in AtT20 cells. In HN9 cells, Pak3b further increased CRHR1-connected CRE-transcription independently of cAMP. Thus, Pak3a and Pak3b seem to modulate different signaling pathways. As in anterior pituitary and AtT-20 cells Pak3a is upregulated by CRH and its knockdown inhibited CRH-induced cell viability (Kageyama *et al.*, 2008), Pak3a may act in corticotrope cells by linking CRHR1-dependent events upstream of cAMP to cell cycle regulating pathways such as growth factor receptor-mediated signal transduction. In neuronal cells the Pak3a and Pak3b kinases activity is likely to positively influence CRH-activated signaling mechanisms such as PKA, MAPK or Ca^{2+}. In corticotrope cells, Pak3b may play a role in

CRHR1 signaling through regulating Nur transcription factors expression via signaling cascades dependently or downstream of cAMP.

The regulator of G protein-signaling 4 (**Rgs4**) was downregulated by CRH after 1 h remaining slightly decreased at all later time points in AtT-20 cell suggesting a CRH-dependent reduction of negative regulation on GPCR signaling. As Rgs4 mRNA is changed by chronic stress in rat locus coeruleus, PVN and pituitary it seems to contribute to the adaptation to stress (Ni *et al.*, 1999). RGS proteins function as GTPase accelerating proteins (GAPs) by binding to the GTP-bound G_{α}-subunits and activating their intrinsic GTPase leading to dampening of the GPCR-mediated signaling. Actually, overexpression of Rgs4 in corticotrope cells diminished CRH-induced CRE transcription as expected while it enhanced CRE-mediated expression after cAMP stimulation suggesting Rgs4 as negative regulator of CRHR1-activated signaling but with another role in cAMP-triggered signaling pathways without GPCR involvement. Indeed, RGS proteins of the R4/B subfamily, where Rgs4 belongs to, appear to bind numerous cellular signaling factors in both G protein-mediated and non GPCR pathways (Bansal *et al.*, 2007). The expression of Rgs4 is enriched in the CNS and the heart in both, humans and rodents (Erdely et al., 2004; Zhang et al., 1998). Rgs4 regulates opioid, cholinergic and serotonergic signaling in the brain and plays a role in Parkinson disease and schizophrenia (Bansal *et al.*, 2007). Inhibition of Rgs4 potentiated serotonergic receptor ($5HT_{1A}$)-mediated regulation of NMDA receptor channels in rat prefrontal cortex neurons whereas Rgs4 overexpression inhibited this response (Gu *et al.*, 2007). In primary hippocampal cells Rgs4 was upregulated at 6 and 12 h of CRH treatment (unpublished data) and enhanced the CRH-induced effect on CRE transcription dependent of cAMP in neuronal HN9 cells. This proposes a new role for Rgs4 via a probable interaction with other signaling molecules potentiating CRHR1-activated signaling downstream/dependent of cAMP in neuronal cells.

Nf2 and Pex13 clustered together in the *Spinecluster* algorithm and with *GeneNet* additionally Cd3e was found coregulated with both candidates because of their common upregulation after 24 hours of CRH stimulation. Therefore, these molecules should not be involved in acute signal transduction, but rather in the modulation of CRH-dependent cellular processes such as proliferation or immune response (Graziani et al., 2007; Karalis et al., 1997; Slominski et al., 2006) Along these lines, all three genes have divergent functions. **Nf2**, a tumor suppressor, plays a critical role in cell proliferation by blocking growth factor receptor-dependent pathways (Lim *et al.*, 2006a). The Cd3-epsilon polypeptide **Cd3e** occurs in the T-cell receptor complex, which couples antigen recognition to several intracellular signal transduction pathways. The peroxisomal biogenesis factor **Pex13** functions as protein transporter in peroxisomes and is related to fatty acid oxidation. As it is known that PKA phosphorylates Nf2 (Alfthan *et al.*, 2004) and

as the regulation of Pex13 and Cd3e was weak and not validated, respectively, the both latter candidates were not further investigated. Nf2, also known as merlin or schwannomin, is predominantly expressed in neurons and mutated in nervous system tumors (Gronholm *et al.*, 2005). It is related to the ezrin-radixin-moesin (ERM) protein family (Rouleau *et al.*, 1993; Trofatter *et al.*, 1993) and links cell membrane proteins with the actin cytoskeleton through its N-terminal FERM (four-point-one protein/ERM) domain (Bretscher *et al.*, 2002; Sun *et al.*, 2002). On the one hand, Nf2 blocks cell growth by inhibition of EGFR signal transduction through sequestration of the EGFR into an insoluble membrane compartment (Cole *et al.*, 2008). On the other hand, Nf2 binds to the Grb2 protein thereby inhibiting growth hormone-activated MAP kinase signaling pathway including Raf1 and ERK (Lim *et al.*, 2006b). Two major alternatively spliced Nf2 variants, Nf2_17 lacking exon 16 and Nf2_16 containing exon 16, are expressed in normal tissues. Nf2_16 encodes a protein with a shorter C-terminus which is not able to block tumor growth as Nf2_17 is (Sherman *et al.*, 1997). Similar effects were detected with a Nf_17 C-terminal truncated version. The effects of all three Nf2 variants plus one N-terminal truncated Nf2 on CRH-induced CRHR1 signaling were analyzed. All Nf2_17 variants were able to further enhance CRH-stimulated CRE and NurRE transcription in AtT-20 cells whereas Nf2_16 only increased NurRE transcription. In the case of the N-terminal and C-terminal truncated Nf2_17, the enhancing effect was weaker as with the full-length version suggesting the importance of both protein parts for efficient protein activity. Only the effect of Nf2_17 on CRE was dependent of cAMP. Nf2 positively influences CRH-activated transcription independently of its N-terminus. The C-terminus seems to be discriminative for CRH-induced CRE transcription but not for NurRE. As only the effect of Nf2_17 on CRE transcription is dependent of cAMP, two different signaling pathways are likely to mediate the Nf2-evoked changes on CRE and NurRE, respectively. Perhaps through interacting with other signal transduction pathways like ErbB receptor signaling, the two different Nf2 variants augment on the one hand cAMP-dependent CRE transcription downstream of PKA whereas on the other hand, NurRE-dependent transcription may be changed by affecting the MAP kinase pathway independently of cAMP. Because of its important role in the brain and its upregulation in primary hippocampal cells upon 6 h of CRH stimulation (unpublished data), the effect of all Nf2 versions on neuronal CRHR1 signal transduction was assessed. Independent of the C- or N-terminus all variants enhanced CRH-stimulated CRE transcription dependent of cAMP proposing a positive regulatory function of Nf2 on CRHR1-mediated signal transduction also in neuronal cells. In both cell types, the exact mechanism of Nf2 to enforce CRH-induced signaling is not clear and has to be further investigated. As CRH is known to regulate cell proliferation Nf2

could be one of the responsible molecules mediating the CRH effect on cell growth (Graziani et al., 2007; Slominski et al., 2006).

Hmgcs1 and **Acsl4**, both revealed by *GeneNet* analysis, were weakly upregulated after 6 and 12 h of CRH treatment. Both genes are involved in lipid metabolism and were found to be connected via the peroxisomal proliferator-activated receptor α (PPARA), which maintains fatty acid homeostasis by induction of fatty acid oxidation and plays a role in controlling peroxisomal proliferation. The Hmgcs1 gene contains a peroxisome proliferator response element (PPRE) in its promoter that binds PPARA/RXR heterodimers. In human liver cells the Hmgcs gene is upregulated by PPARA overexpression (Hsu *et al.*, 2001). Long-chain acyl-CoA synthetases (LC-ACS) like Acsl4 inhibit PPARA-mediated transcription (Hertz *et al.*, 1994) and the blockade of LC-ACS with triascin C results in an increase in PPARA activation *in vitro* (Forman *et al.*, 1997). Acsl4 transcription is activated by cAMP (Cornejo Maciel *et al.*, 2005) and PPARA gets phosphorylated by this second messenger (Lazennec *et al.*, 2000) linking these genes with $G_{\alpha S}$ protein-coupled receptor signaling pathways such as CRHR1. The CRH/CRHR1-dependent regulation of genes involved in lipid metabolism strengthens a potential role of CRH as a modulator of metabolic function. Many psychiatric and neurological disorders coincide with changes in metabolism (Newcomer, 2006; Taylor and MacQueen, 2007). Hmgcs1 together with other genes linked to fatty acid metabolism is upregulated by antipsychotics in human glioma cells (Ferno *et al.*, 2005).

The dual specificity phosphatase 14 (**Dusp14**), also known as MAP kinase phosphatase 6 (Mkp6), is a MAP kinase phosphatase which was shown to be upregulated by ERK activation in mouse striatum (Marie-Claire *et al.*, 2008) but inhibits the activity of ERK1/2, JNK and p38 kinases (Marti *et al.*, 2001) contributing to a direct negative feedback mechanism of MAPK signaling. Actually, the overexpression of Dusp14 in AtT-20 and HN9 cells does not influence CRH-induced MAPK-independent CRE transcription but changes MAPK-dependent NurRE transcription in corticotrope cells. Surprisingly, the overexpression of Dusp14 enhanced CRH-stimulated NurRE-mediated expression. However, this suggests a role for Dusp14 in the inhibition of other, perhaps indirectly by CRH activated, MAP kinase signaling pathways such as receptor tyrosine kinase-dependent signaling mechanisms. By influencing additional signaling cascades, Dusp14 may strengthen CRHR1-dependent NurRE transcription instead of inhibiting directly CRH-activated ERK through dephosphorylation.

The only candidate found CRH/stress- and CRHR1-dependently regulated *in vitro* and *in vivo*, **Errfi1** (ErbB receptor feedback inhibitor 1), also called Mig6 (mitogen-inducible gene 6), is a nonkinase scaffolding adaptor protein known to inhibit ErbB receptor-activated signaling cascades. On the one hand, Errfi1 binds to the receptor tyrosine kinases through

its C-terminal Ack1 homology domain (Anastasi et al., 2003; Fiorentino et al., 2000). On the other hand, it directly interacts with Grb2 via its SH3 domain and the GTPase Cdc42 via its CRIB domain inhibiting RTK-induced signal transduction including PI3 kinase, JNK and p38 MAP kinases (Pante *et al.*, 2005; Xu *et al.*, 2005). Dexamethasone-induced Errfi1 expression in rat fibroblasts inhibits EGFR autophoshorylation and thereby EGF signaling suggesting Errfi1 as connecting molecule in a crosstalk between EGF/ErbB signaling and other mitogenic signaling pathways (Xu *et al.*, 2005). Errfi1 is an immediate early gene whose expression can be rapidly induced by hormones, growth factors and various kinds of stress (Zhang and Vande Woude, 2007) such it was observed in AtT-20 cells after 1 h of CRH stimulation. In the pituitaries of CRHR1-ko mice Errfi1 expression was reduced 3 h after onset of stress compared to CRHR1-wt animals supporting its CRHR1-dependent upregulation *in vitro*. Overexpression of different Errfi1 constructs in AtT-20 cells revealed Errfi1 as a molecule inhibiting CRH- and cAMP-dependent CRE transcription. For the reduction of CRH-stimulated CRE transcription, full-length Errfi1 is required whereas mutants without the CRIB or the Ack1 homology and PDZ domain, or containing only the CRIB domain did not have any effect. Either Errfi1 mediates this inhibition via influencing ErbB receptor signaling through binding to the RTK as well as Grb2 or Cdc42 or Errfi1 uses a new, unknown mechanism to affect CRHR1 signal transduction. In contrast to its CRH-induced upregulation in corticotrope cells, CRH downregulated Errfi1 after 12 h of CRH treatment of hippocampal primary cells (unpublished data) suggesting differences in CRHR1-dependently activated signaling mechanisms in corticotrope and neuronal cells. Indeed, overexpression of Errfi1 in HN9 cells further increased CRH- and cAMP-stimulated CRE transcription. For this effect, all domains besides the CRIB domain seem to be necessary. Therefore, Errfi1 is likely to influence CRHR1 signaling through interaction with ErbB signaling pathways on receptor level but dependent on cAMP.

The only candidate which was validated in all three assessed time points *in vivo* was the heat shock protein 1 (**Hspb1**) showing reduced expression in stressed CRHR1-ko mice. Hspb1 is able to inhibit ERK1/2 activation by H_2O_2 in mouse fibroblasts (Lee *et al.*, 2004) and to reduce apoptosis through blockade of PLCδ (Lee *et al.*, 2005) proposing a regulatory role in CRHR1-dependent signal transduction. Overexpression of Hspb1 and a mutant form, which cannot be phosphorylated, slightly increased CRH-induced NurRE transcription. Hspb1 seems to positively affect PKA and/or MAPK signaling activated by CRHR1 *in vitro* independently of its phosphorylation.

Further candidate genes with increased differential expression comparing stressed CRHR1-ko versus -wt mice were the cold inducible RNA binding protein (**Cirbp**) which downregulates mRNA translation (De Leeuw *et al.*, 2007) and increases ERK phosphorylation (Sakurai *et al.*, 2006), the RNA binding motif protein 3 (**Rbm3**) known to

enhance mRNA translation and thereby protein synthesis (Dresios *et al.*, 2005) and the **9630033F20Rik** with unknown function. The transcription factor **Nr4a2**, also called Nurr1, increases Pomc transcription upon CRH stimulation in AtT-20 cells (Kovalovsky *et al.*, 2002) and **Npn3** (neoplastic progression 3), also called sulfiredoxin 1 homolog (Srxn1), which mediates neuroprotection as answer to oxidative stress and is regulated through members of the AP1-family of transcription factors (Papadia *et al.*, 2008). The latter two genes were less expressed in CRHR1-ko mice after stress compared to CRHR1-wt mice. Besides of Nr4a2, the exact function of these candidate genes in CRHR1-dependent signal transduction remains unclear and has to be further examined.

None of the in depth investigated candidates (Icer, Fosl2, Dusp14, Errfi1, Mpp7, Pak3, Nf2, Rgs4, Hspb1) was able to change CRH-induced Pomc transcription in AtT-20 cells. First, the induction of Pomc by CRH was very weak therefore weak effects of the overexpression of selected candidates may not be detectable. Second, the effects of the candidates on CRE and NurRE transcription are potentiated because of repetitive responsive elements in the luciferase reporter promoter. Maybe these effects get attenuated and therefore lost with the whole Pomc promoter containing only one Creb and Nurr1/Nur77-binding site, respectively (Bousquet C, 2000; Boutillier et al., 1998; Therrien and Drouin, 1991). Third, the chosen candidate genes may affect other targets of CRHR1 signal transduction via influencing CRE- and NurRE-dependent signaling pathways. However, many details are known about CRHR1 signal transduction in corticotrope pituitary cells, but these results establish a basis for further investigation of CRHR1-activated signaling cascades in the brain, especially in neuronal cells. The subset of candidate genes revealed by differential gene expression and reporter assay experiments in AtT-20 cells provided the opportunity for further investigation in neuronal cells as in those cells only CRE could be used as CRH-induced target.

In Figure 27, the proposed role of selected candidate genes in corticotrope CRH/CRHR1-dependent signaling cascades is summarized illustrating the variety of regulatory mechanisms activated or inhibited through CRH-stimulated gene expression changes.

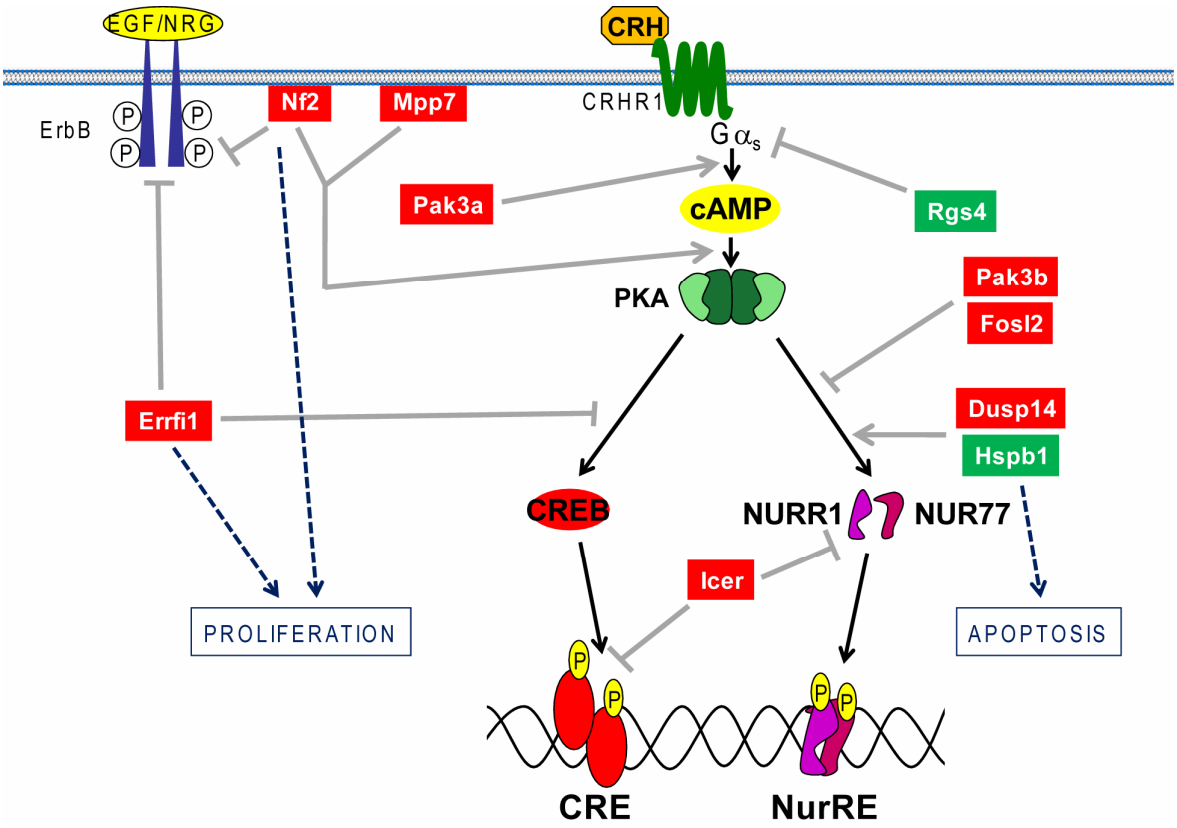

Figure 27. Overview of the potential role of selected candidate genes in known corticotrope CRHR1-dependent signaling cascades. Black lines mark established, gray lines hypothesized connections. Candidate genes are presented in red boxes when upregulated, in green boxes when downregulated by CRH or stress. Lines with an arrowhead reflect positive regulation, other lines indicate inhibition as elicited in functional experiments in AtT-20 cells.

In different brain regions CRHR1 is known to activate ERK1/2-dependent or -undependent signaling pathways (Refojo et al., 2005). In fact, similarities and differences in the role of a subset of candidate genes in corticotrope and neuronal CRHR1-dependent signal transduction were revealed indicating some common and some differing signaling mechanisms depending of the investigated cell type.

The potential functions of some of the candidates in CRH-activated signaling pathways in neuronal cells are summarized in Figure 28. Some of the target genes are not only involved in GPCR- or RTK-induced signaling cascades but are also known to affect neurotransmitter-dependent responses such as Pak3 which alters AMPA receptor expression in hippocampal slice cultures (Boda *et al.*, 2004) and Rgs4 which is able to increase serotonin release (Beyer *et al.*, 2004) and influences muscarinic acetylcholine receptors (mAch-R) (Ding *et al.*, 2006).

Compared to corticotrope CRHR1 signal transduction, Errfi1 and Rgs4 showed opposite effects on CRH-induced CRE transcription in neuronal cells what suggests a distinct role of these CRH-targets in different cell types. Whereas the downregulation of Rgs4 in AtT-20 cells seems to attenuate its negative regulatory role on CRHR1 signaling, the

upregulation of Rgs4 in primary hippocampal cells is likely to further enhance CRHR1-dependent signal transduction. A similar effect was observed for Errfi1. Its upregulation in corticotrope cells may amplify its negative regulatory effect on CRHR1-activated signaling pathways but in neuronal cells its downregulation may reduce further increasing effects on CRE transcription. On the strength of all results, CRH is a multifunctional molecule activating via CRHR1 a multitude of signaling molecules mediating various functions and cross reactions.

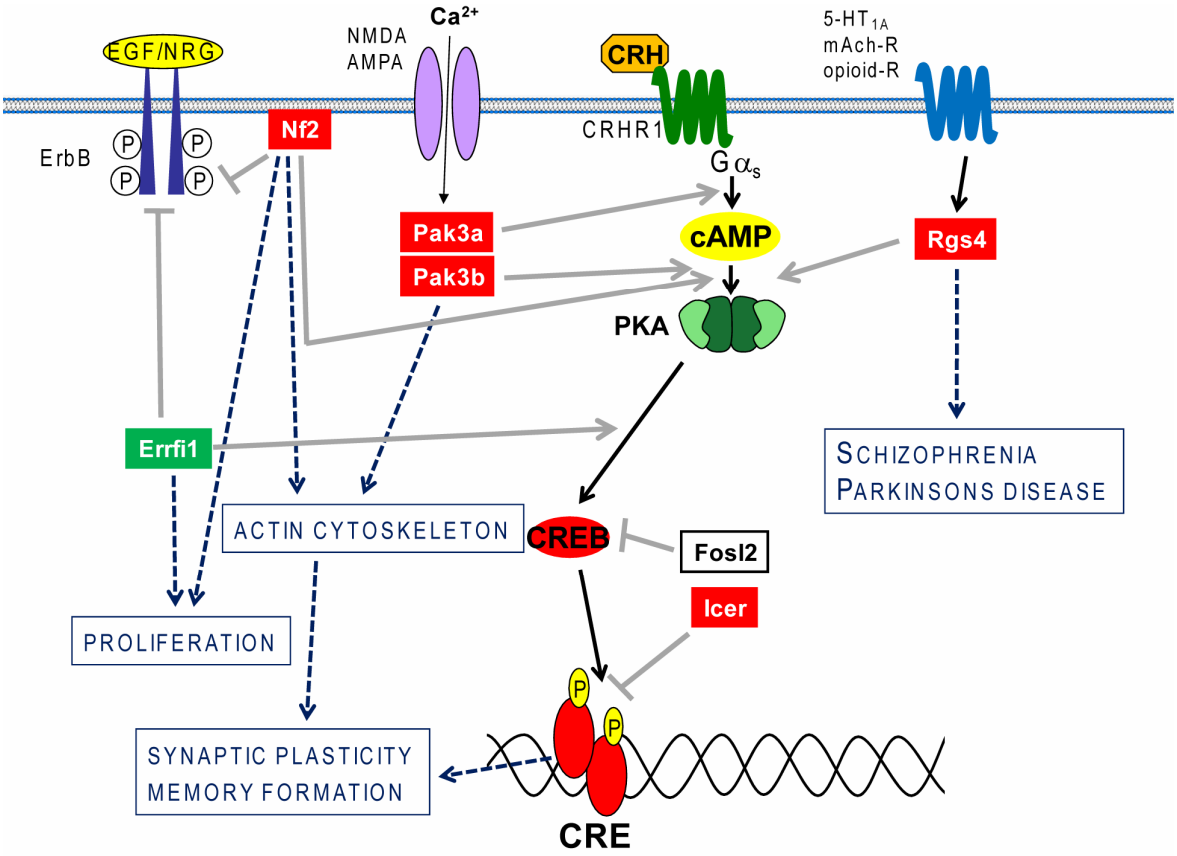

Figure 28. Overview of the potential role of selected candidate genes in known corticotrope CRHR1-dependent signaling cascades. Black lines mark established, gray lines hypothesized connections. Candidate genes are presented in red boxes when upregulated, in green boxes when downregulated by CRH in primary hippocampal cells (unpublished data). Lines with an arrowhead reflect positive regulation, other lines indicate inhibition as elicited in functional experiments in HN9 cells.

In summary, several of the new target genes of CRHR1 signaling showed besides their regulation by CRH an effect on CRHR1-regulated transcription suggesting diverse functions for these candidates in CRH/CRHR1-dependent signaling mechanisms. Nevertheless, exact details of their mode of action remain unclear and have to be further investigated using dominant-negative or knock-down approaches *in vitro*, protein-protein

interaction methods such as yeast- or mammalian-two-hybrid to unravel potential interaction partners or transgenic applications to further examine their functions *in vivo*.

5.4 Interaction of CRH/CRHR1- and ErbB-stimulated signaling cascades

Some of the reported CRHR1 targets play a role in ErbB receptor-dependent signal transduction. The ErbB receptors belong to the family of receptor tyrosine kinases (RTKs). RTKs are single transmembrane cell surface receptors and catalyze the transfer of a phosphate group of ATP to tyrosine residues (Hunter, 1998). Growth factors, cytokines and hormones are ligands of RTKs like epidermal growth factor (EGF) receptor, insulin receptor, plateled-derived growth factor (PDGF) receptor, fibroblast growth factor (FGF) receptor or tropomyosin-receptor-kinase (Trk) receptor and thus, are regulating cellular processes like proliferation and differentiation. Upon ligand binding receptor kinases dimerize and autophosphorylate their cytoplasmic domains leading to activation of a variety of signaling molecules including PI3 kinase/AKT, PLC and MAPK pathways (Lemmon and Schlessinger, 1994; Schlessinger, 2000).

The EGF receptor (EGFR), also called ErbB1, was the first receptor tyrosine kinase to be discovered (Carpenter, 1987). Following the identification of EGFR, three additional members of this receptor family were discovered: ErbB2, ErbB3 and ErbB4. All receptors were found to be expressed in proliferating cells in the CNS. Ligand binding leads to homo- or heterodimerization and autophosphorylation of the ErbB receptor tyrosine kinases. These phosphorylated tyrosines provide docking sites for Src homology-2 (SH2) and phosphotyrosine binding (PTB) domain-containing proteins, which include PI3 kinase, PLCγ and growth factor receptor-bound protein-2 (GRB2). This leads to activation of different signaling pathways such as the MAPK pathway (Alroy and Yarden, 1997; Wong and Guillaud, 2004). Although these receptors share common structural elements, ligands have been identified only for ErbB1, ErbB3 and ErbB4, in particular the EGF family of peptides for EGFR and the neuregulins for ErbB3 and ErbB4. ErbB2 remains an orphan receptor. However, ErbB2 can be transactivated through heterodimerization with other ErbB family members and appears to be their preferred heterodimerization partner. Moreover, ErbB3 has an impaired kinase region due to a mutation in its catalytic domain and is tyrosine phosphorylated by other family members (Citri *et al.*, 2003).

Among the identified CRHR1 targets, Errfi1 and Nf2 are both able to block ErbB-activated signaling cascades whereas Pak3 as a p21-activated kinase transduces phosphorylation from GTPases to downstream targets such as MAP kinases. To elucidate the impact of ErbB receptor-dependent signaling on CRHR1-activated signal transduction, the effect of the overexpression of one member of the ErbB receptor family on CRH-stimulated

transcription in AtT-20 as well as in HN9 cells was examined. As only ErbB2 and ErbB3 were expressed in both investigated cell lines, first experiments were performed with ErbB3. Overexpression of Errfi1, an inhibitor of ErbB signaling, led to a suppression of CRH-induced transcription whereas Nf2, also known as ErbB receptor inhibitor, further increased CRHR1-dependent transcription. This may be due to affecting different ErbB receptors and/or additionally different ErbB-activated signaling pathways. The direct enhancement of ErbB receptor signaling by overexpression of ErbB3 led to a rise of CRH-induced CRE- and NurRE-mediated transcription in AtT-20 and HN9 cells, respectively, suggesting a crosstalk of both signaling pathways. ErbB3 activates upon dimerization with ErbB2 on the one hand the PI3K/AKT pathway; on the other hand, MAP kinase signaling is turned on via Grb2 (Citri *et al.*, 2003). In HEK293 cells Punn *et al.* demonstrated that UCN1-induced activation of CRHR1-dependent signaling needs transactivation of EGFR (Punn *et al.*, 2006). Indeed, transactivation of ErbB receptors by GPCRs is well established. Transactivation may occur e.g. by ectodomain shedding of soluble ligands through metalloproteases (Dziedzic *et al.*, 2003; Shah *et al.*, 2003). But also the activation of GPCRs such as the D4 dopamine receptor causes autophosphorylation of growth receptors through G proteins (Kotecha *et al.*, 2002). Numerous selective cross-communications of RTKs and GPCRs have been shown permitting cells to control multiple regulatory mechanisms (Shah and Catt, 2004). If this is the case for CRHR1 and ErbB2/ErbB3 has to be further explored. Additional overexpression of ErbB2 may unravel if the heterodimer ErbB2/ErbB3 is responsible for the effect on CRH-dependent transcription. First experiments analyzing the consequence of an ErbB-specific kinase inhibitor and an ErbB3-specific agonist (heregulin-1β) on CRH-induced CRE transcription displayed contradictory results. Probably, CRE transcription is not the best read-out for signaling crosstalk studies. Examination of the phosphorylation state of the ErbB receptors themselves or involved signaling molecules such as different components of the MAPK cascade may help to resolve the question of a crosstalk of CRHR1 and ErbB2/3 in corticotrope as well as neuronal cells.

5.5 Errfi1 expression in the murine brain

The only candidate gene which was validated as CRHR1-dependently regulated *in vitro* and *in vivo* is the ErbB receptor feedback inhibitor 1, Errfi1. Furthermore, Errfi1 overexpression showed a regulating effect on CRHR1-activated signal transduction in neuronal cells. To get a first insight into the potential function of Errfi1 in the murine brain, its expression pattern was analyzed using *in situ* hybridization technology. On the one hand, an overlap with CRHR1 expression was expected, on the other hand Errfi1 as

inhibitor of ErbB receptor signaling is anticipated to be coexpressed with members of the ErbB receptor family.

Indeed, Errfi1 mRNA was detected in most of the regions also expressing CRHR1 such as the olfactory bulb, the cortex, the CA1 and CA3 regions of the hippocampus as well as the dentate gyrus, the basolateral and medial amygdala, the substantia nigra and in several thalamic nuclei. These brain regions are involved in different cognitive and behavioral processes. ErbB receptor signaling is known to play an important role in synaptic plasticity and neurogenesis. EGF e.g. enhances the NMDA receptor-mediated increase of the intracellular Ca2+ concentration in cultured rat hippocampal neurons and promotes proliferation and migration of stem or progenitor cells in the normal adult brain. Moreover, EGF also stimulated whereas neuregulins inhibited neurite outgrowth (Pinkas-Kramarski *et al.*, 1997; Wong and Guillaud, 2004). The regulation of Errfi1 by CRHR1 in brain regions expressing members of the ErbB receptor family may connect stress/CRH-dependent signal transduction with proliferation and differentiation processes. The EGFR is expressed in olfactory bulb, cerebral cortex, hippocampus, basal hypothalamus, striatum, thalamus, brainstem and cerebellum (Wong and Guillaud, 2004). ErbB2 is detected in olfactory bulb, cortex, hippocampus, hypothalamus, lateral septum, striatum, thalamus and cerebellum (according to Allen Brain Atlas: http://www.brain-map.org/). The expression patterns of ErbB3 and ErbB4 overlap including olfactory bulb, piriform cortex, cortex, reticular thalamic nucleus, hippocampus, substantia nigra, limbic system, cerebellum and brainstem. While ErbB3 can be found in oligodendrocytes and is mainly involved in the control of proliferation, ErbB4 is expressed in oligodendrocytes as well as in astrocytes and neurons where it is preferentially involved in differentiation processes (Pinkas-Kramarski *et al.*, 1997). In the olfactory bulb, the cortex, the hippocampus and thalamic regions, the mRNA expression of CRHR1, Errfi1 and the ErbB receptors overlap suggesting a possibility for Errfi1 as modulating molecule of both signal transduction pathways.

To confirm CRHR1-dependent regulation of Errfi1, its expression in several brain regions such as CA1, CA3 and medial amygdala was quantified. However, no differences in mRNA levels were observed comparing stressed CRHR1-wt and -ko animals suggesting that Errfi1 does not seem to be regulated by CRHR1 in those brain regions 3 h after stress. If Errfi1 expression is altered by stress and CRHR1-signal transduction in the olfactory bulb, the cortex or thalamic nuclei has still to be examined by extended quantification of the *in situ* hybridizations of brain sections. Furthermore, the analysis of stress-dependent regulation of Errfi1 by comparison of basal and stressed CRHR1-wt mice could help to explain the role of stress on Errfi1 expression in the mouse brain. Obviously, Errfi1 is able to influence neuronal CRHR1-induced signal transduction

suggesting more detailed investigations to examine the molecular and behavioral role of Errfi1 in the brain and its interplay with the CRHR1 which could be assessed using available conditional Errfi-ko mice (Jin *et al.*, 2007).

6. Conclusion

CRHR1 as key molecule of the neuroendocrine and behavioral responses to stress has attracted major interest as a potential novel target for the therapeutic intervention in major depressive disorder. However, CRH/CRHR1-dependent signal transduction mechanisms are only partially understood. Therefore, a more precise understanding of involved intracellular signaling mechanisms is an essential prerequisite towards the development of efficient and less pleitropic CRHR1-specific antagonists. In two approaches, *in vitro* and *in vivo*, time- and CRHR1-dependent changes in gene expression patterns were successfully analyzed in corticotrope cells and pituitary, respectively. About 100 transcripts were found to be regulated *in vitro* in response to CRH stimulation and more than 400 *in vivo* in response to stress and CRHR1 deficiency. Using different bioinformatical approaches *in vitro* plus simple cut off settings *in vitro* and *in vivo* a robust subset of CRHR1 target genes was obtained. In independent material validated CRH/stress-regulated genes are involved e.g. in cAMP, mitogen-activated protein kinase (MAPK) or growth factor receptor signaling. Functional studies using reporter assay experiments elucidated several candidate genes as regulatory molecules in CRHR1-dependent signaling cascades. The multifunctionality of these candidates proposes a variety of regulatory mechanisms modulated by CRHR1-dependent changes of gene expression. Especially ErbB-activated signaling cascades were identified as a novel signaling pathway potentially involved in CRHR1-activated signal transduction via crosstalk mechanisms. Errfi1, the only candidate found differentially expression *in vitro* as well as *in vivo*, raised special interest concerning new mechanisms of CRHR1 signal transduction. Nevertheless, the exact mode of action of the candidate genes is presently only partially understood. The examination of activated signaling molecules on protein level could help to clarify the exact role of CRHR1-regulated genes in CRH-dependent signal transduction. Moreover, targeted overexpression or knockdown of the candidate genes *in vitro* and *in vivo* as well as transgenic approaches should be applied to assess their function not only in signal transduction but also in anxiety- and depression-related behavior. Detailed dissection of these pathways will increase our understanding of the molecular mechanisms underlying stress-related pathologies such as anxiety disorders or depression. In addition, new CRHR1 targets provide the possibility to develop new pharmacological compounds for modulation of CRHR1-dependent signal transduction for the therapeutic intervention in these disorders.

7. Supplementary Data

Table S1. Genes putatively involved in CRH response of AtT-20 cells from mouse as identified by GALGO analyses[a]

spot ID	accession number	gene	description	gene rank 1	2	3	4
Transcription							
4700	**AA254318**	**4930522L14Rik**	**RIKEN cDNA 4930522L14 gene**	**7**	**1**	**2**	**31**
2781	**AI846359**	**Crem**[b]	**CAMP responsive element modulator**	**2**	**20**	**20**	**16**
18869	**BG072398**	**Fosl2**[b]	**Fos-like antigen 2**	**39**	**9**	**17**	**21**
15702	AI415706	Zfp213	Zinc finger protein 213	111	27	14	20
6620	AI835157	Neurod1	Neurogenic differentiation 1	50	81	68	26
20962	AI451115	Tcof1	Treacher Collins Franceschetti syndrome 1, homolog	67	13	90	73
7196	AI854843	Gli3	GLI-Kruppel family member GLI3	117	99	195	39
5075	AI854209	Sf3a1	Splicing factor 3a, subunit 1	268	165	28	54
19524	AI851247	Fosl2	Fos-like antigen 2	40	189	75	227
2656	AI848408	Id2	Inhibitor of DNA binding 2	142	164	205	24
322	AI839114	Sqstm1	Sequestosome 1	239	25	155	265
20114	AA140515	Ythdc1	YTH domain containing 1	166	40	380	161
Nucleotide binding							
1459	**CD776350**	**Pebp1**	**Pebp1 phosphatidylethanolamine-binding protein 1**	**18**	**46**	**21**	**9**
1550	AA270909	Top2a	Topoisomerase (DNA) II alpha	53	17	98	61
5931	AI843104	Ddx3x	DEAD/H (Asp-Glu-Ala-Asp/His) box polypeptide 3, X-linked	78	65	118	47
7671	AI838523	Scaf1	SR-related CTD-associated factor 1	27	113	112	59
8060	AA389327	Skiv2l2	Superkiller viralicidic activity 2-like 2 (S. cerevisiae)	137	145	46	44
21313	AA734490	Abcd4	ATP-binding cassette, sub-family D (ALD), member 4	28	307	256	67
Signal transduction							
5502	**AA185709**	**Cd3e**	**CD3 antigen, epsilon polypeptide**	**4**	**32**	**8**	**15**
5926	AI450767	Mapk1	Mitogen activated protein kinase 1	108	70	135	46
11281	AI449143	Calm1	Calmodulin 1	36	106	104	189
Receptor activity							
2383	AI847223	Sema6c	Sema domain, transmembrane domain (TM), and cytoplasmic domain, (semaphorin) 6C	203	208	56	37
Transport							
11155	**AI450121**	**Pex13**[b]	**Peroxisomal biogenesis factor 13**	**22**	**12**	**7**	**18**
5887	AI841677	Tmed3	Transmembrane emp24 domain containing 3	42	52	23	102
3233	AI117694	Snx11	Sorting nexin 11	26	30	226	22
1296	AI605736	Slc6a11	Solute carrier family 6 (neurotransmitter transporter, GABA), member 11	60	140	30	95
12864	AI850801	Tmed7	Transmembrane emp24 protein transport domain containing 7	86	214	33	40
8536	AI847502	Dld	Dihydrolipoamide dehydrogenase	150	44	173	25
23109	AI843695	Slc37a3	Solute carrier family 37 (glycerol-3-phosphate transporter), member 3	202	168	97	49
17859	AI842864	Rabif	RAB interacting factor	45	101	166	224
15400	AI839164	Tmed10	Transmembrane emp24-like trafficking protein 10 (yeast)	130	47	270	118
21723	AI846151	Rnuxa	RNA U, small nuclear RNA export adaptor	330	48	188	83
Protein binding							
3496	AI847845	Pcdha4	Protocadherin alpha 7	44	160	10	62
4999	AI893639	Anapc1	Anaphase promoting complex subunit 1	144	37	110	100
22642	AI450905	Cep164	Centrosomal protein 164	220	237	11	36
3139	AI847065	Nktr	Natural killer tumor recognition sequence	187	39	79	239
Protein biosynthesis							
18265	AA048130	Rps27l	Ribosomal protein S27-like	62	29	4	30

spot ID	accession number	gene	description	gene rank 1	2	3	4
24169	AA549039	Taf4b	TAF4B RNA polymerase II, TATA box binding protein (TBP)-associated	29	103	91	124
20471	AA182979	Eif2c3	Eukaryotic translation initiation factor 2C, 3	218	305	202	42
Negative regulation of protein kinase activity							
18124	**AI323564**	**Nf2**[b]	**Neurofibromatosis 2**	**10**	**22**	**25**	**45**
1333	AI842320	Nf2	Neurofibromatosis 2	68	180	55	43
Hydrolase activity							
19583	AI844881	Ddx3x	DEAD/H (Asp-Glu-Ala-Asp/His) box polypeptide 3, X-linked	24	73	153	23
15972	AI849987	Smpdl3a	Sphingomyelin phosphodiesterase, acid-like 3A	30	111	95	65
23726	AA268030	Dpysl5	Dihydropyrimidinase-like 5	77	107	39	94
15156	W41539	Pnpla1	Patatin-like phospholipase domain containing 1	213	19	82	285
18134	AI848680	Nt5dc2	5'-nucleotidase domain containing 2	37	157	251	158
Transferase activity							
2363	**AI849149**	**Mat2a**	**Methionine adenosyltransferase II, alpha**	**5**	**36**	**16**	**3**
15752	AI426672	Dnttip2	Deoxynucleotidyltransferase, terminal, interacting protein 2	123	162	36	35
16573	AI447731	Cmas	Cytidine monophospho-N-acetylneuraminic acid synthetase	34	8	217	175
21246	W35091	Coq2	Coenzyme Q2 homolog, prenyltransferase (yeast)	17	204	203	137
Oxidoreductase activity							
2336	**AI451727**	**0610012D14Rik**	**RIKEN cDNA 0610012D14 gene**	**35**	**45**	**27**	**34**
4730	AI661450	Idh2	Isocitrate dehydrogenase 2 (NADP+), mitochondrial	32	85	117	273
19778	AA259765	Prdx5	Peroxiredoxin 5	76	35	341	108
Lipid metabolism							
6750	**AI846046**	**Acsl4**[b]	**Acyl-CoA synthetase long-chain family member 4**	**38**	**18**	**1**	**33**
16977	**AI843116**	**Hmgcs1**	**3-hydroxy-3-methylglutaryl-Coenzyme A synthase 1**	**33**	**24**	**273**	**10**
6705	**AI841574**	**Hmgcs1**[b]	**3-hydroxy-3-methylglutaryl-Coenzyme A synthase 1**	**3**	**3**	**5**	**346**
6715	AA060369	Hmgcr	3-hydroxy-3-methylglutaryl-Coenzyme A reductase	61	193	47	127
Apoptosis							
4606	AI841410	Tax1bp1	Tax1 (human T-cell leukemia virus type I) binding protein 1	23	97	76	125
12328	AI327173	Aplp1	Amyloid beta (A4) precursor-like protein 1	210	127	161	41
15853	AA615635	Egln3	EGL nine homolog 3 (C. elegans)	368	195	50	364
Cytoskeleton							
9477	AI835922	Kif3a	Kinesin family member 3A	65	14	37	60
12686	AI429298	Kif3a	Kinesin family member 3A	19	38	62	72
21425	NM_008744	Ntn1	Netrin 1	8	11	178	14
8837	AA200002	Kif17	Kinesin family member 17	118	42	142	145
21350	AI854113	Sdc2	Syndecan 2	235	28	41	291
6645	AI846131	Kif3c	RIKEN cDNA 1110002L01 gene	13	314	262	345
Mitochondrion							
4880	AI840657	Cox7a2l	Cytochrome c oxidase subunit VIIa polypeptide 2-like	75	55	26	4
9331	AI839512	Timm17a	Translocator of inner mitochondrial membrane 17a	173	77	32	38
10489	AI847956	Pigy	Phosphatidylinositol glycan anchor biosynthesis, class Y	121	49	175	70
Biological process unknown							
13207	AA718111	Fgfr1op	Fgfr1 oncogene partner	11	34	24	51
15947	AI841252	Cnpy2	Canopy 2 homolog (zebrafish)	214	95	35	119
6037	AI847392	Gbas	Glioblastoma amplified sequence	158	43	45	243
Others							
7181	**AI227072**	**Malat1**	**Metastasis-associated lung adenocarcinoma transcript 1 (non-coding RNA)**	**1**	**2**	**3**	**1**
19276	**AA816221**	**6720467C03Rik**	**RIKEN cDNA 6720467C03 gene**	**12**	**5**	**6**	**13**

spot ID	accession number	gene	description	gene rank 1	2	3	4
2698	**AI846018**		**Transcribed locus**	**15**	**7**	**19**	**12**
8648	**AA269410**	**Loxl3**	**Lysyl oxidase-like 3**	**9**	**16**	**12**	**17**
Others							
3931	**AI450057**	**A430097D04Rik**	**DNA segment, Chr 15, Brigham & Women's Genetics 0759 expressed**	**25**	**26**	**31**	**19**
19692	W58944	3200002M19Rik	RIKEN cDNA 3200002M19 gene	20	23	67	6
15482	AI465375	Misc12	MIS12 homolog (yeast)	16	21	74	11
3185	AI853444		Predicted gene, ENSMUSG00000063277	57	31	13	27
5478	AA387159	Wdr40c	WD repeat domain 40C	6	105	84	8
22725	AI447476	Mfap3	Microfibrillar-associated protein 3	46	72	109	74
16322	AI661037	Neil3	Nei like 3 (E. coli)	43	53	9	198
20310	AI448474		Transcribed locus	51	4	222	29
1103	AI849707	Myeov2	Myeloma overexpressed 2	104	150	54	7
16577	AI837598			64	188	38	28
14534	AI413090	BC037034	CDNA sequence BC037034	176	33	18	106
9017	AI837674	2610040E16Rik	Leucine rich repeat containing 40	41	87	48	167
5666	AA259694	Suv420h2	Suppressor of variegation 4-20 homolog 2 (Drosophila)	101	62	183	2
6201	AI837840			63	143	29	126
8023	AI323897	Tmod2	Tropomodulin 2	244	6	66	128
5491	AI847942	Sept4	Septin 4	66	172	194	32
17312	AI845689	Lamp1	Lysosomal membrane glycoprotein 1	182	116	42	134
3000	AA415398	MGC73851	Expressed sequence AA415398	14	58	133	270
9279	AA437817	Tfpi	Tissue factor pathway inhibitor	48	126	160	147
4267	AI449074		Transcribed locus	47	108	64	272
14161	AI841985		Transcribed locus	141	50	93	218
6684	AI842055	AW554918	Expressed sequence AW554918	136	15	72	305
5427	AI842990		Transcribed locus	107	286	134	5
4831	AI894247	Tubb5	Tubulin, beta 5	205	152	44	141
13825	AA120647			49	228	163	130
11316	AA433626	Thnsl2	Threonine synthase-like 2 (bacterial)	249	166	40	129
20965	AI839696	Fkbp2	FK506 binding protein 2	93	41	255	231
20153	AI853067	Csnk1a1	Casein kinase 1, alpha 1	87	134	43	368
8047	AI449795	Usp48	Ubiquitin-specific peptidase 48	245	75	350	48
13118	AI854682	BC005561	CDNA sequence BC005561	21	300	49	358
22422	AI414820	Rrp1b	Ribosomal RNA processing 1 homolog B (S. cerevisiae)	112	10	387	234
5299	AI839515	Tbcd	Tubulin-specific chaperone d	31	223	345	165
7845	AI850268		Transcribed locus	342	200	34	211
7590	AI842091	Tgoln1	Trans-golgi network protein	273	199	330	50
1852	AI450720		Transcribed locus	289	342	22	205

[a]Functional classification was based on Gene Ontology (GO) categories according to NCBI. All genes were obtained by four separated GALGO analyses of all preselected genes and merged in this table. Those genes with boldface occur in four analyses among the topmost 50 ranked genes or occurred twice in at least three runs and were – after elimination of RIKEN clones and unknown transcripts – chosen for modeling of interactions with GeneNet. Genes that fall in the same GO category are sorted in ascending order by the sum of the Gene Ranks for all four analyses.

[b]Candidate genes validated over time by qRT-PCR.

Table S2. Significantly CRH-dependently regulated genes revealed by microarray data[a]; cut-off: |fold regulation|>1.3, accept2=true or p<0.05, mean expression > 950, at at least one time point

spot ID	accession number	gene symbol	description	fold regulation				
				1 h	3 h	6 h	12 h	24 h
transcription								
2781	AI846359	Crem[b,10,G]	cAMP responsive element modulator	3.13	2.02	1.28	1.66	1.11
3550	AI414446	Eya2[4]	Eyes absent 2 homolog (Drosophila)	1.16	1.22	1.13	-1.43	1.14
18869	AI848789	Fosl2[b,10,G]	Fos-like antigen 2	2.51	1.46	1.39	1.40	1.16
19524	AI851247	Fosl2[b,10]	Fos-like antigen 2	1.80	1.36	1.17	1.28	1.13
7196	AI854843	Gli3[4]	GLI-Kruppel family member GLI3	1.55	-1.05	1.12	-1.03	-1.15
16804	AI451211	Med6[4]	Mediator of RNA polymerase II transcription, subunit 6 homolog (yeast)	1.12	1.03	1.11	1.42	1.07
6620	AI835157	Neurod1[8]	Neurogenic differentiation 1	1.14	-1.47	-1.14	-1.35	-1.53
16853	AI848790	Pbx1[7]	Pre B-cell leukemia transcription factor 1	-1.02	1.50	1.22	1.25	1.01
12670	AI841402	Rb1cc1[4]	RB1-inducible coiled-coil 1	1.33	-1.07	-1.03	-1.33	-1.43
nucleic acid binding								
13802	AI661472	Clk2	CDC-like kinase 2	-1.09	-1.05	-1.50		
9815	AI841344	Hspca[4]	Heat shock protein 1, alpha	-1.37	-1.15	1.14	1.67	-1.23
5239	AI846216	Zcchc12[7]	Zinc finger, CCHC domain containing 12	-1.03	1.35	1.56	1.57	1.10
signal transduction								
5502	AA185709	Cd3e[4,G]	CD3 antigen, epsilon polypeptide	-1.13	-1.31	-1.20	1.05	1.50
5962	AA543402	Ect2[4]	Ect2 oncogene	-1.20	-1.37	1.08	1.48	-1.01
2197	AI853531	Errfi1[b,1]	ERBB receptor feedback inhibitor 1	1.87	1.06	1.01	1.09	1.08
8856	AI323945	Igfbp4[4]	Insulin-like growth factor binding protein 4	1.06	1.14	1.01	1.16	1.43
4123	AI841111	Ly6e[7]	Lymphocyte antigen 6 complex, locus E	-1.31	1.47	-1.02	1.06	1.23
20150	AI848679	Pea15[4]	Phosphoprotein enriched in astrocytes 15	-1.45	1.25	-1.09	1.01	1.01
16914	AI847765	Rgs4[b,7]	Regulator of G protein-signaling 4	-1.84	-1.33	-1.22	-1.52	-1.45
5934	AI850105	Stmn1[4]	Stathmin 1	-1.47	1.07	-1.15	1.00	1.04
8023	AI323897	Tmod2[8]	Tropomodulin 2	-1.00	-1.40	-1.12	-1.01	-1.86
calcium ion transport								
11281	AI449143	Calm1[7]	Calmodulin 1	-1.05	1.39	1.17	1.37	1.49
20027	AI852446	Pcdh21[4]	Protocadherin 21	-1.05	1.04	-1.08	-1.48	1.06
kinases								
8455	AI852492	Pak3[b,7]	P21 (CDKN1A)-activated kinase 3	-1.06	1.34	1.86	1.81	1.33
7882	AI839355	Pctk1[4]	PCTAIRE-motif protein kinase 1	-1.57	-1.02	-1.00	1.20	1.22
phosphatases								
5034	AI851272	Dusp14[b]	Dual specificity phosphatase 14	1.84	1.64	1.30		-1.19
1282	AI327145	Dusp19[4]	Dual specificity phosphatase 19	1.03	-1.02	1.06	1.44	1.07
transport								
7849	AA028501	Cox8b	Cytochrome c oxidase, subunit VIIIb	1.08	-1.10	-1.14		-1.61
6751	AI843967	Syt4[10]	Synaptotagmin IV	1.33	1.65	1.62	1.72	1.29
15969	AI843138	Syt4[10]	Synaptotagmin IV	1.67	1.56	1.32	1.58	1.26
20962	AI451115	Tcof1[4]	Treacher Collins Franceschetti syndrome 1, homolog	1.11	-1.26	1.04	-1.31	-1.45
12097	AI414363	Timm13a[4]	Translocase of inner mitochondrial membrane 13 homolog a (yeast)	-1.54	1.16	-1.09	-1.06	-1.03
11995	AI450028	Trappc1[7]	Trafficking protein particle complex 1	-1.11	1.01	-1.05	1.63	1.14
2774	AI431077	Ttyh1[7]	Tweety homolog 1 (Drosophila)	-1.01	1.38	1.41	1.53	1.59
apoptosis								
2321	AI849021	Axud1[4]	AXIN1 up-regulated 1	1.45	-1.02	1.05	-1.08	-1.08
5760	AI836867	Bag1[4]	Bcl2-associated athanogene 1	-1.22	1.01	1.04	-1.01	1.49
15058	AI323713	Dad1[7]	Defender against cell death 1	-1.42	1.55	1.14	1.51	1.14
18930	AI847764	Dad1[7]	Defender against cell death 1	-1.57	1.43	1.06	1.35	1.25
2960	AI121214	Elmo1[4]	Engulfment and cell motility 1, ced-12 homolog (C. elegans)	-1.01	-1.13	-1.11	-1.42	-1.16
metabolic enzymes								
6750	AI846046	Acsl4[b,4,G]	Acyl-CoA synthetase long-chain family member 4	1.18	-1.14	1.36	1.22	-1.46
13294	AI324267	Dio2[4]	Deiodinase, iodothyronine, type II	1.06	-1.14	1.24	-1.47	1.06
13429	AI842311	Eprs[7]	Glutamyl-prolyl-tRNA synthetase	-1.27	1.02	1.18	1.54	1.05

spot ID	accession number	gene symbol	description	fold regulation				
				1 h	3 h	6 h	12 h	24 h
6705	AI841574	Hmgcs1[b,8,G]	3-hydroxy-3-methylglutaryl-Coenzyme A synthase 1	-1.07	-1.02	1.37	1.32	-1.76
ubiquitin-dependent protein catabolic process								
2471	AI854059	Nedd8[6]	Neural precursor cell expressed, developmentally down-regulated gene 8	-1.59	1.30	1.04	1.11	1.15
3562	AI852729	Psmb7[3]	Proteasome (prosome, macropain) subunit, beta type 7	-1.28	1.46	-1.01	-1.02	1.29
9985	AI847441	Psmc5[6]	Protease (prosome, macropain) 26S subunit, ATPase 5	-1.35	1.42	1.06	1.23	1.11
21954	AI847785	Ube1x[6]	Ubiquitin-activating enzyme E1, Chr X	-1.13	1.43	1.07	-1.01	1.03
proteolysis								
16939	AI853552	Cct8[7]	Chaperonin subunit 8 (theta)	-1.38	1.46	-1.03	1.50	1.06
protein binding								
3899	AI853569	Mphosph6	M phase phosphoprotein 6	-1.11	1.42	1.12	1.33	1.04
20776	AI839890	Mpp6[7]	Membrane protein, palmitoylated 6 (MAGUK p55 subfamily member 6)	-1.14	1.40	1.09	1.44	1.38
7645	AI415104	Mpp7[b,7]	Membrane protein, palmitoylated 7 (MAGUK p55 subfamily member 7	-1.03	2.23	1.01	1.09	1.24
1333	AI842320	Nf2[b,9]	Neurofibromatosis 2	-1.15	-1.23	-1.02	-1.06	1.83
18124	AI323564	Nf2[b,9,G]	Neurofibromatosis 2	-1.14	-1.48	-1.12	1.10	2.16
cell adhesion								
7248	AI452101	Cd47[4]	CD47 antigen (Rh-related antigen, integrin-associated signal transducer)	-1.09	1.41	1.02	1.10	1.18
22031	AI413655	Cdh4[1]	Cadherin 4	1.44	-1.10	-1.13	-1.22	1.10
625	AA048249	Xlkd1[7]	Extra cellular link domain-containing 1	-1.43	1.53	1.10	1.16	1.32
microtubule-based movement								
9477	AI835922	Kif3a[9]	Kinesin family member 3A	-1.14	-1.30	-1.13	-1.13	1.79
12686	AI429298	Kif3a[10]	Kinesin family member 3A	1.80	1.26	1.25	1.27	1.01
others								
7155	W64453	2410030K01Rik[7]	Spindle pole body component 24 homolog (S. cerevisiae)	-1.16	1.21	1.31	1.47	1.10
1737	W40649	Amelx[7]	Amelogenin X chromosome	-1.29	1.46	1.05	1.15	1.18
3391	AI847243	Apobec2[4]	Apolipoprotein B editing complex 2	-1.32	-1.26	-1.09	-1.54	-1.08
20310	AI448474	Leng8[4]	Leukocyte receptor cluster (LRC) member 8	-1.02	1.31	-1.08	1.15	1.47
21120	AI851292	Stip1[4]	Stress-induced phosphoprotein 1	-1.01	1.43	1.06	1.04	1.06
1095	AI447316	Ugcg[4]	UDP-glucose ceramide glucosyltransferase	1.57	-1.06	-1.00	1.12	1.14
biological process unknown								
20569	AI847949	0610007H07Rik[4]	RIKEN cDNA 0610007H07 gene	-1.42	1.23	1.09	-1.07	1.03
2336	AI451727	0610012D14Rik[10,G]	RIKEN cDNA 0610012D14 gene	1.57	1.65	1.31	1.18	1.20
12762	W48899	0610012G03Rik[4]	RIKEN cDNA 0610012G03 gene	-1.20	1.54	1.06	1.05	1.05
7173	AI850687	0610038F07Rik[6]	RIKEN cDNA 0610038F07 gene	-1.44	1.13	1.05	1.26	1.04
23111	AI849195	1110019C08Rik	RIKEN cDNA 1110019C08 gene	1.10	1.65	1.09		
22566	AI845039	1110038O08Rik	RIKEN cDNA 1110038O08 gene	-1.23	1.68	1.22		
23635	AI847924	2210011C24Rik[7]	RIKEN cDNA 2210011C24 gene	1.03	1.59	1.56	1.67	1.38
7181	AI227072	2210401K01Rik[8,G]	Metastasis associated lung adenocarcinoma transcript 1 (non-coding RNA)	-1.11	-1.26	1.16	-1.48	-1.80
12480	AI836697	2310008M10Rik[7]	RIKEN cDNA 2310008M10 gene	-1.16	1.25	1.25	1.63	1.04
1634	AA259726	2610311I19Rik[4]	Yip1 domain family, member 5	-1.17	1.42	1.08	-1.01	1.10
5024	AI465414	2610311I19Rik[7]	Yip1 domain family, member 5	-1.02	1.08	1.51	1.38	1.10
5	AI836168	2810405K02Rik[6]	RIKEN cDNA 2810405K02 gene	-1.44	1.14	-1.08	-1.15	1.01
8404	AI448906	3000004C01Rik[7]	RIKEN cDNA 3000004C01 gene	-1.15	1.21	1.02	1.53	1.03
8627	AA388754	3930401K13Rik[10]	RIKEN cDNA 3930401K13 gene	1.67	1.60	1.33	1.27	1.20
17119	AI449756	4922501K12Rik[7]	RIKEN cDNA 4922501K12 gene	-1.56	1.50	1.07	1.10	1.37
7460	AI465327	5730494M16Rik[3]	RIKEN cDNA 5730494M16 gene	-1.12	1.45	1.05	-1.06	1.11
7671	AI838523	AI480556[9]	Expressed sequence AI480556	-1.04	-1.22	-1.01	1.03	1.68
1321	AA764584	Atp6v0d2[4]	RIKEN cDNA 4833419A21 gene	-1.02	-1.01	1.06	-1.10	-1.43
13701	AI842153	AW049604[4]	Expressed sequence AW049604	-1.07	-1.02	-1.05	-1.51	1.16
5626	AA691795	BC034054[7]	CDNA sequence BC034054	-1.25	1.49	1.02	1.10	1.25
9199	AI413641	D11Bwg0434e[3]	DNA segment, Chr 11, Brigham & Women's Genetics 0434 expressed	-1.74	1.29	-1.14	-1.12	1.17
7634	AI849637	Dp1[7]	Deleted in polyposis 1	-1.11	1.37	1.11	1.19	1.45
14302	AI324241	Dp1[7]	Deleted in polyposis 1	-1.16	1.46	1.19	1.11	1.21
16207	AA048628	E130112L23Rik	RIKEN cDNA E130112L23 gene	-1.16	1.53	-1.01	1.33	

spot ID	accession number	gene symbol	description	fold regulation				
				1 h	3 h	6 h	12 h	24 h
19440	W10141	Gsdm1[7]	Gasdermin 1	-1.38	1.39	1.17	1.60	1.57
12495	BE135684	Odc1[7]	ornithine decarboxylase, structural 1	1.12	1.75	1.12	1.44	1.10
23178	AI851260	Rpl41[7]	Ribosomal protein L41	-1.57	1.64	1.03	1.20	1.37
11085	AA273481	Tmem27[4]	Transmembrane protein 27	1.08	-1.09	-1.04	1.45	-1.17
15245	AI227127	Xist[4]	X (inactive)-specific transcript, antisense	1.14	-1.38	-1.17	1.42	-1.02
936	AI850053[7]		Transcribed locus	1.20	1.70	1.73	1.59	1.48
4962	AI837001[4]		Transcribed locus	-1.06	-1.07	-1.06	-1.04	-1.48
8675	AI429183[7]		Transcribed locus, weakly similar to NP_919328.1 hypothetical protein LOC278676 [Mus musculus]	-1.03	1.60	1.33	1.52	1.34
8932	AI841851[4]			-1.18	-1.17	1.17	1.44	-1.21
9287	p23[4]			-1.06	-1.02	1.11	-1.07	-1.52
9352	AI839173[1]			1.63	-1.06	-1.07	1.08	1.06
15828	W14341[7]			1.32	1.08	1.20	1.48	1.90
19100	AI848698[7]		Similar to Ornithine decarboxylase (ODC)	1.09	1.62	1.40	1.40	1.07
22356	AI850470		Transcribed locus	-1.17	1.50	1.03	1.30	1.12

[a]Functional classification was based on Gene Ontology categories according to NCBI.

[b] Microarray data validated by qRT-PCR in independent material.

[1-10] Number of corresponding cluster revealed by Bayesian hierarchical co-clustering.

[G] Genes occurring in the top 16 candidates found by *GALGO* analysis.

8. References

Abbud Ra, Kelleher R and Melmed S (2004): Cell-Specific Pituitary Gene Expression Profiles after Treatment with Leukemia Inhibitory Factor Reveal Novel Modulators for Proopiomelanocortin Expression. *Endocrinology* 145(2): 867-880.

Aguilera G, Harwood Jp, Wilson Jx, Morell J, Brown Jh and Catt Kj (1983): Mechanisms of action of corticotropin-releasing factor and other regulators of corticotropin release in rat pituitary cells. *J Biol Chem* 258(13): 8039-45.

Alfthan K, Heiska L, Gronholm M, Renkema Gh and Carpen O (2004): Cyclic AMP-dependent Protein Kinase Phosphorylates Merlin at Serine 518 Independently of p21-activated Kinase and Promotes Merlin-Ezrin Heterodimerization. *J. Biol. Chem.* 279(18): 18559-18566.

Allison Db, Cui X, Page Gp and Sabripour M (2006): Microarray data analysis: from disarray to consolidation and consensus. *Nat Rev Genet* 7(1): 55-65.

Alroy I and Yarden Y (1997): The ErbB signaling network in embryogenesis and oncogenesis: signal diversification through combinatorial ligand-receptor interactions. *FEBS Lett* 410(1): 83-6.

Anastasi S, Fiorentino L, Fiorini M, Fraioli R, Sala G, Castellani L, Alema S, Alimandi M and Segatto O (2003): Feedback inhibition by RALT controls signal output by the ErbB network. *Oncogene* 22(27): 4221-34.

Aoki Y, Iwasaki Y, Katahira M, Oiso Y and Saito H (1997): Regulation of the Rat Proopiomelanocortin Gene Expression in AtT-20 Cells. I: Effects of the Common Secretagogues. *Endocrinology* 138(5): 1923-1929.

Arzt E and Holsboer F (2006): CRF signaling: molecular specificity for drug targeting in the CNS. *Trends Pharmacol Sci.* 27(10): 531-538.

Bale Tl, Contarino A, Smith Gw, Chan R, Gold Lh, Sawchenko Pe, Koob Gf, Vale Ww and Lee K-F (2000): Mice deficient for corticotropin-releasing hormone receptor-2 display anxiety-like behaviour and are hypersensitive to stress. *Nat Genet* 24(4): 410-414.

Bale Tl and Vale Ww (2004): CRF AND CRF RECEPTORS: Role in Stress Responsivity and Other Behaviors. *Annu Rev Pharmacol Toxicol.* 44(1): 525-557.

Bansal G, Druey Km and Xie Z (2007): R4 RGS proteins: regulation of G-protein signaling and beyond. *Pharmacol Ther* 116(3): 473-95.

Barnes M, Freudenberg J, Thompson S, Aronow B and Pavlidis P (2005): Experimental comparison and cross-validation of the Affymetrix and Illumina gene expression analysis platforms. *Nucleic Acids Res* 33(18): 5914-23.

Becquet D, Guillaumond F, Bosler O and Francois-Bellan Am (2001): Long-term variations of AP-1 composition after CRH stimulation: consequence on POMC gene regulation. *Mol Cell Endocrinol* 175(1-2): 93-100.

Beyer Ce, Ghavami A, Lin Q, Sung A, Rhodes Kj, Dawson La, Schechter Le and Young Kh (2004): Regulators of G-protein signaling 4: modulation of 5-HT1A-mediated neurotransmitter release in vivo. *Brain Res* 1022(1-2): 214-20.

Boda B, Alberi S, Nikonenko I, Node-Langlois R, Jourdain P, Moosmayer M, Parisi-Jourdain L and Muller D (2004): The mental retardation protein PAK3 contributes to synapse formation and plasticity in hippocampus. *J Neurosci* 24(48): 10816-25.

Bohl J, Brimer N, Lyons C and Vande Pol Sb (2007): The stardust family protein MPP7 forms a tripartite complex with LIN7 and DLG1 that regulates the stability and localization of DLG1 to cell junctions. *J Biol Chem* 282(13): 9392-400.

Bousquet C Zm, Melmed S. (2000): Direct regulation of pituitary proopiomelanocortin by STAT3 provides a novel mechanism for immuno-neuroendocrine interfacing. *J Clin Invest.* 106(11): 1417-25.

Boutillier Al, Gaiddon C, Lorang D, Roberts Jl and Loeffler Jp (1998): Transcriptional Activation of the Proopiomelanocortin Gene by Cyclic AMP-responsive Element Binding Protein. *Pituitary* 1(1): 33-43.

Brauns O, Liepold T, Radulovic J and Spiess J (2001): Pharmacological and chemical properties of astressin, antisauvagine-30 and alpha-helCRF: significance for behavioral experiments. *Neuropharmacology* 41(4): 507-16.

Bretscher A, Edwards K and Fehon Rg (2002): ERM proteins and merlin: integrators at the cell cortex. *Nat Rev Mol Cell Biol* 3(8): 586-99.

Britton Kt, Lee G, Vale W, Rivier J and Koob Gf (1986): Corticotropin releasing factor (CRF) receptor antagonist blocks activating and 'anxiogenic' actions of CRF in the rat. *Brain Res* 369(1-2): 303-6.

Bucan M and Abel T (2002): The mouse: genetics meets behaviour. *Nat Rev Genet* 3(2): 114-23.

Buchwald G, Hostinova E, Rudolph Mg, Kraemer A, Sickmann A, Meyer He, Scheffzek K and Wittinghofer A (2001): Conformational switch and role of phosphorylation in PAK activation. *Mol Cell Biol* 21(15): 5179-89.

Bunney We, Bunney Bg, Vawter Mp, Tomita H, Li J, Evans Sj, Choudary Pv, Myers Rm, Jones Eg, Watson Sj*, et al.* (2003): Microarray technology: a review of new strategies to discover candidate vulnerability genes in psychiatric disorders. *Am J Psychiatry* 160(4): 657-66.

Buonassisi V, Sato G and Cohen Ai (1962): Hormone-producing cultures of adrenal and pituitary tumor origin. *Proc.Natl.Acad Sci U.S.A* 48: 1184-1190.

Canales Rd, Luo Y, Willey Jc, Austermiller B, Barbacioru Cc, Boysen C, Hunkapiller K, Jensen Rv, Knight Cr, Lee Ky*, et al.* (2006): Evaluation of DNA microarray results with quantitative gene expression platforms. *Nat Biotech* 24(9): 1115-1122.

Carpenter G (1987): Receptors for epidermal growth factor and other polypeptide mitogens. *Annu Rev Biochem* 56: 881-914.

Carroll Bj (1982): Clinical applications of the dexamethasone suppression test for endogenous depression. *Pharmacopsychiatria* 15(1): 19-25.

Chadee Dn, Xu D, Hung G, Andalibi A, Lim Dj, Luo Z, Gutmann Dh and Kyriakis Jm (2006): Mixed-lineage kinase 3 regulates B-Raf through maintenance of the B-Raf/Raf-1 complex and inhibition by the NF2 tumor suppressor protein. *Proc.Natl.Acad Sci U.S.A* 103(12): 4463-4468.

Chalifour Le, Fahmy R, Holder El, Hutchinson Ew, Osterland Ck, Schipper Hm and Wang E (1994): A method for analysis of gene expression patterns. *Anal Biochem* 216(2): 299-304.

Chalmers Dt, Lovenberg Tw and De Souza Eb (1995): Localization of novel corticotropin-releasing factor receptor (CRF2) mRNA expression to specific subcortical nuclei in rat brain: comparison with CRF1 receptor mRNA expression. *J Neurosci* 15(10): 6340-50.

Chen R, Lewis Ka, Perrin Mh and Vale Ww (1993): Expression cloning of a human corticotropin-releasing-factor receptor. *Proc Natl Acad Sci U S A* 90(19): 8967-71.

Chrousos Gp (1998): Stressors, Stress, and Neuroendocrine Integration of the Adaptive Response: The 1997 Hans Selye Memorial Lecture. *Annals of the New York Academy of Sciences* 851(STRESS OF LIFE: FROM MOLECULES TO MAN): 311-335.

Citri A, Skaria Kb and Yarden Y (2003): The deaf and the dumb: the biology of ErbB-2 and ErbB-3. *Exp Cell Res* 284(1): 54-65.

Cole Bk, Curto M, Chan Aw and Mcclatchey Ai (2008): Localization to the cortical cytoskeleton is necessary for Nf2/merlin-dependent epidermal growth factor receptor silencing. *Mol Cell Biol* 28(4): 1274-84.

Cornejo Maciel F, Maloberti P, Neuman I, Cano F, Castilla R, Castillo F, Paz C and Podesta Ej (2005): An arachidonic acid-preferring acyl-CoA synthetase is a hormone-dependent and obligatory protein in the signal transduction pathway of steroidogenic hormones. *J Mol Endocrinol* 34(3): 655-666.

Coste Sc, Kesterson Ra, Heldwein Ka, Stevens Sl, Heard Ad, Hollis Jh, Murray Se, Hill Jk, Pantely Ga, Hohimer Ar*, et al.* (2000): Abnormal adaptations to stress and impaired cardiovascular function in mice lacking corticotropin-releasing hormone receptor-2. *Nat Genet* 24(4): 403-9.

Cuevas B, Lu Y, Watt S, Kumar R, Zhang J, Siminovitch Ka and Mills Gb (1999): SHP-1 Regulates Lck-induced Phosphatidylinositol 3-Kinase Phosphorylation and Activity. *J. Biol. Chem.* 274(39): 27583-27589.

Dal-Zotto S, Marti O and Armario A (2003): Glucocorticoids are involved in the long-term effects of a single immobilization stress on the hypothalamic-pituitary-adrenal axis. *Psychoneuroendocrinology* 28(8): 992-1009.

Dautzenberg Fm and Hauger Rl (2002): The CRF peptide family and their receptors: yet more partners discovered. 23(2): 71-77.

De Kloet Er, Joels M and Holsboer F (2005): Stress and the brain: from adaptation to disease. *Nat Rev Neurosci* 6(6): 463-75.

De Leeuw F, Zhang T, Wauquier C, Huez G, Kruys V and Gueydan C (2007): The cold-inducible RNA-binding protein migrates from the nucleus to cytoplasmic stress granules by a methylation-dependent mechanism and acts as a translational repressor. *Exp Cell Res* 313(20): 4130-44.

Deak T, Nguyen Kt, Ehrlich Al, Watkins Lr, Spencer Rl, Maier Sf, Licinio J, Wong Ml, Chrousos Gp, Webster E*, et al.* (1999): The impact of the nonpeptide corticotropin-releasing hormone antagonist antalarmin on behavioral and endocrine responses to stress. *Endocrinology* 140(1): 79-86.

Debold C, Sheldon W, Decherney G, Jackson R, Alexander A, Vale W, Rivier J and Orth D (1984): Arginine vasopressin potentiates adrenocorticotropin release induced by ovine corticotropin-releasing factor. *J Clin Invest.* 73(2): 533–538.

Dekloet Er (2004): Hormones and the Stressed Brain. *Annals of the New York Academy of Sciences* 1018(1): 1-15.

Delibrias Cc, Floettmann Je, Rowe M and Fearon Dt (1997): Downregulated Expression of SHP-1 in Burkitt Lymphomas and Germinal Center B Lymphocytes. *J. Exp. Med.* 186(9): 1575-1583.

Dere E, Boverhof D, Burgoon L and Zacharewski T (2006): In vivo - in vitro toxicogenomic comparison of TCDD-elicited gene expression in Hepa1c1c7 mouse hepatoma cells and C57BL/6 hepatic tissue. *BMC Genomics* 7(1): 80.

Desouza E (1985): Conspectus. Corticotropin-releasing factor. *Compr Ther.* 11(6): 3-5.

Dettling M and Buhlmann P (2003): Boosting for tumor classification with gene expression data. *Bioinformatics* 19(9): 1061-1069.

Deussing Jm (2006): Animal models of depression. *Drug Discovery Today: Dis. Models* 3(4): 375-383.

Deussing Jm, Kuhne C, Putz B, Panhuysen M, Breu J, Stenzel-Poore Mp, Holsboer F and Wurst W (2007): Expression profiling identifies the CRH//CRH-R1 system as a modulator of neurovascular gene activity. *J Cereb Blood Flow Metab* 27(8): 1476-1495.

Deussing Jm and Wurst W (2005): Dissecting the genetic effect of the CRH system on anxiety and stress-related behaviour. *C R Biol* 328(2): 199-212.

Deutsch Jm (2003): Evolutionary algorithms for finding optimal gene sets in microarray prediction. *Bioinformatics* 19(1): 45-52.

Ding J, Guzman Jn, Tkatch T, Chen S, Goldberg Ja, Ebert Pj, Levitt P, Wilson Cj, Hamm He and Surmeier Dj (2006): RGS4-dependent attenuation of M4 autoreceptor function in striatal cholinergic interneurons following dopamine depletion. *Nat Neurosci* 9(6): 832-42.

Dresios J, Aschrafi A, Owens Gc, Vanderklish Pw, Edelman Gm and Mauro Vp (2005): Cold stress-induced protein Rbm3 binds 60S ribosomal subunits, alters microRNA levels, and enhances global protein synthesis. *Proc Natl Acad Sci U S A* 102(6): 1865-70.

Dudoit S, Fridlyand J and Speed Tp (2002): Comparison of discrimination methods for the classification of tumors using gene expression data. *J Amer Statist Assoc* 97: 77 - 87.

Dunn Aj and Berridge Cw (1990): Physiological and behavioral responses to corticotropin-releasing factor administration: is CRF a mediator of anxiety or stress responses? *Brain Res Brain Res Rev* 15(2): 71-100.

Dziedzic B, Prevot V, Lomniczi A, Jung H, Cornea A and Ojeda Sr (2003): Neuron-to-glia signaling mediated by excitatory amino acid receptors regulates ErbB receptor function in astroglial cells of the neuroendocrine brain. *J Neurosci* 23(3): 915-26.

Edgar R, Domrachev M and Lash Ae (2002): Gene Expression Omnibus: NCBI gene expression and hybridization array data repository. *Nucl. Acids Res.* 30(1): 207-210.

Erdely Ha, Lahti Ra, Lopez Mb, Myers Cs, Roberts Rc, Tamminga Ca and Vogel Mw (2004): Regional expression of RGS4 mRNA in human brain. *Eur J Neurosci* 19(11): 3125-8.

Ferguson Gd, Herschman Hr and Storm Dr (2004): Reduced anxiety and depression-like behavior in synaptotagmin IV (-/-) mice. *Neuropharmacology* 47(4): 604-11.

Ferno J, Raeder Mb, Vik-Mo Ao, Skrede S, Glambek M, Tronstad K-J, Breilid H, Lovlie R, Berge Rk, Stansberg C*, et al.* (2005): Antipsychotic drugs activate SREBP-regulated expression of lipid biosynthetic genes in cultured human glioma cells: a novel mechanism of action? 5(5): 298-304.

Fickel J, Papsdorf G, Putscher I, Winkler A and Melzig Mf (1994): Compensation of CRH induced ACTH secretion by substance P (SP) in AtT20 mouse pituitary tumor cells under serum reduced conditions. *Regulatory Peptides* 53(Supplement 1): S117-S118.

Fiorentino L, Pertica C, Fiorini M, Talora C, Crescenzi M, Castellani L, Alema S, Benedetti P and Segatto O (2000): Inhibition of ErbB-2 mitogenic and transforming activity by RALT, a mitogen-induced signal transducer which binds to the ErbB-2 kinase domain. *Mol Cell Biol* 20(20): 7735-50.

Forman Bm, Chen J and Evans Rm (1997): Hypolipidemic drugs, polyunsaturated fatty acids, and eicosanoids are ligands for peroxisome proliferator-activated receptors α and δ. *PNAS* 94(9): 4312-4317.

Gabriel Kr (1971): The biplot graphic display of matrices with application to principal component analysis. *Biometrica* 58: 453-467.

Gold Pw, Goodwin Fk and Chrousos Gp (1988): Clinical and biochemical manifestations of depression. Relation to the neurobiology of stress (2). *N Engl J Med* 319(7): 413-420.

Gower Jc and Hand Dj (1996): Biplots. London, *Chapman and Hall*.

Grammatopoulos Dk and Chrousos Gp (2002): Functional characteristics of CRH receptors and potential clinical applications of CRH-receptor antagonists. 13(10): 436-444.

Graziani G, Tentori L, Muzi A, Vergati M, Tringali G, Pozzoli G and Navarra P (2007): Evidence that corticotropin-releasing hormone inhibits cell growth of human breast cancer cells via the activation of CRH-R1 receptor subtype *Mol. Cell. Endocrinol.* 264(1-2): 44-49

Grigoriadis De (2005): The corticotropin-releasing factor receptor: a novel target for the treatment of depression and anxiety-related disorders. *Expert Opinion on Therapeutic Targets* 9(4): 651-684.

Gronholm M, Teesalu T, Tyynela J, Piltti K, Bohling T, Wartiovaara K, Vaheri A and Carpen O (2005): Characterization of the NF2 protein merlin and the ERM protein ezrin in human, rat, and mouse central nervous system. *Mol Cell Neurosci* 28(4): 683-93.

Gu Z, Jiang Q and Yan Z (2007): RGS4 modulates serotonin signaling in prefrontal cortex and links to serotonin dysfunction in a rat model of schizophrenia. *Mol Pharmacol* 71(4): 1030-9.

Gutkind Js (1998): The Pathways Connecting G Protein-coupled Receptors to the Nucleus through Divergent Mitogen-activated Protein Kinase Cascades. *J. Biol. Chem.* 273(4): 1839-1842.

Hastie T, Tibshirani R and Friedman J (2001a): The Elements of Statistical Learning - Data Mining, Inference, and Prediction. Heidelberg, *Springer-Verlag*.

Hastie T, Tibshirani R and Friedman J (2001b): Elements of statistical learning: Data mining, inference and prediction. *Springer-Verlag, Berlin, Germany.*

Hauger R and Dautzenberg F (1999): Regulation of the stress response by corticotropin-releasing factor receptors. *Neuroendocrinology in Physiology and Medicine (Conn PM andFreedman ME eds), Humana Press, Inc., Totowa, NJ*: 261-286.

Hauger Rl, Grigoriadis De, Dallman Mf, Plotsky Pm, Vale Ww and Dautzenberg Fm (2003): International Union of Pharmacology. XXXVI. Current status of the nomenclature for receptors for corticotropin-releasing factor and their ligands. *Pharmacol Rev* 55(1): 21-6.

Hauger Rl, Risbrough V, Brauns O and Dautzenberg Fm (2006): Corticotropin releasing factor (CRF) receptor signaling in the central nervous system: new molecular targets. *CNS Neurol Disord Drug Targets* 5(4): 453-79.

Heard N, Holmes C and Stephens D (2006): A quantitative study of gene regulation involved in the immune response of Anopheline mosquitoes: An application of Bayesian hierarchical clustering of curves. *Journal of the American Statistical Association* 101(473): 18-29.

Heinrichs Sc, Stenzel-Poore Mp, Gold Lh, Battenberg E, Bloom Fe, Koob Gf, Vale Ww and Pich Em (1996): Learning impairment in transgenic mice with central overexpression of corticotropin-releasing factor. *Neuroscience* 74(2): 303-11.

Herman Jp, Figueiredo H, Mueller Nk, Ulrich-Lai Y, Ostrander Mm, Choi Dc and Cullinan We (2003): Central mechanisms of stress integration: hierarchical circuitry controlling hypothalamo-pituitary-adrenocortical responsiveness. *Front Neuroendocrinol* 24(3): 151-180.

Hertz R, Berman I and Bar-Tana J (1994): Transcriptional activation by amphipathic carboxylic peroxisomal proliferators is induced by the free acid rather than the acyl-CoA derivative. *Eur J Biochem.* 221(1): 611-615.

Hillhouse Ew and Grammatopoulos Dk (2006): The molecular mechanisms underlying the regulation of the biological activity of corticotropin-releasing hormone receptors: implications for physiology and pathophysiology. *Endocrine Reviews* 27(3): 260-86.

Holsboer F (2000): The corticosteroid receptor hypothesis of depression. *Neuropsychopharmacology* 23(5): 477-501.

Holsboer F and Ising M (2008): Central CRH system in depression and anxiety -- Evidence from clinical studies with CRH1 receptor antagonists. *European Journal of Pharmacology* 583(2-3): 350-357.

Hsu M-H, Savas U, Griffin Kj and Johnson Ef (2001): Identification of Peroxisome Proliferator-responsive Human Genes by Elevated Expression of the Peroxisome Proliferator-activated Receptor alpha in HepG2 Cells. *J. Biol. Chem.* 276(30): 27950-27958.

Hsu Sy and Hsueh Aj (2001): Human stresscopin and stresscopin-related peptide are selective ligands for the type 2 corticotropin-releasing hormone receptor. *Nat Med* 7(5).

Hunter T (1998): The Croonian Lecture 1997. The phosphorylation of proteins on tyrosine: its role in cell growth and disease. *Philos Trans R Soc Lond B Biol Sci* 353(1368): 583-605.

Hunter Wm and Greenwood Fc (1962): Preparation of iodine-131 labelled human growth hormone of high specific activity. *Nature* 194: 495-6.

Iredale Pa and Duman Rs (1997): Glucocorticoid regulation of corticotropin-releasing factor1 receptor expression in pituitary-derived AtT-20 cells. *Mol Pharmacol* 51(5): 794-9.

Ising M and Holsboer F (2006): Genetics of stress response and stress-related disorders. *Dialogues Clin Neurosci* 8(4): 433-44.

Ising M, Zimmermann Us, Kunzel He, Uhr M, Foster Ac, Learned-Coughlin Sm, Holsboer F and Grigoriadis De (2007): High-Affinity CRF1 Receptor Antagonist NBI-34041: Preclinical and Clinical Data Suggest Safety and Efficacy in Attenuating Elevated Stress Response. *Neuropsychopharmacology* 32(9): 1941-1949.

Jaffer Zm and Chernoff J (2002): p21-activated kinases: three more join the Pak. *Int J Biochem Cell Biol* 34(7): 713-7.

Jin N, Gilbert Jl, Broaddus Rr, Demayo Fj and Jeong Jw (2007): Generation of a Mig-6 conditional null allele. *Genesis* 45(11): 716-21.

Jirapech-Umpai T and Aitken S (2005): Feature selection and classification for microarray data analysis: Evolutionary methods for identifying predictive genes. *BMC Bioinformatics* 6(1): 148.

Juruena Mf, Cleare Aj and Pariante Cm (2004): The Hypothalamic Pituitary Adrenal axis, Glucocorticoid receptor function and relevance to depression. *Revista Brasileira de Psiquiatria* 26: 189-201.

Kageyama K, Hanada K, Moriyama T, Imaizumi T, Satoh K and Suda T (2007): Differential regulation of CREB and ERK phosphorylation through corticotropin-releasing factor receptors type 1 and 2 in AtT-20 and A7r5 cells. *Mol Cell Endocrinol.* 263(1-2): 90-102.

Kageyama K, Sakihara S and Suda T (2008): Regulation and role of p21-activated kinase 3 by corticotropin-releasing factor in mouse pituitary. *Regulatory Peptides* In Press, Corrected Proof.

Kalin Nh, Sherman Je and Takahashi Lk (1988): Antagonism of endogenous CRH systems attenuates stress-induced freezing behavior in rats. *Brain Res* 457(1): 130-5.

Karalis K, Muglia L, Bae D, Hilderbrand H and Majzoub J (1997): CRH and the immune system. *J Neuroimmunol.* 72(2): 131-136

Keck Me (2006): Corticotropin-releasing factor, vasopressin and receptor systems in depression and anxiety. *Amino Acids* 31(3): 241-50.

Kessler Rc, Berglund P, Demler O, Jin R, Koretz D, Merikangas Kr, Rush Aj, Walters Ee and Wang Ps (2003): The epidemiology of major depressive disorder: results from the National Comorbidity Survey Replication (NCS-R). *Jama* 289(23): 3095-105.

Kim E and Sheng M (2004): PDZ domain proteins of synapses. *Nat Rev Neurosci* 5(10): 771-81.

Kishimoto T, Radulovic J, Radulovic M, Lin Cr, Schrick C, Hooshmand F, Hermanson O, Rosenfeld Mg and Spiess J (2000): Deletion of Crhr2 reveals an anxiolytic role for corticotropin-releasing hormone receptor-2. *Nat Genet* 24(4): 415-9.

Kissil Jl, Wilker Ew, Johnson Kc, Eckman Ms, Yaffe Mb and Jacks T (2003): Merlin, the Product of the Nf2 Tumor Suppressor Gene, Is an Inhibitor of the p21-Activated Kinase, Pak1. *Molecular Cell* 12(4): 841-849.

Knauf U, Jakob U, Engel K, Buchner J and Gaestel M (1994): Stress- and mitogen-induced phosphorylation of the small heat shock protein Hsp25 by MAPKAP kinase 2 is not essential for chaperone properties and cellular thermoresistance. *EMBO J.* 13(1): 54-60.

Knaus Ug and Bokoch Gm (1998): The p21Rac/Cdc42-activated kinases (PAKs). *Int J Biochem Cell Biol* 30(8): 857-62.

Knaus Ug, Morris S, Dong Hj, Chernoff J and Bokoch Gm (1995): Regulation of human leukocyte p21-activated kinases through G protein--coupled receptors. *Science* 269(5221): 221-3.

Koob Gf (1999): Corticotropin-releasing factor, norepinephrine, and stress *Biological Psychiatry* 46(9): 1167-1180.

Korte Sm, Korte-Bouws Ga, Bohus B and Koob Gf (1994): Effect of corticotropin-releasing factor antagonist on behavioral and neuroendocrine responses during exposure to defensive burying paradigm in rats. *Physiol Behav* 56(1): 115-20.

Kotecha Sa, Oak Jn, Jackson Mf, Perez Y, Orser Ba, Van Tol Hh and Macdonald Jf (2002): A D2 class dopamine receptor transactivates a receptor tyrosine kinase to inhibit NMDA receptor transmission. *Neuron* 35(6): 1111-22.

Kothapalli R, Yoder Sj, Mane S and Loughran Tp, Jr. (2002): Microarray results: how accurate are they? *BMC Bioinformatics* 3: 22.

Kovalovsky D, Refojo D, Liberman Ac, Hochbaum D, Pereda Mp, Coso Oa, Stalla Gk, Holsboer F and Arzt E (2002): Activation and Induction of NUR77/NURR1 in Corticotrophs by CRH/cAMP: Involvement of Calcium, Protein Kinase A, and MAPK Pathways. *Mol Endocrinol* 16(7): 1638-1651.

Kromer Sa, Kessler Ms, Milfay D, Birg In, Bunck M, Czibere L, Panhuysen M, Putz B, Deussing Jm, Holsboer F*, et al.* (2005): Identification of glyoxalase-I as a protein marker in a mouse model of extremes in trait anxiety. *J Neurosci* 25(17): 4375-84.

Kronsbein Hc, Jastorff Am, Maccarrone G, Stalla G, Wurst W, Holsboer F, Turck Cw and Deussing Jm (2008): CRHR1-dependent effects on protein expression and posttranslational modification in AtT-20 cells. *Mol Cell Endocrinol.* 292(1-2): 1-10.

Krzanowski Wj, Jonathan P, Mccarthy Wv and Thomas Mr (1995): Discriminant analysis with singular covarince matrices: Methods and applications to spectroscopic data. *Appl. Statist.* 44: 101-115.

Kuo Wp, Jenssen Tk, Butte Aj, Ohno-Machado L and Kohane Is (2002): Analysis of matched mRNA measurements from two different microarray technologies. *Bioinformatics* 18(3): 405-12.

Lamas M and Sassone-Corsi P (1997): The Dynamics of the Transcriptional Response to Cyclic Adenosine 3',5'-Monophosphate: Recurrent Inducibility and Refractory Phase. *Mol Endocrinol* 11(10): 1415-1424.

Läuter J, Glimm E and Kropf S (1998): Multivariate tests based on leftspherically distributed linear scores. *The Annals of Statistics* 27(26): 1441.

Lazennec G, Canaple L, Saugy D and Wahli W (2000): Activation of Peroxisome Proliferator-Activated Receptors (PPARs) by Their Ligands and Protein Kinase A Activators. *Mol Endocrinol* 14(12): 1962-1975.

Ledoit O and Wolf M (2003): A well-conditioned estimator for large-dimensional covariance matrices. *Journal of Multivariate Analysis* 88: 365-411.

Lee Hj, Hammond Dn, Large Th, Roback Jd, Sim Ja, Brown Da, Otten Uh and Wainer Bh (1990): Neuronal properties and trophic activities of immortalized hippocampal cells from embryonic and young adult mice. *J.Neurosci.* 10(6): 1779-1787.

Lee Yj, Cho Hn, Jeoung Di, Soh Jw, Cho Ck, Bae S, Chung Hy, Lee Sj and Lee Ys (2004): HSP25 overexpression attenuates oxidative stress-induced apoptosis: roles of ERK1/2 signaling and manganese superoxide dismutase. *Free Radic Biol Med* 36(4): 429-44.

Lee Yj, Lee Dh, Cho Ck, Bae S, Jhon Gj, Lee Sj, Soh Jw and Lee Ys (2005): HSP25 inhibits protein kinase C delta-mediated cell death through direct interaction. *J Biol Chem* 280(18): 18108-19.

Lefkowitz Rj, Pierce Kl and Luttrell Lm (2002): Dancing with different partners: protein kinase a phosphorylation of seven membrane-spanning receptors regulates their G protein-coupling specificity. *Mol Pharmacol* 62(5): 971-4.

Lemmon Ma and Schlessinger J (1994): Regulation of signal transduction and signal diversity by receptor oligomerization. *Trends Biochem Sci* 19(11): 459-63.

Lewis K, Li C, Perrin Mh, Blount A, Kunitake K, Donaldson C, Vaughan J, Reyes Tm, Gulyas J, Fischer W*, et al.* (2001): Identification of urocortin III, an additional member of the corticotropin-releasing factor (CRF) family with high affinity for the CRF2 receptor. *Proc Natl Acad Sci U S A* 98(13).

Li W, Fan J and Woodley Dt (2001): Nck/Dock: an adapter between cell surface receptors and the actin cytoskeleton. *Oncogene* 20(44): 6403-17.

Liebsch G, Landgraf R, Engelmann M, Lorscher P and Holsboer F (1999): Differential behavioural effects of chronic infusion of CRH 1 and CRH 2 receptor antisense oligonucleotides into the rat brain. *J Psychiatr Res* 33(2): 153-63.

Lim Jy, Kim H, Jeun S-S, Kang S-G and Lee K-J (2006a): Merlin inhibits growth hormone-regulated Raf-ERKs pathways by binding to Grb2 protein. *Biochemical and Biophysical Research Communications* 340(4): 1151-1157.

Lim Jy, Kim H, Jeun Ss, Kang Sg and Lee Kj (2006b): Merlin inhibits growth hormone-regulated Raf-ERKs pathways by binding to Grb2 protein. *Biochemical and Biophysical Research Communications* 340(4): 1151-1157.

Liu Xs, Zhang Zg, Zhang Rl, Gregg Sr, Meng H and Chopp M (2007): Comparison of in vivo and in vitro gene expression profiles in subventricular zone neural progenitor cells from the adult mouse after middle cerebral artery occlusion. *Neuroscience* 146(3): 1053-61.

Liu Y, Kalintchenko N, Sassone-Corsi P and Aguilera G (2006): Inhibition of corticotrophin-releasing hormone transcription by inducible cAMP-early repressor in the hypothalamic cell line, 4B. *J.Neuroendocrinol.* 18(1): 42-49.

Livak Kj and Schmittgen Td (2001): Analysis of Relative Gene Expression Data Using Real-Time Quantitative PCR and the 2-[Delta][Delta]CT Method. *Methods* 25(4): 402-408.

Lockhart Dj, Dong H, Byrne Mc, Follettie Mt, Gallo Mv, Chee Ms, Mittmann M, Wang C, Kobayashi M, Horton H*, et al.* (1996): Expression monitoring by hybridization to high-density oligonucleotide arrays. *Nat Biotechnol* 14(13): 1675-80.

Lowry Pj, Koerber Sc, Woods Rj, Baigent S, Sutton S, Behan Dp, Vale W and Rivier J (1996): Nature of ligand affinity and dimerization of corticotrophin-releasing factor-binding protein may be detected by circular dichroism. *J Mol Endocrinol* 16(1): 39-44.

Lu A, Steiner Ma, Whittle N, Vogl Am, Walser Sm, Ableitner M, Refojo D, Ekker M, Rubenstein Jl, Stalla Gk*, et al.* (2008): Conditional mouse mutants highlight mechanisms of corticotropin-releasing hormone effects on stress-coping behavior. *Mol Psychiatry* 13(11): 1028-42.

Lundkvist J, Chai Z, Teheranian R, Hasanvan H, Bartfai T, Jenck F, Widmer U and Moreau Jl (1996): A non peptidic corticotropin releasing factor receptor antagonist attenuates fever and exhibits anxiolytic-like activity. *Eur J Pharmacol* 309(2): 195-200.

Luttrell Lm (2002): Activation and targeting of mitogen-activated protein kinases by G-protein-coupled receptors. *Can J Physiol Pharmacol* 80(5): 375-82.

Luttrell Lm and Lefkowitz Rj (2002): The role of beta-arrestins in the termination and transduction of G-protein-coupled receptor signals. *J Cell Sci* 115(Pt 3): 455-65.

Manser E, Huang Hy, Loo Th, Chen Xq, Dong Jm, Leung T and Lim L (1997): Expression of constitutively active alpha-PAK reveals effects of the kinase on actin and focal complexes. *Mol Cell Biol* 17(3): 1129-43.

Marie-Claire C, Benturquia N, Lundqvist A, Courtin C and Noble F (2008): Characteristics of dual specificity phosphatases mRNA regulation by 3,4-methylenedioxymethamphetamine acute treatment in mice striatum. *Brain Research* 1239: 42-48.

Marti F, Krause A, Post Nh, Lyddane C, Dupont B, Sadelain M and King Pd (2001): Negative-feedback regulation of CD28 costimulation by a novel mitogen-activated protein kinase phosphatase, MKP6. *J Immunol* 166(1): 197-206.

Mccarthy Jr, Heinrichs Sc and Grigoriadis De (1999): Recent advances with the CRF1 receptor: design of small molecule inhibitors, receptor subtypes and clinical indications. *Curr Pharm Des* 5(5): 289-315.

Mckinney Wt, Jr. and Bunney We, Jr. (1969): Animal model of depression. I. Review of evidence: implications for research. *Arch Gen Psychiatry* 21(2): 240-8.

Mcphie Dl, Coopersmith R, Hines-Peralta A, Chen Y, Ivins Kj, Manly Sp, Kozlowski Mr, Neve Ka and Neve Rl (2003): DNA synthesis and neuronal apoptosis caused by familial Alzheimer disease mutants of the amyloid precursor protein are mediated by the p21 activated kinase PAK3. *J Neurosci* 23(17): 6914-27.

Meng J, Meng Y, Hanna A, Janus C and Jia Z (2005): Abnormal long-lasting synaptic plasticity and cognition in mice lacking the mental retardation gene Pak3. *J Neurosci* 25(28): 6641-50.

Muller Mb, Zimmermann S, Sillaber I, Hagemeyer Tp, Deussing Jm, Timpl P, Kormann Msd, Droste Sk, Kuhn R, Reul Jmhm*, et al.* (2003): Limbic corticotropin-releasing hormone receptor 1 mediates anxiety-related behavior and hormonal adaptation to stress. *Nat Neurosci* 6(10): 1100-1107.

Mutarelli M, Cicatiello L, Ferraro L, Grober Om, Ravo M, Facchiano Am, Angelini C and Weisz A (2008): Time-course analysis of genome-wide gene expression data from hormone-responsive human breast cancer cells. *BMC Bioinformatics* 9 Suppl 2: S12.

Nemeroff C (1996): The corticotropin-releasing factor (CRF) hypothesis of depression: new findings and new directions. *Mol Psychiatry.* 1(4): 336-42.

Nemeroff C, Widerlöv E, Bissette G, Walléus H, Karlsson I, Eklund K, Kilts C, Loosen P and Vale W (1984): Elevated concentrations of CSF corticotropin-releasing factor-like immunoreactivity in depressed patients. *Science* 226(4680): 1342-4.

Nemeroff Cb (1988): The role of corticotropin-releasing factor in the pathogenesis of major depression. *Pharmacopsychiatry* 21(2): 76-82.

Nestler Ej, Barrot M, Dileone Rj, Eisch Aj, Gold Sj and Monteggia Lm (2002): Neurobiology of Depression. 34(1): 13-25.

Newcomer J (2006): Medical risk in patients with bipolar disorder and schizophrenia. *J Clin Psychiatry.* 67(11): e16.

Ni Yg, Gold Sj, Iredale Pa, Terwilliger Rz, Duman Rs and Nestler Ej (1999): Region-specific regulation of RGS4 (Regulator of G-protein-signaling protein type 4) in brain by stress and glucocorticoids: in vivo and in vitro studies. *J Neurosci* 19(10): 3674-80.

Olianas Mc, Lampis G and Onali P (1995): Coupling of corticotropin-releasing hormone receptors to adenylyl cyclase in human Y-79 retinoblastoma cells. *J Neurochem* 64(1): 394-401.

Ooi Ch and Tan P (2003): Genetic algorithms applied to multi-class prediction for the analysis of gene expression data. *Bioinformatics* 19(1): 37-44.

Pante G, Thompson J, Lamballe F, Iwata T, Ferby I, Barr Fa, Davies Am, Maina F and Klein R (2005): Mitogen-inducible gene 6 is an endogenous inhibitor of HGF/Met-induced cell migration and neurite growth. *J Cell Biol* 171(2): 337-48.

Papadia S, Soriano Fx, Leveille F, Martel Ma, Dakin Ka, Hansen Hh, Kaindl A, Sifringer M, Fowler J, Stefovska V*, et al.* (2008): Synaptic NMDA receptor activity boosts intrinsic antioxidant defenses. *Nat Neurosci* 11(4): 476-87.

Park P, Pagano M and Bonetti M (2001): A nonparametric scoring algorithm for identifying informative genes from microarray data. *Pac. Symp. Biocomput.* 6: 52-63.

Patterson Ta, Lobenhofer Ek, Fulmer-Smentek Sb, Collins Pj, Chu Tm, Bao W, Fang H, Kawasaki Es, Hager J, Tikhonova Ir*, et al.* (2006): Performance comparison of one-color and two-color platforms within the MicroArray Quality Control (MAQC) project. *Nat Biotechnol* 24(9): 1140-50.

Peeters Pj, Fierens Fl, Van Den Wyngaert I, Goehlmann Hw, Swagemakers Sm, Kass Su, Langlois X, Pullan S, Stenzel-Poore Mp and Steckler T (2004a): Gene expression profiles highlight adaptive brain mechanisms in corticotropin releasing factor overexpressing mice. *Brain Res Mol Brain Res* 129(1-2): 135-50.

Peeters Pj, Gohlmann Hw, Van Den Wyngaert I, Swagemakers Sm, Bijnens L, Kass Su and Steckler T (2004b): Transcriptional Response to Corticotropin-Releasing Factor in AtT-20 Cells. *Mol Pharmacol* 66(5): 1083-1092.

Perrin M, Donaldson C, Chen R, Blount A, Berggren T, Bilezikjian L, Sawchenko P and Vale W (1995): Identification of a second corticotropin-releasing factor receptor gene and characterization of a cDNA expressed in heart. *Proc Natl Acad Sci U S A* 92(7): 2969-73.

Pierce Kl, Premont Rt and Lefkowitz Rj (2002): Seven-transmembrane receptors. *Nat Rev Mol Cell Biol* 3(9): 639-50.

Pinkas-Kramarski R, Eilam R, Alroy I, Levkowitz G, Lonai P and Yarden Y (1997): Differential expression of NDF/neuregulin receptors ErbB-3 and ErbB-4 and involvement in inhibition of neuronal differentiation. *Oncogene* 15(23): 2803-15.

Potter E, Behan Dp, Linton Ea, Lowry Pj, Sawchenko Pe and Vale Ww (1992): The central distribution of a corticotropin-releasing factor (CRF)-binding protein predicts multiple sites and modes of interaction with CRF. *Proc Natl Acad Sci U S A* 89(9): 4192-6.

Punn A, Levine Ma and Grammatopoulos Dk (2006): Identification of Signaling Molecules Mediating Corticotropin-Releasing Hormone-R1{alpha}-Mitogen-Activated Protein Kinase (MAPK) Interactions: The Critical Role of Phosphatidylinositol 3-Kinase in Regulating ERK1/2 But Not p38 MAPK Activation. *Mol Endocrinol* 20(12): 3179-3195.

Raadsheer Fc, Hoogendijk Wj, Stam Fc, Tilders Fj and Swaab Df (1994): Increased numbers of corticotropin-releasing hormone expressing neurons in the hypothalamic paraventricular nucleus of depressed patients. *Neuroendocrinology* 60(4): 436-44.

Radulovic J, Ruhmann A, Liepold T and Spiess J (1999): Modulation of Learning and Anxiety by Corticotropin-Releasing Factor (CRF) and Stress: Differential Roles of CRF Receptors 1 and 2. *J. Neurosci.* 19(12): 5016-5025.

Refojo D, Echenique C, Muller Mb, Reul Jm, Deussing Jm, Wurst W, Sillaber I, Paez-Pereda M, Holsboer F and Arzt E (2005): Corticotropin-releasing hormone activates ERK1/2 MAPK in specific brain areas. *Proc Natl Acad Sci U S A* 102(17): 6183-8.

Reul Jmhm and Holsboer F (2002): Corticotropin-releasing factor receptors 1 and 2 in anxiety and depression. *Curr Opin Pharmacol.* 2(1): 23-33.

Rosendale Be, Jarrett Db and Robinson Ag (1987): Identification of a corticotropin-releasing factor-binding protein in the plasma membrane of AtT-20 mouse pituitary tumor cells and its regulation by dexamethasone. *Endocrinology* 120(6): 2357-66.

Rouleau Ga, Merel P, Lutchman M, Sanson M, Zucman J, Marineau C, Hoang-Xuan K, Demczuk S, Desmaze C, Plougastel B*, et al.* (1993): Alteration in a new gene encoding a putative membrane-organizing protein causes neuro-fibromatosis type 2. *Nature* 363(6429): 515-21.

Rousseau V, Goupille O, Morin N and Barnier Jv (2003): A new constitutively active brain PAK3 isoform displays modified specificities toward Rac and Cdc42 GTPases. *J.Biol.Chem.* 278(6): 3912-3920.

Sajdyk Tj and Gehlert Dr (2000): Astressin, a corticotropin releasing factor antagonist, reverses the anxiogenic effects of urocortin when administered into the basolateral amygdala. *Brain Res* 877(2): 226-34.

Sakurai T, Itoh K, Higashitsuji H, Nonoguchi K, Liu Y, Watanabe H, Nakano T, Fukumoto M, Chiba T and Fujita J (2006): Cirp protects against tumor necrosis factor-alpha-induced apoptosis via activation of extracellular signal-regulated kinase. *Biochim Biophys Acta* 1763(3): 290-5.

Sapolsky Rm, Romero Lm and Munck Au (2000): How Do Glucocorticoids Influence Stress Responses? Integrating Permissive, Suppressive, Stimulatory, and Preparative Actions. *Endocrine Reviews* 21(1): 55-89.

Schäfer J, Opgen-Rhein R and Strimmer K (2006): Reverse engineering genetic networks using the GeneNet package. *R News* 6: 50-53.

Schäfer J and Strimmer K (2005a): An empirical Bayes approach to inferring large-scale gene association networks. *Bioinformatics* 21(6): 754-764.

Schäfer J and Strimmer K (2005b): A shrinkage approach to large-scale covariance matrix estimation and implications for functional genomics. *Stat Appl Genet Mol Biol* 4(1): Article:32.

Schena M, Shalon D, Davis Rw and Brown Po (1995): Quantitative monitoring of gene expression patterns with a complementary DNA microarray. *Science* 270(5235): 467-70.

Schlessinger J (2000): Cell signaling by receptor tyrosine kinases. *Cell* 103(2): 211-25.

Schulz Dw, Mansbach Rs, Sprouse J, Braselton Jp, Collins J, Corman M, Dunaiskis A, Faraci S, Schmidt Aw, Seeger T*, et al.* (1996): CP-154,526: a potent and selective nonpeptide antagonist of corticotropin releasing factor receptors. *Proc Natl Acad Sci U S A* 93(19): 10477-82.

Schwenger Gtf, Kok Cc, Arthaningtyas E, Thomas Ma, Sanderson Cj and Mordvinov Va (2002): Specific Activation of Human Interleukin-5 Depends on de Novo Synthesis of an AP-1 Complex. *J. Biol. Chem.* 277(49): 47022-47027.

Selye H (1951): The general-adaptation-syndrom and the gastrointestinal diseases of adaptation. *Am J Proctol.* 2(4): 167-84.

Seong E, Seasholtz Af and Burmeister M (2002): Mouse models for psychiatric disorders. *Trends Genet* 18(12): 643-50.

Shah Bh and Catt Kj (2004): GPCR-mediated transactivation of RTKs in the CNS: mechanisms and consequences. *Trends Neurosci* 27(1): 48-53.

Shah Bh, Soh Jw and Catt Kj (2003): Dependence of gonadotropin-releasing hormone-induced neuronal MAPK signaling on epidermal growth factor receptor transactivation. *J Biol Chem* 278(5): 2866-75.

Sherman L, Xu Hm, Geist Rt, Saporito-Irwin S, Howells N, Ponta H, Herrlich P and Gutmann Dh (1997): Interdomain binding mediates tumor growth suppression by the NF2 gene product. *Oncogene* 15(20): 2505-2509.

Shi L, Reid Lh, Jones Wd, Shippy R, Warrington Ja, Baker Sc, Collins Pj, De Longueville F, Kawasaki Es, Lee Ky*, et al.* (2006): The MicroArray Quality Control (MAQC) project shows inter- and intraplatform reproducibility of gene expression measurements. *Nat.Biotechnol.* 24(9): 1151-1161.

Skutella T, Probst Jc, Renner U, Holsboer F and Behl C (1998): Corticotropin-releasing hormone receptor (type I) antisense targeting reduces anxiety. *Neuroscience* 85(3): 795-805.

Slominski A, Zbytek B, Pisarchik A, Slominski R, Zmijewski M and Wortsman J (2006): CRH functions as a growth factor/cytokine in the skin. *J Cell Physiol.* 206(3): 780-791.

Smith Gw, Aubry Jm, Dellu F, Contarino A, Bilezikjian Lm, Gold Lh, Chen R, Marchuk Y, Hauser C, Bentley Ca*, et al.* (1998): Corticotropin releasing factor receptor 1-deficient mice display decreased anxiety, impaired stress response, and aberrant neuroendocrine development. *Neuron* 20(6): 1093-102.

Spessert R, Rapp M, Jastrow H, Karabul N, Blum F and Vollrath L (2000): A differential role of CREB phosphorylation in cAMP-inducible gene expression in the rat pineal. *Brain Research* 864(2): 270-280.

Stalla Gk, Stalla J, Von Werder K, Muller Oa, Gerzer R, Hollt V and Jakobs Kh (1989): Nitroimidazole derivatives inhibit anterior pituitary cell function apparently by a direct effect on the catalytic subunit of the adenylate cyclase holoenzyme. *Endocrinology* 125(2): 699-706.

Stenzel-Poore Mp, Heinrichs Sc, Rivest S, Koob Gf and Vale Ww (1994): Overproduction of corticotropin-releasing factor in transgenic mice: a genetic model of anxiogenic behavior. *J Neurosci* 14(5 Pt 1): 2579-84.

Sun Cx, Robb Va and Gutmann Dh (2002): Protein 4.1 tumor suppressors: getting a FERM grip on growth regulation. *J Cell Sci* 115(Pt 21): 3991-4000.

Swanson Lw, Sawchenko Pe, Rivier J and Vale Ww (1983): Organization of ovine corticotropin-releasing factor immunoreactive cells and fibers in the rat brain: an immunohistochemical study. *Neuroendocrinology* 36(3).

Tan Pk, Downey Tj, Spitznagel El, Jr., Xu P, Fu D, Dimitrov Ds, Lempicki Ra, Raaka Bm and Cam Mc (2003): Evaluation of gene expression measurements from commercial microarray platforms. *Nucleic Acids Res* 31(19): 5676-84.

Tarcic N, Ovadia H, Weiss Dw and Weidenfeld J (1998): Restraint stress-induced thymic involution and cell apoptosis are dependent on endogenous glucocorticoids. *J Neuroimmunol* 82(1): 40-6.

Taylor V and Macqueen G (2007): Cognitive dysfunction associated with metabolic syndrome. *Obesity Reviews* 8(5): 409-418.

Therrien M and Drouin J (1991): Pituitary pro-opiomelanocortin gene expression requires synergistic interactions of several regulatory elements. *Mol. Cell. Biol.* 11(7): 3492-3503.

Timpl P, Spanagel R, Sillaber I, Kresse A, Reul Jm, Stalla Gk, Blanquet V, Steckler T, Holsboer F and Wurst W (1998): Impaired stress response and reduced anxiety in mice lacking a functional corticotropin-releasing hormone receptor 1. *Nat.Genet.* 19(2): 162-166.

Todorovic C, Jahn O, Tezval H, Hippel C and Spiess J (2005): The role of CRF receptors in anxiety and depression: implications of the novel CRF1 agonist cortagine. *Neurosci Biobehav Rev* 29(8): 1323-33.

Trevino V and Falciani F (2006): GALGO: an R package for multivariate variable selection using genetic algorithms. *Bioinformatics* 22(9): 1154-1156.

Trofatter Ja, Maccollin Mm, Rutter Jl, Murrell Jr, Duyao Mp, Parry Dm, Eldridge R, Kley N, Menon Ag, Pulaski K*, et al.* (1993): A novel moesin-, ezrin-, radixin-like gene is a candidate for the neurofibromatosis 2 tumor suppressor. *Cell* 72(5): 791-800.

Tronche F, Kellendonk C, Kretz O, Gass P, Anlag K, Orban Pc, Bock R, Klein R and Schutz G (1999): Disruption of the glucocorticoid receptor gene in the nervous system results in reduced anxiety. *Nat Genet* 23(1): 99-103.

Tsigos C and Chrousos G (2002): Hypothalamic-pituitary-adrenal axis, neuroendocrine factors and stress. *J Psychosom Res* 53: 865– 871.

Tsolakidou A, Trumbach D, Panhuysen M, Putz B, Deussing J, Wurst W, Sillaber I, Holsboer F and Rein T (2008): Acute stress regulation of neuroplasticity genes in mouse hippocampus CA3 area - possible novel signalling pathways. *Mol Cell Neurosci* 38(3): 444-52.

Vale W, Rivier C, Brown Mr, Spiess J, Koob G, Swanson L, Bilezikjian L, Bloom F and Rivier J (1983): Chemical and biological characterization of corticotropin releasing factor. *Recent Prog Horm Res* 39 245-70.

Vale W, Spiess J, Rivier C and Rivier J (1981): Characterization of a 41-residue ovine hypothalamic peptide that stimulates secretion of corticotropin and beta-endorphin. *Science* 213(4514): 1394-7.

Van Gaalen Mm, Stenzel-Poore Mp, Holsboer F and Steckler T (2002): Effects of transgenic overproduction of CRH on anxiety-like behaviour. *Eur J Neurosci* 15(12): 2007-15.

Van Pett K, Viau V, Bittencourt Jc, Chan Rk, Li Hy, Arias C, Prins Gs, Perrin M, Vale W and Sawchenko Pe (2000): Distribution of mRNAs encoding CRF receptors in brain and pituitary of rat and mouse. *J Comp Neurol* 428(2): 191-212.

Vaughan J, Donaldson C, Bittencourt J, Perrin Mh, Lewis K, Sutton S, Chan R, Turnbull Av, Lovejoy D, Rivier C*, et al.* (1995): Urocortin, a mammalian neuropeptide related to fish urotensin I and to corticotropin-releasing factor. *Nature* 378(6554): 287-92.

Vila G, Papazoglou M, Stalla J, Theodoropoulou M, Stalla Gk, Holsboer F and Paez-Pereda M (2005): Sonic hedgehog regulates CRH signal transduction in the adult pituitary. *Faseb J* 19(2): 281-3.

Wong Rw and Guillaud L (2004): The role of epidermal growth factor and its receptors in mammalian CNS. *Cytokine Growth Factor Rev* 15(2-3): 147-56.

Xu D, Makkinje A and Kyriakis Jm (2005): Gene 33 is an endogenous inhibitor of epidermal growth factor (EGF) receptor signaling and mediates dexamethasone-induced suppression of EGF function. *J Biol Chem* 280(4): 2924-33.

Yang Yh, Dudoit S, Luu P, Lin Dm, Peng V, Ngai J and Speed Tp (2002): Normalization for cDNA microarray data: a robust composite method addressing single and multiple slide systematic variation. *Nucl. Acids Res.* 30(4): e15.

Zhang Q, Fukuda M, Van Bockstaele E, Pascual O and Haydon Pg (2004): Synaptotagmin IV regulates glial glutamate release. *Proc Natl Acad Sci U S A* 101(25): 9441-6.

Zhang S, Han J, Sells Ma, Chernoff J, Knaus Ug, Ulevitch Rj and Bokoch Gm (1995): Rho family GTPases regulate p38 mitogen-activated protein kinase through the downstream mediator Pak1. *J Biol Chem* 270(41): 23934-6.

Zhang S, Watson N, Zahner J, Rottman Jn, Blumer Kj and Muslin Aj (1998): RGS3 and RGS4 are GTPase activating proteins in the heart. *J Mol Cell Cardiol* 30(2): 269-76.

Zhang Yw and Vande Woude Gf (2007): Mig-6, signal transduction, stress response and cancer. *Cell Cycle* 6(5): 507-13.

Zobel Aw, Nickel T, Kunzel He, Ackl N, Sonntag A, Ising M and Holsboer F (2000): Effects of the high-affinity corticotropin-releasing hormone receptor 1 antagonist R121919 in major depression: the first 20 patients treated. *J Psychiatr Res* 34(3): 171-81.

9. Acknowledgements

First of all, I want to express my gratitude to Dr. Jan Deussing for the helpful guidance, his faith in my abilities and for giving me the scope to pursue own ideas. Moreover, I would like to thank him for the thorough proofreading of this PhD thesis.
I am grateful to Prof. Dr. Wolfgang Wurst, the supervisor of my doctoral thesis, for the opportunity to work on this fascinating topic.
I would also like to thank Prof. Dr. Dieter Langosch and Prof. Dr. Alfons Gierl for their readiness to invest their time in the evaluation and examination of my thesis.

Sincere thanks go to the members of the microarray facility, Claudia Kühne, Peter Weber, Dr. Benno Pütz and Dr. Marcus Panhyusen, for their patient help and support in every step of the microarray analyses. For bioinformatical analyses of the huge data sets I give special thanks to Dr. Benno Pütz and Dr. Dietrich Trümbach, who never became desperate to explain me the secrets of bioinformatical algorithms.

Furthermore, I am indebted to Dr. Damian Refojo for his motivating scientific input in desponding moments.

Many thanks go to Claudia Kühne, the heart and soul of our lab. Whatever problem or question I had she always solved it. Moreover, I like to acknowledge Tanja Orschmann, Marcel Schieven and Jessica Köpke for their help with the animals. Furthermore, I thank Johanna Stalla, Ursula Habersetzer and Dr. Chadi Touma for the hormone measurements.
Altogether, I am grateful to all members of the group for their permanent support in practical and scientific questions, for funny and serious conversations and a relaxed and inspiriting atmosphere. I really enjoyed working with you.

As well, I am thankful to Ludwig Czibere and Dr. Timo Rieg for the careful proofreading of my thesis.

For enduring encouragement, new ideas and diverting evenings I like to show my gratitude to Ludwig Czibere, Dr. Miriam Bunck, Regina Knapp and Claudia Liebl. Thanks a lot for your support and friendship!

Last but not least I thank all the people who accompanied and motivated me in the last years, in particular my family for their constant faith in me.

10. Curriculum Vitae

EDUCATION

since 07/2005	Graduate studies in Molecular Neurogenetics, Max-Planck-Institute of Psychiatry / Technical University Munich
07/2004 - 03/2005	Diploma student, Institute for Pharmacology and Toxicology, Tübingen Diploma thesis: "Analysis of the role of the gap-junction protein Connexin 32 in the hepatocancerogenesis of mice"
10/2004 - 02/2005	Student assistant, Eberhard-Karls-University Tübingen, Germany
04/2000 - 03/2005	Studies in Biochemistry, Eberhard-Karls-University Tübingen, Germany Exams in Analytical Chemistry, Pharmacology/Toxicology and Biochemistry

PRESENTATIONS

05/2008	Keystone Symposia Meeting: G Protein-Coupled Receptors: New Insights in Functional Regulation and Clinical Application, Killarney, Ireland: "New candidate genes in CRHR1-dependent signalling in mouse corticotrope cells" (Poster)
10/2007	25. AGNP Symposium, Munich, Germany: "Dissecting CRHR1-mediated pathways by microarray technology" (Poster)
08/2007	World Conference of Stress, Budapest, Hungary: "Dissecting CRHR1-mediated pathways by microarray technology" (Talk)
07/2007	2nd Interdisciplinary Max-Planck PhDnet Workshop COMMUNICATION, Frankfurt/Main, Deutschland: "Activation of Intracellular Communication by Corticotropin-Releasing Hormone (CRH) and its receptor CRHR1" (Poster)
08/2006	1st Interdisciplinary Max-Planck PhDnet Workshop GLOBAL CHANGES, Köln: "Effects of stress – a gene expression study" (Poster)

11. List of Publications

Brenz Verca M.S., Weber P., Mayer C., **Graf C.**, Refojo D., Kuhn R., Grummt I., Lutz B. (2007). Development of a species-specific RNA polymerase I-based shRNA expression vector, *Nucleic Acids Res.*;35(2):e10.

Bunck M.*, Czibere L.*, Horvath C., **Graf C**., Murgatroyd C., Müller-Myhsok B., Gonik M., Muigg P., Singewald N., Kessler M. S., Frank E., Bettecken T., Deussing J. M., Holsboer F., Spengler D. and Landgraf R.: A hypomorphic vasopressin allele prevents anxiety-related behaviour. *PLoS ONE* (submitted)

* Authors contributed equally

Trümbach D.*, **Graf C.***, Pütz B., Kühne C., Panhuysen M., Weber P., Holsboer F., Wurst W., Welzl G., Deussing J.M.: Deducing corticotropin-releasing hormone receptor type 1 signaling networks from gene expression data by combining genetic algorithm with graphical Gaussian models. (in preparation)

* Authors contributed equally

Graf C., Pütz B., Kühne C., Panhuysen M., Weber P., Holsboer F., Wurst W., Deussing J.M.: Dissecting corticotrope and neuronal CRHR1-signaling pathways: common target genes. (in preparation)

Czibere L., Baur-Jaronowski L. A., Zeiner K., Bunck M., Prigl J., Weber P., Putz B., **Graf C.**, Kuhne C., Panhuysen M., Holsboer F., Deussing J. M. and Landgraf R.: Profiling anxiety: A comprehensive gene expression study in mice bred for extremes in trait anxiety. (in preparation)

12. Declaration / Erklärung

Hiermit versichere ich, Cornelia Graf, dass ich mich zu keiner Zeit anderweitig um die Erlangung des Doktorgrades beworben habe.

Ferner versichere ich, dass ich die vorliegende Arbeit selbstständig und ohne fremde Hilfe verfasst habe und keine anderen als die hier vorliegenden Quellen und Hilfsmittel benutzt und die den verwendeten Werken wörtlich oder inhaltlich entnommenen Stellen als solche kenntlich gemacht habe.

München, den

Cornelia Graf